



SCHOOL of
GRADUATE STUDIES
EAST TENNESSEE STATE UNIVERSITY

East Tennessee State University
Digital Commons @ East
Tennessee State University

Electronic Theses and Dissertations

Student Works

8-2012

Immobilized Bis-Indenyl Ligands for Stable and Cost-Effective Metallocene Catalysts of Hydrogenation and Polymerization Reactions

Thomas Max Simerly
East Tennessee State University

Follow this and additional works at: <https://dc.etsu.edu/etd>



Part of the [Polymer Chemistry Commons](#)

Recommended Citation

Simerly, Thomas Max, "Immobilized Bis-Indenyl Ligands for Stable and Cost-Effective Metallocene Catalysts of Hydrogenation and Polymerization Reactions" (2012). *Electronic Theses and Dissertations*. Paper 1473. <https://dc.etsu.edu/etd/1473>

This Thesis - Open Access is brought to you for free and open access by the Student Works at Digital Commons @ East Tennessee State University. It has been accepted for inclusion in Electronic Theses and Dissertations by an authorized administrator of Digital Commons @ East Tennessee State University. For more information, please contact digilib@etsu.edu.

Immobilized Bis-Indenyl Ligands for Stable and Cost-Effective Metallocene Catalysts of
Hydrogenation and Polymerization Reactions

A thesis
presented to
the faculty of the Department of Chemistry
East Tennessee State University

In partial fulfillment
of the requirements for the degree
Master of Science in Chemistry

by
Thomas Max Simerly
August 2012

Dr. Aleksey N. Vasiliev, Chair
Dr. Ismail O. Kady
Dr. Yu Lin Jiang

Keywords: Immobilization, Ethylene *Bis*-Indenyl Ligands, Thiol-ene Coupling, Functionalized Silica Gel

ABSTRACT

Immobilized Bis-Indenyl Ligands for Stable and Cost-Effective Metallocene Catalysts of Hydrogenation and Polymerization Reactions

by

Thomas Max Simerly

Reactions of catalytic hydrogenations and polymerizations are widely used in industry for manufacture of fine chemicals, pharmaceuticals, and plastics. Homogeneous catalysts for the processes that have low stability and their separation is difficult. Therefore, the development of new highly active and stable catalysts for hydrogenations and polymerizations is a necessity. The objective of this research was the development of a strategy for immobilization of heterogeneous metallocene catalysts. First, a methodology of immobilization of *bis*-indenyl ligands on the surface of mesoporous silica gel was designed. Four *bis*-indenyl ligands containing functionalized tethers of various lengths with terminal alkene groups were synthesized. All *bis*-indenyl ligands were immobilized on the surface of mesoporous functionalized silica gel by two methods: hydrosilylation and thiol-ene coupling of the double bond. After comparing the results, the second strategy was chosen as more efficient. The materials can be used further as intermediates for synthesis of supported metallocene catalysts.

DEDICATION

This work is dedicated in loving memory of my grandmother, Eva “Lena” Simerly.

ACKNOWLEDGEMENTS

First and foremost, I must thank God for guiding me through this journey. Though I am not worthy, he has given me so much with so little in return. I am truly blessed.

I must also thank my parents Max and Teresa Simerly for helping me through the years, always providing me with what I needed, motivating me, and for putting up with me when no one else would.

A large thanks goes to Dr. Aleksey Vasiliev. Not only was he wise, but he was also a friend. Thank you for all of the guidance and mentorship given to me. Because of Dr. Aleksey Vasiliev, I know I am ready to get my Ph.D. at Virginia Tech.

For serving on my committee, thank you Dr. Ismail Kady and Dr. Yu Lin Jiang. I have learned a lot from my committee that I will take with me to my next step in life.

For encouraging me to pursue my Ph.D. after my Masters Degree, thank you Dr. Phillip Cook. I am glad that I listened to what he said. His wisdom is greatly appreciated.

For proofreading my thesis and making suggestions, thank you Dr. Scott Kirkby. I enjoyed the conversations that he and I frequently had.

I want to also thank my dear friends, Myles Keck, Loren Brown, Cornelius Ndi, Kolade Ojo, Stanley Jing, and Jude Lakbub for all of the times we have shared and for being my friends. I have enjoyed getting to know everyone. I wish each and every one the best in their future endeavors.

Lastly, I want to thank all of my fellow graduate students. Each and every one has made the Chemistry Department a close family. Not only have I had a great time with everyone for the past two years, but I have also learned so much.

CONTENTS

	Page
ABSTRACT	2
DEDICATION	3
ACKNOWLEDGEMENTS	4
LIST OF TABLES	8
LIST OF FIGURES	9
LIST OF SCHEMES	12
Chapter	
1. INTRODUCTION	13
Importance of Metallocene Catalysts.....	13
Metallocene Catalysts of Hydrogenations	16
Carbon-Carbon Double Bonds (C=C).....	16
Carbon-Nitrogen Double Bonds (C=N).....	19
Carbon-Oxygen Double Bonds (C=O)	21
Metallocene Catalysts of Polymerizations.....	22
Other Applications of Chiral Metallocenes	25
Structure and Synthesis of Non-Tethered Bridged Bis-Indenyl Ligands	26
Heterogeneous vs. Homogeneous Catalysts	30
Synthesis of Tethered Bridged Bis-Indenyl Ligands	32
Research Objective	35
2. EXPERIMENTAL	37
Structure, Purity, and Manufacturer of Synthetic Reagents	37
Synthesis of Bis-Indenyl Ligands	38

First Step: Synthesis of Indenyl Alcohols.....	39
Second Step: Synthesis of Iodoalkenyl Indenes	40
Third Step: Synthesis of Alkenediyl-bis-indenes	41
Immobilization of the Ligands By Hydrosilyation	42
Immobilization of the Ligands By Thiol-ene Coupling.....	42
Characterization of the Products.....	44
TLC.....	44
FT-IR.....	44
LC-MS	44
¹ H NMR	44
¹³ C NMR	45
Porosimetry	45
Atomic Absorption.....	45
3. RESULTS	46
Yields and Properties of the Compounds	46
NMR Spectral Data.....	47
FT-IR Spectral Data.....	50
MS Spectral Data	51
Porosimetry Data	52
Elemental Analysis Data.....	52
Atomic Absorption data.....	54
4. DISCUSSION	55
Synthesis of Bis-Indenyl Ligands	55
Immobilization of the Ligands on Porous Support.....	57
Summary.....	59
BIBLIOGRAPHY.....	62
APPENDICES	75

APPENDIX A: NMR Spectrums	75
APPENDIX B: FT-IR Spectrums	91
APPENDIX C: Porosimetry Graphs	99
APPENDIX D: Atomic Absorption Calibration Curve	119
VITA	120

LIST OF TABLES

Table	Page
1. Structure, Purity, and Manufacturer of Synthetic Reagents	37
2. Yields and Properties of the Compounds.....	46
3. NMR Spectral Data.....	47
4. FT-IR Spectral Data.....	50
5. MS Spectral Data	51
6. Loading of the Ligands on the Silica Surface and Porous Characteristics of Products 19 -26	52
7. Contents of Metallic Pt on Silica Samples 20-23 After Hydrosilylation.....	54

LIST OF FIGURES

Figure	Page
1. Structure of Indinavir, which contains 5 chiral centers	14
2. A picture displaying children with mycophelia	15
3. <i>S</i> Enantiomer (left) and <i>R</i> Enantiomer (right) of Thalidomide	15
4. An example displaying the tacticity of a polymer	23
5. Polypropylene tacticity vs. metallocene catalyst symmetry	24
6. FT-IR Spectra of Samples 24 and 25	51
7. Adsorption/Desorption Isotherms and Pore Size Distributions of 19 and 20	53
8. Adsorption/Desorption Isotherms and Pore Size Distributions of 24 and 25	54
9. The Volumes of the Ligand Molecules	60
10. Dependence of the Ligand Loading on the Molecular Size	61
11. ¹ H NMR Spectrum of 7	75
12. ¹³ C NMR Spectrum of 7	76
13. ¹ H NMR Spectrum of 8	77
14. ¹³ C NMR Spectrum of 8	78
15. ¹ H NMR Spectrum of 9	79
16. ¹³ C NMR Spectrum of 9	80
17. ¹ H NMR Spectrum of 10	81
18. ¹³ C NMR Spectrum of 10	82
19. ¹ H NMR Spectrum of 15	83
20. ¹³ C NMR Spectrum of 15	84
21. ¹ H NMR Spectrum of 16	85
22. ¹³ C NMR Spectrum of 16	86
23. ¹ H NMR Spectrum of 17	87

24. ^{13}C NMR Spectrum of 17	88
25. ^1H NMR Spectrum of 18	89
26. ^{13}C NMR Spectrum of 18	90
27. FT-IR of 7	91
28. FT-IR of 8	92
29. FT-IR of 9	93
30. FT-IR of 10	94
31. FT-IR of 15	95
32. FT-IR of 16	96
33. FT-IR of 17	97
34. FT-IR of 18	98
35. Adsorption/Desorption Isotherm of 19	99
36. Pore Size Distribution of 19	100
37. Adsorption/Desorption Isotherm of 20	101
38. Pore Size Distribution of 20	102
39. Adsorption/Desorption Isotherm of 21	103
40. Pore Size Distribution of 21	104
41. Adsorption/Desorption Isotherm of 22	105
42. Pore Size Distribution of 22	106
43. Adsorption/Desorption Isotherm of 23	107
44. Pore Size Distribution of 23	108
45. Adsorption/Desorption Isotherm of 24	109
46. Pore Size Distribution of 24	110
47. Adsorption/Desorption Isotherm of 25	111
48. Pore Size Distribution of 25	112
49. Adsorption/Desorption Isotherm of 26	113
50. Pore Size Distribution of 26	114

51. Adsorption/Desorption Isotherm of 27	115
52. Pore Size Distribution of 27	116
53. Adsorption/Desorption Isotherm of 28	117
54. Pore Size Distribution of 28	118
55. Calibration Curve of Pt Standards for AAS.....	119

LIST OF SCHEMES

Scheme	Page
1. Hydrogenation of <i>E</i> and <i>Z</i> -alkene by a <i>bis</i> -indenyl metallocene catalyst.....	19
2. Hydrogenation of an acyclic imine by titanocene.....	21
3. Hydrogenation of a ketone by a titanocene catalyst	22
4. Generalized insertion of alkenes by the Cossee-Arman mechanism	25
5. Preparation of the ethano bridged <i>bis</i> -indenyl ligand	27
6. Preparation of tetrahydroindenyl lithium (6)	28
7. Preparation of silyl-bridged <i>bis</i> -indenyl ligand	28
8. Preparation of the binaphthalenyl bridged <i>bis</i> -indenyl ligand.....	30
9. Generalized rearrangement and deactivation of a metallocene catalyst	31
10. Synthesis of an EBI ligand containing a functional tether.....	33
11. A general reaction for the formation of functionalized tethered-EBI ligands	34
12. The immobilization and side reaction of a tethered metallocene	35
13. A complete reaction scheme of the synthesis of <i>bis</i> -indenyl ligands	39
14. Reaction scheme of the immobilization of ligands by hydrosilylation.....	43
15. Reaction scheme of the immobilization of ligands by thiol-ene coupling.....	43

CHAPTER 1

INTRODUCTION

Importance of Metallocene Catalysts

Metallocene catalysts are often used in synthesis due to their ability to induce a high level of enantioselectivity. Many reasons exist to use metallocene catalysts, whether it be controlling the isomers that are produced or producing structured polymers [1, 2, 34, 41]. Enantioselectivity in organic synthesis is often very important. The importance of enantioselectivity can be most observed in the pharmaceutical and fine chemical industries. The Food and Drug Administration (FDA) mandates a high level of purity for drugs [1, 2]. Many enantiomers or diastereomers of drugs are biologically inactive or even toxic [3].

For example, Indinavir is a drug, produced by Merck that is used to aid and treat Human Immunodeficiency Virus (HIV) [4]. Thirty-two stereoisomers exist, yet only one isomer of this compound ((2*S*)-1-[(2*S*,4*R*)-4-benzyl-2-hydroxy-4-[[[(1*S*,2*R*)-2-hydroxy-2,3-dihydro-1*H*-inden-1-yl]carbamoyl]butyl]-*N*-*tert*-butyl-4-(pyridin-3-ylmethyl)piperazine-2-carboxamide) is effective in treating HIV; Indinavir contains five chiral centers [1, 4]. Therefore, catalysts selective enough to produce one of two possible isomers are of high interest or worth for each step in the multistep synthesis of drugs. If the reactions are not enantioselective, the yield of the desired isomer is very low. However, if the reactions are enantioselective, the yield of the desired isomer is much higher. Also, when the reaction is enantioselective, separation of isomers is not necessary. The structure of Indinavir is presented in Figure 1 [1].

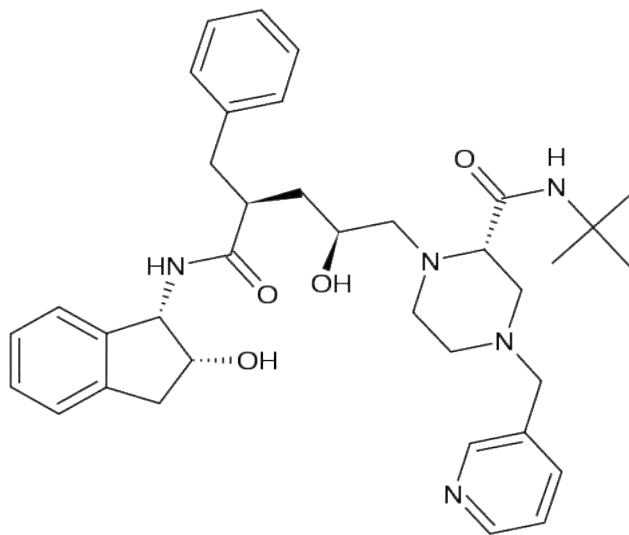


Figure 1. Structure of Indinavir, which contains 5 chiral centers [1].

Most notable of isomeric drugs is thalidomide, gaining its popularity in the late 1950s to the early 1960s. Thalidomide is a racemic mixture correctly titled (*RS*)-2-(2,6-dioxopiperidin-3-yl)-1*H*-isoindole-1,3(2*H*)-dione [5]. One isomer, the *R* enantiomer, is effective in treating multiple myeloma, leprosy, and morning sickness during pregnancy [5]. The other isomer, the *S* enantiomer, is teratogenic, causing mycophelia, or birth defects such as deformed or misplaced appendages [5].

A picture displaying some of the possible birth defects may be observed in Figure 2. The structures of both isomers of thalidomide are shown in Figure 3. Most reactions in organic synthesis, including enantioselective reactions, require the use of a catalyst. Therefore, the use of an enantioselective catalyst increases the yield of the desired isomer.

Metallocene catalysts are highly asymmetrical and, therefore, minimize the number of possible isomeric catalyst-substrate complexes that could form due to steric hindrance from ligands of the catalyst [2]. Based on the orientation of the ligands in the metallocene catalyst, different isomers will be produced. Reducing the number of isomeric complexes induces a high degree of enantiocontrol and, thus, enantioselectivity [2]. In addition to this, enantioselectivity

can be furthermore increased by the addition of steric bulk to the metallocene catalysts, which reduces possible flexibility of the metallocene [2]. The increase in steric bulk can be accomplished by addition of substituents and/or bridges [2]. Metallocene catalysts possess the ability to produce single isomers of compounds, preventing life-altering effects to humans, such as that observed from thalidomide.



Figure 2. A picture displaying children with mycophelia [5].

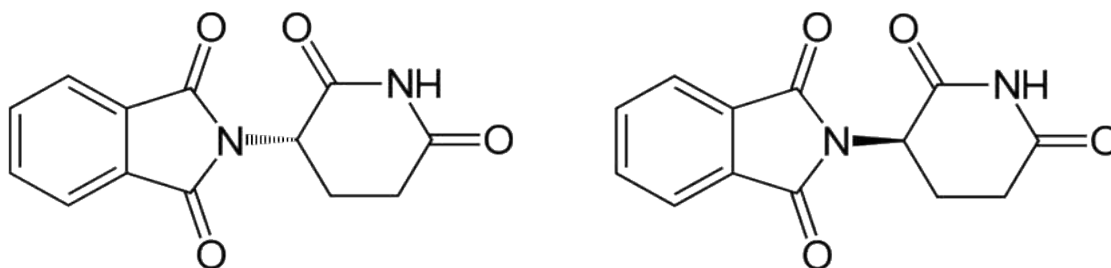


Figure 3. *S*-Enantiomer (left) and *R*-Enantiomer (right) of Thalidomide [5].

Metallocene catalysts also prove useful in the catalysis of polymerization reactions. Use of metallocene catalysts produce syndiotactic or isotactic polymers as compared to atactic polymers produced from typical free-radical reactions [6]. The order of a polymer greatly affects its worth and properties, such as rigidity, melting point, flexibility, crystallinity, etc [6]. This is yet another example and reason for the use of metallocene catalysts in reactions where enantiocontrol and enantioselectivity are of high importance.

Metallocene Catalysts of Hydrogenations

Carbon-Carbon Double Bonds (C=C)

Titanocene and zirconocene complexes are optically active themselves and are in high demand due to their ability to execute asymmetric homogeneous catalysis in various types of reactions [7, 8]. The wide range of uses for metallocene catalysts stems from considerable structural features: (a) metallocenes whose chirality is determined by only one ligand; (b) symmetrical dimers that possess chiral ligands constructed of cyclopentadienes; (c) metallocenes that contain two chiral cyclopentadienes of differing type [9]. High levels of enantioselectivity are observed for titanocenes because chirality is induced when the two carbon atoms directly linked to the cyclopentadiene are substituted with alkyl groups [9]. However, some substituents of the metallocene, increasing in size, sterically hinder the binding site and, therefore, greatly limit the facial discrimination of the metallocene as the double bonded-carbon approaches; this can be an alkene, imine, or ketone [9].

One such way to acquire optically pure compounds is by using the asymmetric hydrogenation of alkenes [10-12]. Alkenes with a high degree of substitution are of high interest. However, a great degree of substitution lowers the reactivity of alkenes; steric hindrance of the substituted alkene restricts their ability to bind to organometallic complexes [10]. For

trisubstituted alkenes, hydrogenations that yielded an enantiomeric excess (ee) of 83-99% have been performed by using (S,S)-(ETBHI)TiH (ETBHI = ethylene-*bis*-tetrahydroindenyl) as a catalyst [10, 13]. Some of the hydrogenations of this type took several days to reach completion due to steric hindrance; tetrasubstituted alkenes are expected to react much more slowly [10].

Another idea for metallocene catalyzed hydrogenations is the use of cationic titanocene and zirconocene complexes for sterically hindered alkenes such as tri- and tetrasubstituted alkenes [10]. The basis for this idea is that highly electrophilic cationic metallocenes would be quite effective at binding highly substituted alkenes such as tri- and tetrasubstituted alkenes [10].

Metallocenes must be converted to the catalytically active cationic hydride complex in a hydrogen atmosphere [10, 14]. Troutman *et al.* created cationic metallocene hydride complexes first by using (EBTHI)ZrMe₂ in the presence of either methylaluminoxane or [PhMe₂NH]⁺[Co(C₂B₉H₁₁)₂]⁻ for the asymmetric hydrogenation of 1,1-disubstituted alkenes, but the ee's of the products were low, not exceeding 36% [10, 15, 16]. Second, Troutman *et al.* noticed that when generating a metallocene hydride complex using (EBTHI)ZrMe₂ in the presence of [PhMe₂NH]⁺[B(C₆F₅)₄]⁻, one is able to hydrogenate tetrasubstituted alkenes with very high enantioselectivity [10].

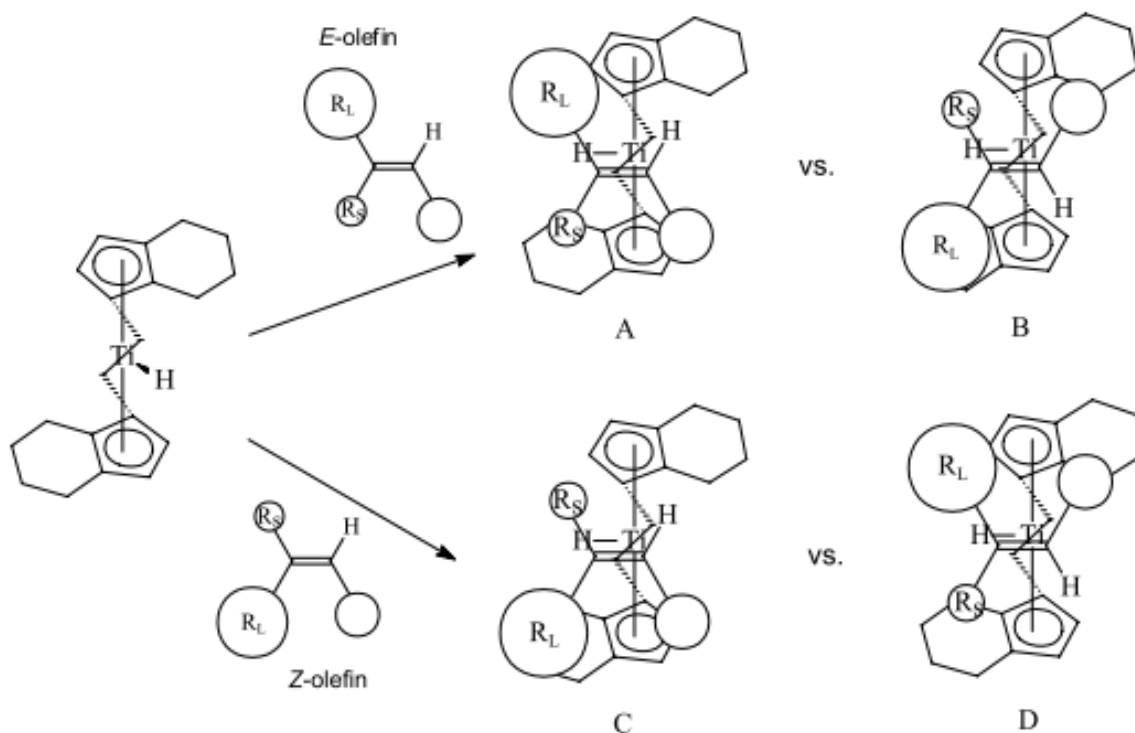
The ability of titanocenes and zirconocenes to catalyze hydrogenations is not equal. The catalytic activity of chiral zirconocenes is substantially lower than that of the chiral titanocenes [9]. Hydrogenations on titanocenes are typically able to proceed at lower temperatures (~-20°C), shorter reaction times (~48 h), and lower hydrogen pressures (~20 psi) [9]. For titanocenes, the level of selectivity typically increased with decreases in temperature [9]. At conditions similar to this, zirconocenes are typically unreactive [9]. For hydrogenations using zirconocenes, the reaction conditions require higher temperatures (~+20°C), much longer reaction times (~4-32

days), and higher hydrogen pressures (~40 psi) [9]. Nevertheless, enantioselectivity must still be considered in lieu of the lower catalytic activity of zirconocenes. Chiral titanocene catalysts also deliver a wider range of utility than that of zirconocenes in enantioselective hydrogenations [17].

The mechanisms of such hydrogenations are presumed to be similar, if not alike, to the mechanism for the hydrogenation of trisubstituted alkenes [10, 13]. The mechanism begins with the carbon-carbon double bond inserting itself into the titanocene hydride complex to form intermediates **A-D** (Scheme 1) [13, 18], differing in amounts produced, which undergoes hydrogenolysis [10, 13, 14]. From this mechanism, it is easily deduced that products stemming from the hydrogenation of cyclic substrates have *cis* configuration [10]. This is an important aspect because enantioselectivity is of high interest in metallocene catalysts. Many factors affect the approach of the alkene to the metallocene. The first factor that affects the approach of the alkene is non-bonded interactions [9]. As the alkene approaches the metallocene, and the complexation continues, a second interaction takes place in which the wedge between the ligands must be at its widest point for the alkene to incorporate correctly [9]. However, the degree of tilting becomes so sizeable that the mutual compression of the ligands must be considered and may not be extreme [9]. Due to overlap between the alkene being inserted and the *bis*-indenyl metallocene, only one isomer is preferred; **A** and **D** are low in energy and are preferred, **B** and **C** are not energetically favorable. [13, 18]. Another point that must be noted is the use of a bridge between the metallocenes, connecting them, that does not allow them to continue to rotate, therefore inducing enantioselectivity. Without a bridge, ligands of the metallocenes are free to rotate in any direction. A schematic of the selectivity of a *bis*-indenyl metallocene is displayed in Scheme 1.

Carbon-Nitrogen Double Bonds (C=N)

Enantiomerically pure compounds containing nitrogen are highly important in pharmaceutical and agrochemical industries, therefore, drawing much attention to the asymmetric hydrogenations of imines to enantiomerically rich amines [21]. High enantioselectivity is yielded under a wide range of conditions when performing asymmetric hydrogenations of cyclic ketimines with chiral titanocene catalysts [21]. Interestingly enough, no coordination group is required to yield high levels of enantioselectivity because the titanocene catalyst only discriminates based on the shape of the substrate of question [21].



Scheme 1. Hydrogenation of *E* and *Z*-alkene by a *bis*-indenyl metallocene catalyst [13, 18].

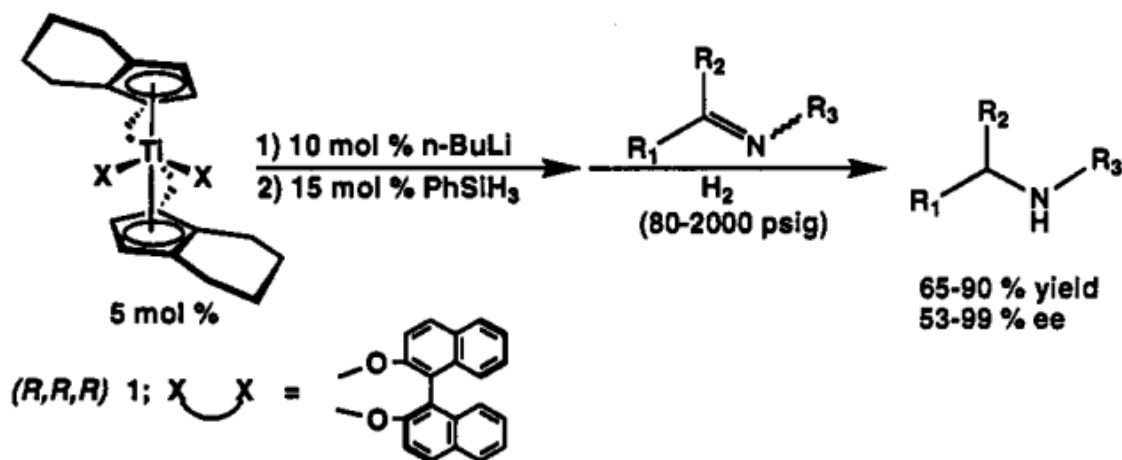
The imines of discussion here are acyclic imines and cyclic imines. Analogous to the reduction of ketones to alcohols, the synthesis of enantiopure amines from imines has a lower yield than expected [22-29]. Asymmetric hydrogenation of acyclic imines presents an attractive method for acquiring enantiomerically enriched amines; the ratio of *anti*:*syn* ranges from 3.3:1 to

44:1 [21]. Cyclic imines tend to only have moderately successful yields, while even lower yields are observed with the later transition metal containing metallocene catalysts [20, 24, 27, 30]. The type of metallocene that works best for the hydrogenations of imines is typically a titanium metallocene catalyst [31-34].

Initially, Willoughby and Buchwald were interested in the development of an asymmetric catalyst for hydrosilylation of imines and ketones, but it was soon discovered that hydrogen was a more effective and attractive choice for the stoichiometric reduction of imines [35]. It was even found that asymmetric hydrogenation of cyclic imines, ketimines specifically, when using a chiral titanocene catalyst, yielded amines with spectacular enantioselectivity under a wide range of conditions; low temperature and high pressure, or high temperature and low pressure [20, 21]. The first method of asymmetric hydrogenation of acyclic imines involved lithiating of the titanocene, followed by treatment by phenylsilane for the purpose of forming the titanium (III) hydride catalyst for hydrogenation [34]. This investigation by Brintzinger was novel, being that it was the first example of reducing imines with a metallocene catalyst of this type [20]. One downside of hydrogenating acyclic imines is the mixture of products that are yielded [36]. One receives a mixture of *anti* and *syn* isomers [36]. It has been shown that the *anti*-isomer is produced in excess to the *syn* isomer in a ratio range of 3.3:1 to 44:1 [36]. Another downside is that hydrogenating acyclic imines requires high hydrogen pressures to achieve desired ee's [36]. A schematic of the reaction can be observed in Scheme 2.

Cyclic imines are important because they make up a large percentage of naturally occurring and medicinal compounds [20]. The most effective metallocene catalyst for the hydrogenation of cyclic imines appears to be titanocene complexes [20]. Many of the late transition metal catalysts have had low yields [20]. Though the yields for catalytic and stoichiometric asymmetric

hydrogenations of cyclic imines are only moderately successful, the enantiopurity of the cyclic amine product is much higher [20, 21].



Scheme 2. Hydrogenation of an acyclic imine by titanocene [36].

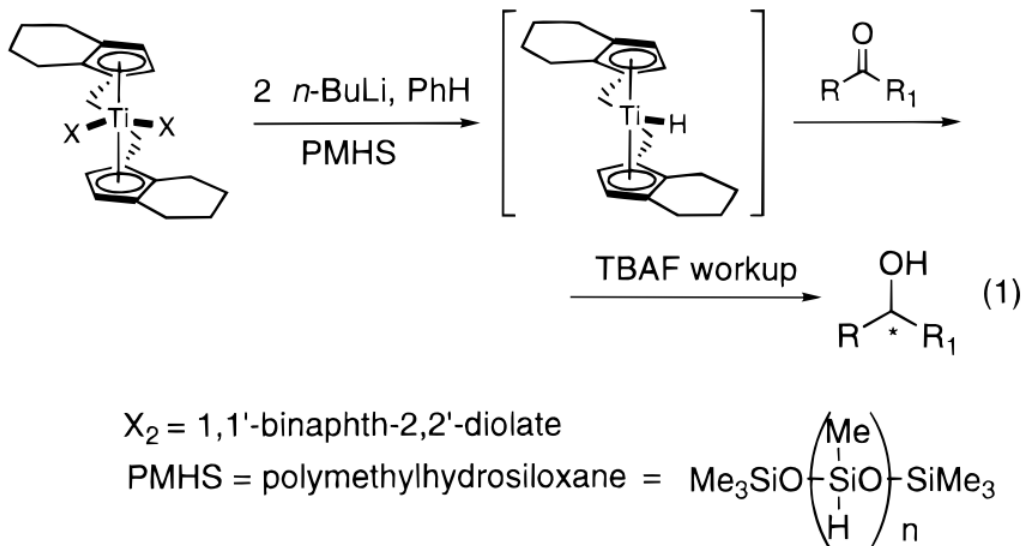
Another advantage of hydrogenating cyclic imines by the use of a titanocene catalyst is that the hydrogenation can be carried out under much lower hydrogen pressures compared to the hydrogenation of acyclic imines [20, 21]. One can hydrogenate cyclic imines to cyclic amines with spectacular levels of ee when using low pressure with high temperature or when using medium pressure with low temperature [20, 21]. When using a titanocene catalyst, the hydrogenation of cyclic imines to amines yields ee's of 95-99% [20].

Carbon-Oxygen Double Bonds (C=O)

A method of hydrogenating imines by hydrosilylation was proposed by Yun and Buchwald, which has been investigated and shown to hydrogenate ketones with high enantiopurity while exhibiting the degree of enantioselectivity of titanocene catalysts [37-39]. First, a simple hydrogenation of ketones was explored using chiral titanocene catalysts, which yielded corresponding alcohols in high enantiomeric purity [40]. A schematic of the reaction may be observed in Scheme 3.

Metallocene Catalysts of Polymerizations

The properties of polymers are highly related to their molecular structure, which is dependent upon the catalyst used and the conditions under which it is formed [6]. The geometry of the metallocene catalysts plays a key role in formation of polymers [6]. For example, traditional metallocene catalysts for the formation of polypropylene from propylene yields low melting, atactic polymers [6]. However, if metallocene catalysts that possess a specific geometry are used, the formation of stereo regular isotactic and syndiotactic polypropylene is highly possible [6].



Scheme 3. Hydrogenation of a ketone by a titanocene catalyst [40].

To achieve such geometry, Britzinger bridged two indenyl ligands, forming *ansa*-metallocenes [34]. When using a C_2 -symmetric *rac*-(ethylene-*bis*-indenyl) titanium complex, isotactic polypropylene is obtained, but not nearly as high isotacticity as with zirconium analogues [34, 41]. However, when performing the polymerization while using the zirconium analogues, it must be noted that it must be performed at low temperatures; isotacticity of the polymer drops with high temperatures [42]. It was then observed that the substitution of large

substituents at the 4 position of the indenyl molecule raised the isotacticity to well over 95% [43]. High isotacticity of the polypropylene is also possible at high temperatures due to the increased selectivity of the metallocene resulting from the introduction of larger substituents to the indenyl molecule [43]. An example displaying tacticity can be observed in Figure 4.

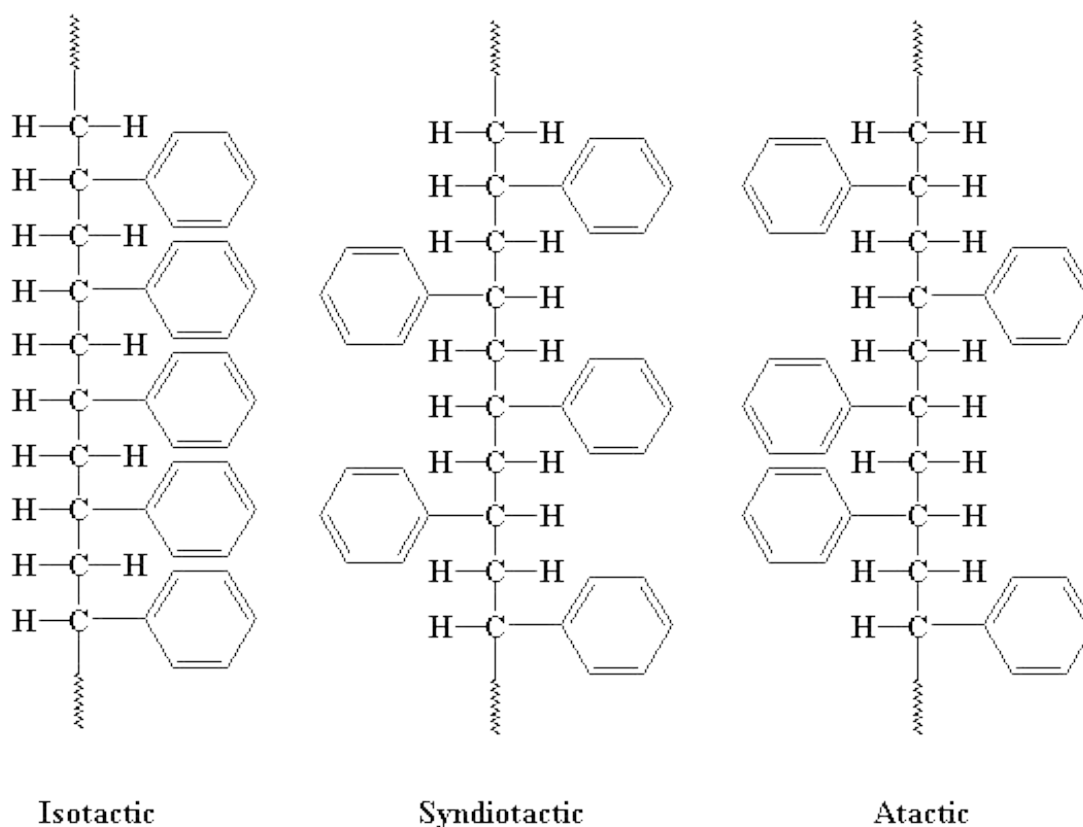


Figure 4. An example displaying the tacticity of a polymer [34, 41].

If syndiotactic polypropylene is of interest, it is possible to attain such by using C_s -symmetric fluorenyl linked cyclopentadienyl zirconium metallocene catalysts [44-46]. Properties of the produced polymer are influenced highly by the substituents at the β -position of the cyclopentadienyl ring; smaller substituents, such as methyl groups, produced hemi-isotactic polymers while larger substituents, such as *t*-butyl groups, produced isotactic polymers [47]. A

schematic of the tacticity of polypropylene vs. the symmetry of the metallocene catalyst is displayed in Figure 5.

Cationic metallocenes, type $[\text{Cp}_2\text{-Mme}]^+$ ($\text{M} = \text{Ti}, \text{Zr}$) [10, 48, 49], have been of high interest in Ziegler-Natta-type polymerizations [10, 50-53]. When using homogeneous metallocene catalysts for polymerization, it must be noted that ancillary ligands are not only used to stabilize the metal center, but they also help to tune the electronic properties and steric hindrance around the metal center [6].

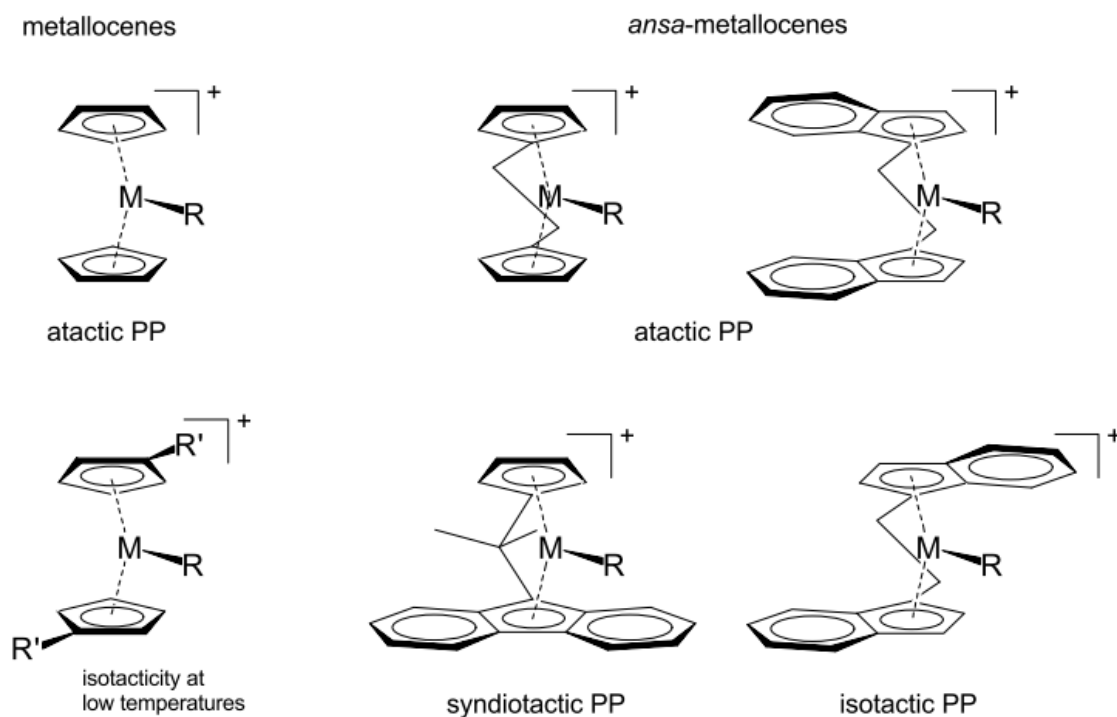
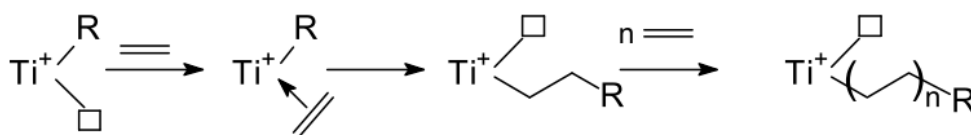
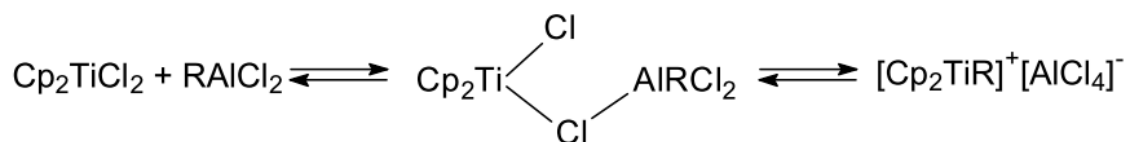


Figure 5. Polypropylene tacticity vs. metallocene catalyst symmetry [6, 34].

Therefore, the choice of the ligand is one of the most important factors in stability, activity, and selectivity of the metallocene catalyst [6]. Kinetic studies have been performed on Ziegler-Natta type catalytic systems such as homogeneous metallocenes, $\text{Cp}_2\text{TiRCl}/\text{AlR}'\text{Cl}_2$ [44-46, 54-56]. The study suggested that two equilibria lead to the species having such active catalytic abilities [44-46, 54-56]. A scheme of the two equilibria is displayed in Scheme 4. For this mechanism to

be successful, the formation of a vacant coordination site on a cationic group 4 metal center is necessary [57-59]. Polymerization is believed to involve the coordination of an alkene to one of the vacant coordination sites of the activated Ti-R (Ti is used as an example group 4 metal) catalytic species and, subsequently, the insertion into the Ti-R bond, which is referred to as the Cossee-Arlman mechanism [60, 61]. Some of the most known active homogeneous catalysts for the polymerization of ethene, cationic group 4 metallocene complexes, are observed to be *iso*-electronic when found with neutral group 3 and lanthanide complexes [62-68].



Scheme 4. Generalized insertion of alkenes by the Cossee-Arlman mechanism [6].

Other Applications of Chiral Metallocenes

Group 4 (*ansa*-)metallocenes are highly effective catalytic agents in more than just the polymerization of alkenes [6]. They are also used as reagents by catalyzing C-C bond formations such as allylation of aldehydes and coupling of alkynes to ketones [69-71], functionalization of pyridines [72], cyclopolymerization of dienes [73, 74], Diels-Alder reactions [75, 76], and carbomagnesation reactions [77, 78]; C-H bond formations such as hydrogenation of enamines [11, 79], hydrosilylation of alkenes [80], and hydrosilylation of imines [81]; C-N bond

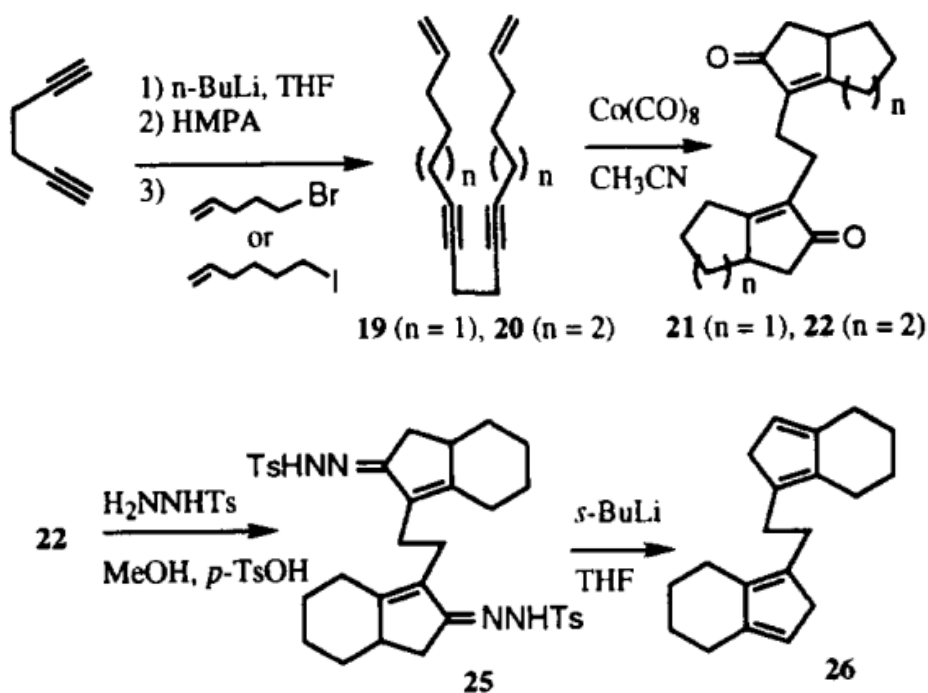
formations such as hydroamination of alkynes [82]; C-O bond formations such as epoxidation of alkenes [83].

Structure and Synthesis of Non-Tethered Bridged Bis-Indenyl Ligands

Bridged *bis*-indenyl ligands have been an area of interest in catalysis for many years. The idea that these bridged *bis*-indenyl ligands can be metalated to form metallocenes for use in catalyzing hydrogenation and polymerization reactions has sparked a large amount of research into the synthesis and characterization of these metalated complexes. Therefore, there has been much investigation into the most appropriate methodology for synthesis of bridged *bis*-indenyl ligands. The question of interest is what type of bridge works best? Should the bridge be comprised of carbon only, or should the bridge contain other atoms? The structures and syntheses of different bridged *bis*-indenyl ligands are now discussed.

The first bridge is a simple hydrocarbon bridge between each indene. In the following reaction, the Pauson-Khand cyclization reaction is used with 1,5-hexadiynes [84]. The Pauson-Khand reaction is simply a means by which cyclopentenones can be synthesized from diynes [84]. This synthesis of discussion involves a Pauson-Khand cyclization of diynes to form *bis*-indenones, which are aminated and then protonated to form *bis*-indenyl ligands [84]. 1,17-octadeca-7,11-diyne (**20**) was synthesized by first introducing 1,5-hexadiyne, in an inert environment, to *n*-BuLi to give a 1,5-hexadiynyl lithium salt, which was then introduced to 6-iodo-1-hexene [84]. Cyclization of the 1,17-octadeca-7,11-diyne, to give cyclopentenones, was performed when a solution of 1,17-octadeca-7,11-diyne and acetonitrile was introduced to dicobalt octacarbonyl in an inert environment, yielded 1,2-ethylene-*bis*(9-bicyclo[4.3.0]-non-1(9)-en-8-one) (**22**) [84]. The *bis*-cyclopentenonyl compound was then converted to sulfonylhydrazonyl compound by adding CH₃OH to a mixture of *p*-toluenesulfonylhydrazide, *p*-

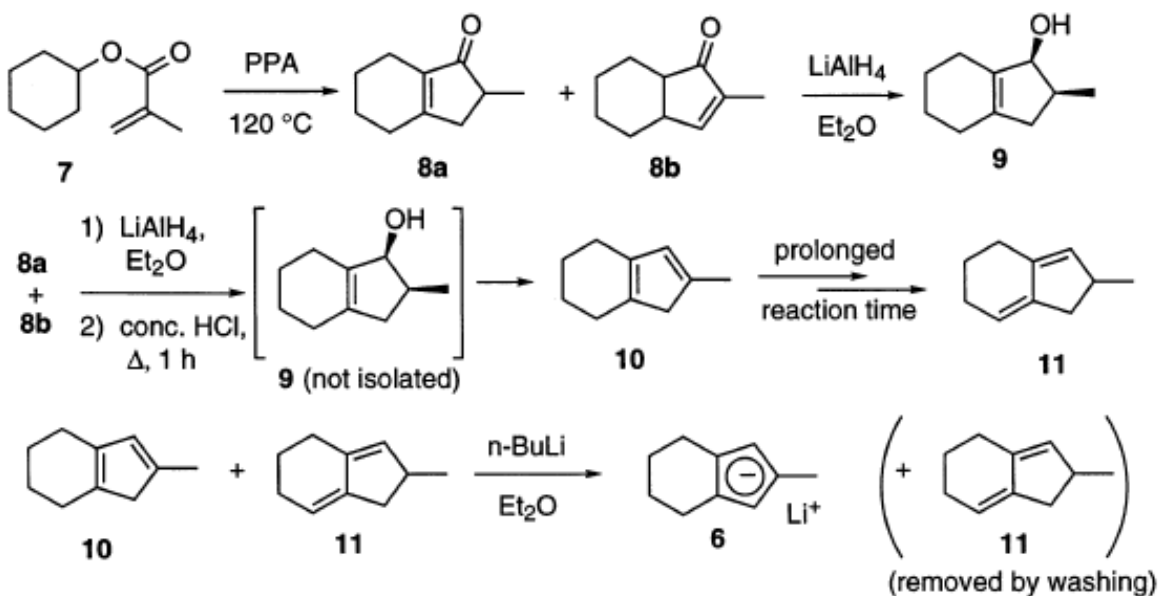
toluenesulfonic acid, and 1,2-ethylene-*bis*(9-bicyclo[4.3.0]-non-1(9)-en-8-one) in an inert environment to yield 1,2-ethylene-*bis*(9-bicyclo[4.3.0]-non-1(9)-en-8-one-4-methylbenzene sulfonylhydrazone (**25**) [84]. Lastly, 1,2-ethylene-*bis*(9-bicyclo[4.3.0]-non-1(9)-en-8-one-4-methylbenzene sulfonylhydrazone was reacted with *s*-BuLi in the presence of THF to remove the sulfonylhydrazone and lead to the formation of the ethano-bridged *bis*(cyclopentadiene), 1,2-ethylene-*bis*(9-bicyclo[4.3.0]-nona-1(6),6-diene (**26**) [84]. A schematic of the reaction can be observed in Scheme 5.



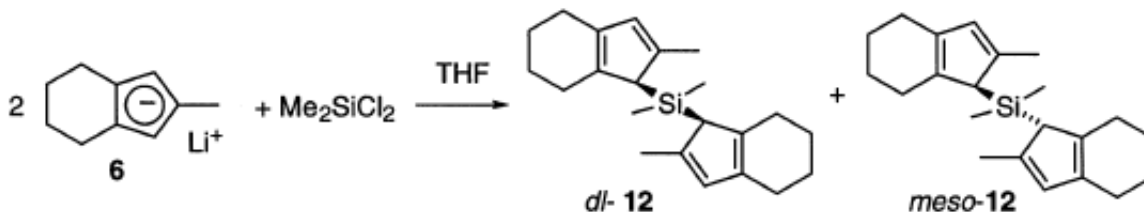
Scheme 5. Preparation of the ethano bridged *bis*-indenyl ligand [84].

Bridges of *bis*-indenyl ligands can be comprised of atoms other than carbon. One such example was synthesized by Halterman *et al.* [85]. It has been reported that dimethylsilyl bridged *bis*(2-methyltetrahydroindene) was successfully synthesized and then metalated to yield *ansa*-zirconocene and titanocene dichlorides and yttrium and lutetium chlorides [85]. This was accomplished by first isolating an isomeric mixture of 2-methyltetrahydroindenones (**8a,b**) from

the rearrangement and PPA-promoted Nazarov cyclization of cyclohexylmethacrylate (**7**) at a high temperature of 120°C [85]. The isomeric mixture of 2-methyltetrahydroindenones was reduced to yield 1H-2-methyl-2,3,4,5,6,7-hexahydroindan-1-ol (**9**) when treated with excess LiAlH₄ [85]. Once the alcohol was formed, it was immediately acidified by the addition of concentrated HCl and heated to yield 2-methyltetrahydroindene (**10** and **11**), which, if the reaction time was prolonged or the indenyl product was stored, rearranged to form the more stable isomer [85]. This was acceptable, however, because treatment of the isomers with *n*-BuLi in hexane yielded the reactive 2-methyl-4,5,6,7-tetrahydroindenyllithium (**6**) [85].



Scheme 6. Preparation of tetrahydroindenyl lithium (**6**) [85].

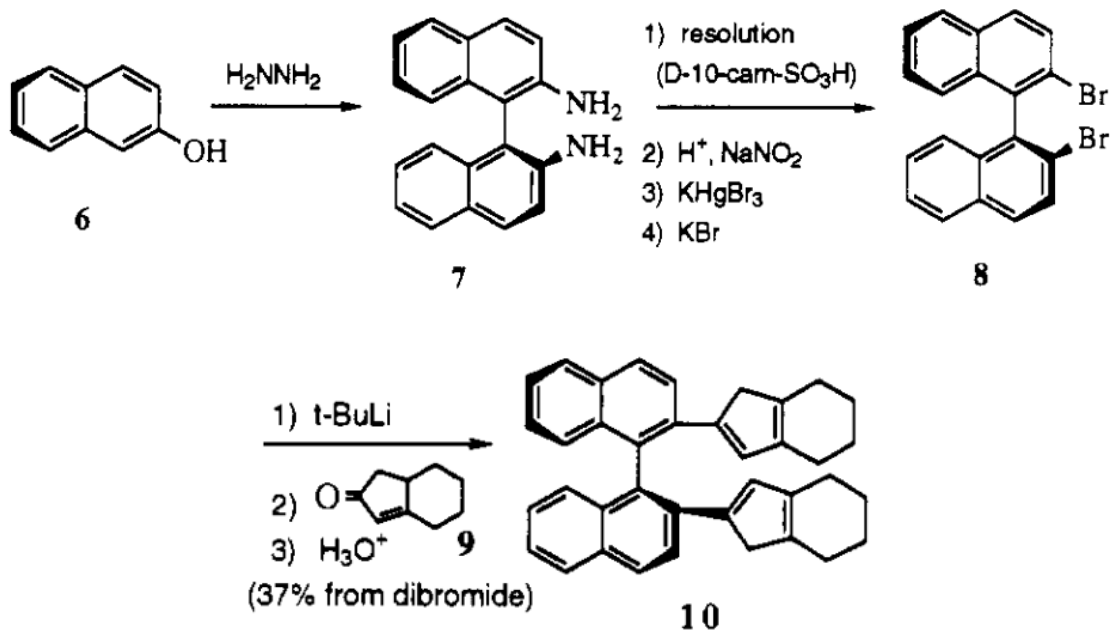


Scheme 7. Preparation of silyl-bridged *bis*-indenyl ligand [85].

Treatment of the indenyllithium compound with dichlorodimethylsilane yielded the desired silyl-bridged *bis*(tetrahydroindene) in a stereoisomeric mixture [85]. Schematics of the reactions can be observed in Scheme 6 and 7.

For carbon containing bridges, one must not limit bridges only to chains; the bridges can contain many functional groups as well. Halterman *et al.* reported an example of this. It was reported that 2-naphthol (**6**) could be inexpensively coupled, yielding 1,1'-binaphthalene-2,2'-diamine (**7**), when in the presence of hydrazine, and that it can be easily resolved in a favorable amount during the recrystallization of the diastereomeric salts of D-10-camphorsulfonic acid (D-10-cam-SO₃H) to yield 1,1'-binaphthalene-2,2'-dibromide (**8**) [17]. To increase its reactivity, 1,1'-binaphthalene-2,2'-dibromide was lithiated by treatment of *t*-BuLi to yield 1,1'-binaphthalene-2,2'-dilithium, which, when reacted in the presence of 1,4,5,6,7,7a-hexahydro-2H-inden-2-one (**9**), yielded 1,1'-binaphthalene-2,2'-*bis*(4,5,6,7-tetrahydro-1H-2-indenyl)-2,2'-diol [17]. The diol was then protonated to form 2,2'-*bis*(4,5,6,7-tetrahydro-1H-2-indenyl)-1,1'-binaphthalene (**10**) [17]. A schematic of the reaction can be observed in Scheme 8.

Bridges of *bis*-indenyl ligands can contain any amount of atoms, whether it is silicon, carbon, or any other atom. The three examples discussed contained one, two, and four atoms [17, 84, 85]. Also, there are various means of synthesizing the bridged *bis*-indenyl ligands; more than are discussed in this section. One such synthesis is the utilization of the Nazarov cyclization of a cyclic ester, followed by reduction of the hydroxyl group to an indenyl product, which is then bridged by a silicon containing compound [85].



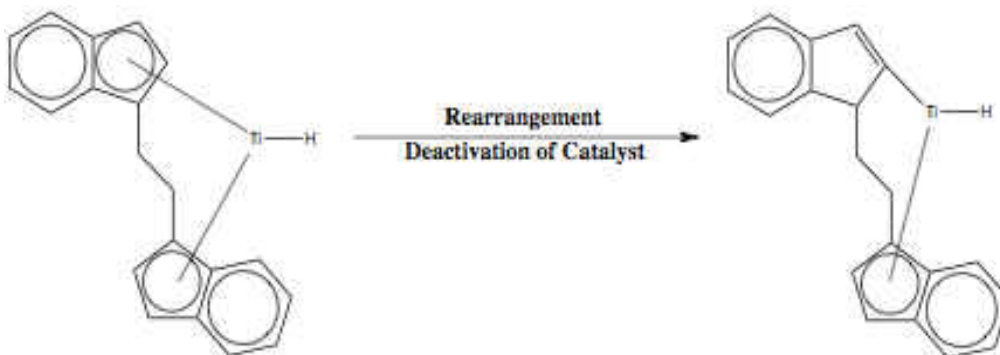
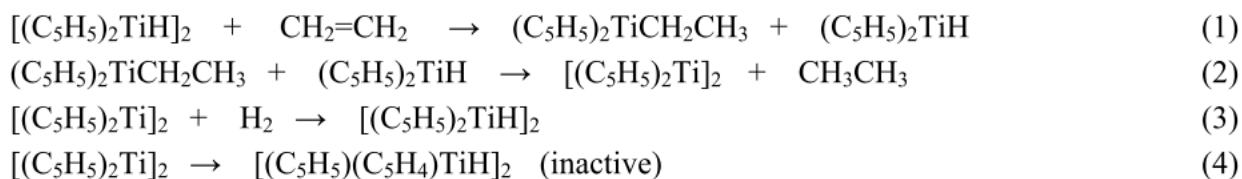
Scheme 8. Preparation of the binaphthalenyl bridged *bis*-indenyl ligand [17].

Another method of producing a bridged *bis*-indenyl ligand is by the amination of an enol, forming a diamine, which is brominated, reacted with a cyclopentenone, and followed by reduction to form a bridged *bis*-indenyl diol, which is dehydrated to form a bridged *bis*-indenyl ligand [17]. Though the synthesis may have minor differences, each yields the same general structure; two indene molecules, bound by a bridge containing one or more atoms.

Heterogeneous vs. Homogeneous Catalysts

Homogeneous metallocene catalysts, discussed above, are very active and prosperous in hydrogenation and polymerization reactions of alkenes, carbonyls, and imines [6]. However, homogeneous catalysts have a few downfalls. Removal of the catalyst from the reaction mixture is difficult and results in high costs of the final product [86-93]. In addition to increased costs, due to removal, the catalyst cannot be recycled and reused [86-93]. This is highly unattractive to industry due to the cost of purchasing and using new catalyst for each hydrogenation or polymerization. As a result of the homogeneous catalyst freely moving about in solution, and as

a result of the polymerization reaction taking place, many side products are formed such as alcohols, HCl, etc. [94, 95, 102]. Homogeneous catalysts, despite their high catalytic activity, decompose during the catalyzing of reactions [86-93]. In addition, dimerization of the homogeneous catalyst is very likely, resulting in deactivation of the catalyst; hydrogenation or polymerization reactions cease [86-93]. Chemical equations demonstrating the rearrangement and deactivation of a metallocene catalyst may be observed below. Also, a schematic of the rearrangement and deactivation of a metallocene catalyst is displayed in Scheme 9 [18, 31].



Scheme 9. Generalized rearrangement and deactivation of a metallocene catalyst.

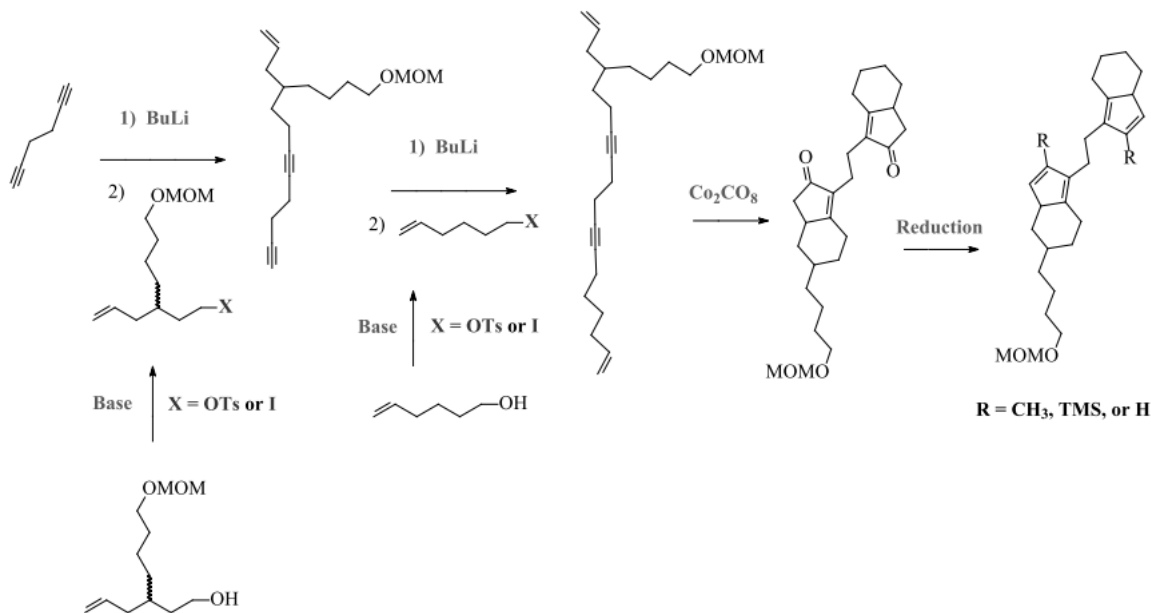
However, homogeneous catalysts do have some positive characteristics. Homogeneous catalysts are easily improved and tailored to the reaction of interest in addition to possessing a higher catalytic activity than heterogeneous catalysts [86-94].

Heterogeneous catalysts are of high interest today. By grafting a homogeneous metallocene catalyst onto a solid support, one resolves the problem of decomposition, dimerization/deactivation, and more importantly one is able to recover and recycle/reuse the

catalyst for further reactions [86-95, 98-104]. It is true that once immobilized, heterogeneous metallocene catalysts do lose a small amount of catalytic activity [86-94], however, due to being able to easily remove the catalyst from the reaction mixture (filtration), and being able to recycle/reuse the catalyst, one is able to generate cleaner, more pure compounds in an economical range [1]. Over 80% of the total cost of pharmaceuticals is attributed to the removal of the catalyst from the reaction mixture [1]. Another positive aspect of heterogeneous catalysts is that the Federal Drug Administration (FDA) mandates that the catalyst be removed from the reaction mixture down to a very low level [1]. Therefore, due to the positive aspects of heterogeneous catalysts outweighing those of homogeneous catalysts, it is apparent that heterogeneous catalysts are far more environmentally and economically desirable than homogeneous catalysts.

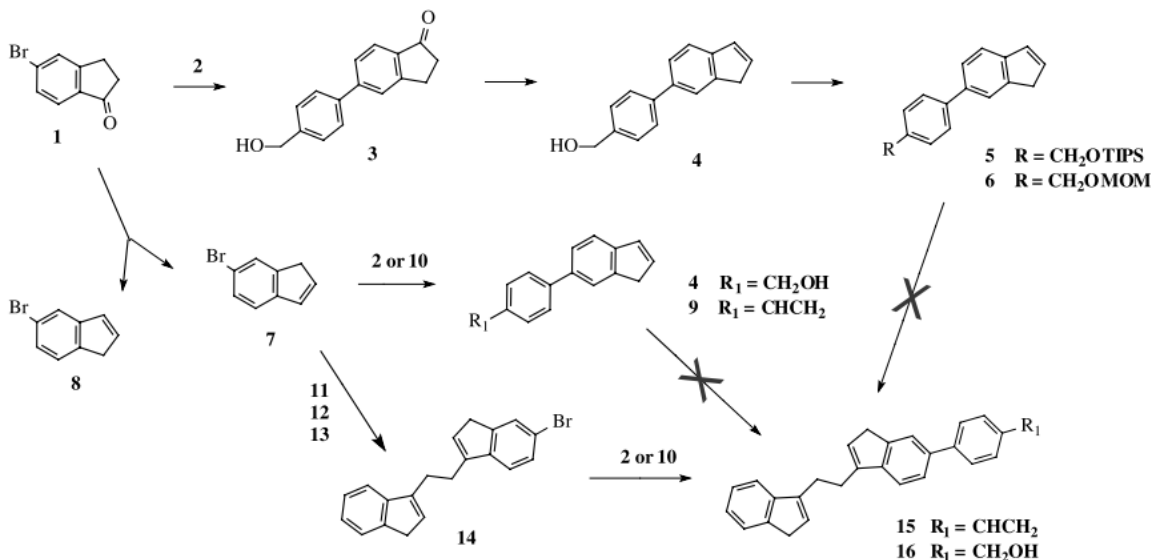
Synthesis of Tethered Bridged Bis-Indenyl Ligands

Panarello et al. investigated how to attach a functionalized tether to an ethylene-*bis*(tetrahydroindenyl) ligand (EBTHI) [105]. Their first problem was attaching a functionalized tether to either the EBTHI or EBI ligand due to no reactive functional groups being attached to the ligand [105]. Therefore, Panarello *et al.* investigated the double alkylation of a 1,5-hexadiyne, then a Pauson-Khand cyclization to form an ethylene-*bis*(hydroindeneone), followed by a Shapiro elimination reaction [84, 105]. However, this method was not found to be efficient. Due to very low stability of the ligand and extremely low yield >10%, the synthesis was deemed unsuccessful [105]. It must also be noted that the R-group attached to the tetrahydroindenyl ring did not affect the synthesis of the ligand [105]. A general reaction involving the double alkylation, Pauson-Khand cyclization, and Shapiro elimination can be observed in Scheme 10.



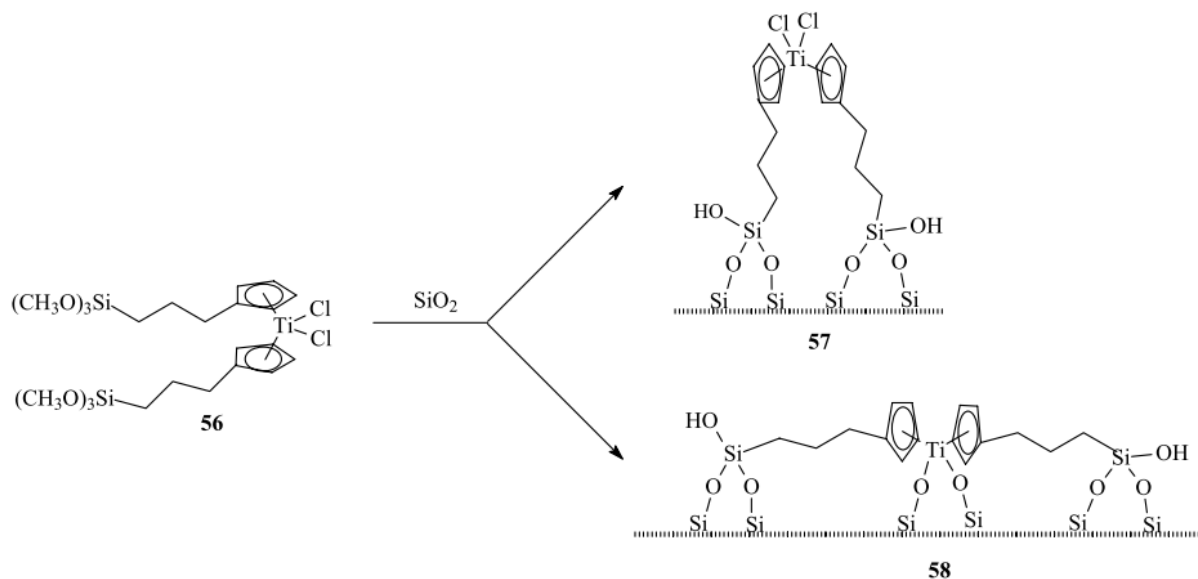
Scheme 10. Synthesis of an EBI ligand containing a functional tether [105].

Panarello *et al.* next expanded their above mentioned concept to ethylene-*bis*(indenyl) ligands (EBI) [105, 106]. In their investigation, EBI ligands were coupled to different aryl borates [106]. Panarello *et al.* began by reducing 5-bromo-indanone (**1**) to yield both 6-bromoindene (**7**) and its isomer 5-bromoindene (**8**) [106]. Direct coupling with the aryl borates yielded a compound that was not further reactive in forming the tethered-EBI ligand [106]. However, when reacted with functionalized indenenes, 2-(3*H*-inden-1'-yl)-ethyl ester (**11**), 3-(2'-bromoethyl)-1*H*-indene (**12**), and 3-(2''chloroethyl)-1*H*-indene (**13**), a EBI ligand (**14**) was produced that could easily be coupled to aryl borates to yield a functionalized tethered-EBI ligand [106]. Of the three functionalized indenenes used, it must be noted that (**11**) afforded the best yields with the easiest separation [106]. This methodology is much more successful than the previous method used by Panarello *et al.* Stability and yield were much higher for the tethered-EBI ligands synthesized by this methodology [106]. A general reaction showing the formation of a functionalized tethered-EBI ligand can be observed in Scheme 11.



Scheme 11. A general reaction for the formation of functionalized tethered-EBI ligands [106].

It must be noted that most functional groups on tethers that are used for immobilization reactions are trialkylsilyl groups, which are very reactive towards surface silanol groups due to their very low pK_a of 4.8-8.5 [18, 107]. For example, some work done by Ofunne *et al.* showed that functionalized tethers with trialkoxysilyl groups produced two products; one product was bound to the surface only with alkoxy groups, while in the other product both the TiCl₂ and alkoxy groups were bound to the surface of the support by interaction with the silanol groups [18, 107]. This is in part due to the pK_a of silanol groups being 4.9-8.5; they are very acidic. Due to the low pH of the silanol groups, they are very reactive to the TiCl₂ groups of the *bis*-indenyl metallocenes [18, 107]. The reaction between the metal center and the silanol groups is hydrolysis. A reaction displaying the immobilization and side reaction can be observed in Scheme 12. Also, it must be noted that most tethers are currently functionalized trialkoxysilyl, hydroxyl, carboxyl, or amino groups [18]. The first solution to this problem is to find a new functionalized tether that works well in the immobilization of metallocenes on silica surfaces without producing side-reactions.



Scheme 12. The immobilization and side reaction of a tethered metallocene [18].

It is known that alkenes are effective in immobilization reactions due to their ability to react with silica hydride groups [18]. Therefore, the investigation into a methodology of synthesis of ligands containing a tether with a terminal alkene was necessary. Some *bis*-indenyl ligands containing terminal alkene groups were synthesized due to their ability to induce high selectivity in catalysis [18].

Research Objective

As mentioned earlier, there are many disadvantages of using homogeneous metallocene catalysts such as the difficulty of removal from the reaction mixture, deactivation by rearrangement of the metal-carbon bond, and the inability of reuse/recycling due to decomposition [86-95, 102]. Due to the disadvantages, heterogeneous metallocene catalysts are preferred despite their lowered catalytic ability [86-94]. Also, due to the above-mentioned disadvantages of current methods of immobilization (side reactions affording deactivated immobilized catalysts due to Si-O-M bonds, and side reactions of the functionalized tether) an investigation into new methods of immobilization is necessary. The objectives of this research

are to develop a methodology into the synthesis of *bis*-indenyl ligands for the purpose of metallocene catalysts, and to develop methods of immobilization of highly reactive metal complexes that do not involve reactions of the metal center with functional groups on the surface of the solid support. Therefore, a tether that does not involve trialkoxysilyl groups will be investigated. Lastly, silica supports must be functionalized by weakly or non-acidic functional groups in order to prevent formation of Si-O-M bonds by means of hydrolysis.

CHAPTER 2

EXPERIMENTAL

High purity reagents were used in the synthesis of compounds **7-18**, and the immobilization of compounds **19-28**. The structure, purity, and manufactures may be observed in Table 1.

Table 1. Structure, Purity, and Manufacturer of Synthetic Reagents

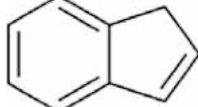
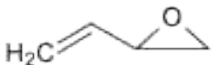
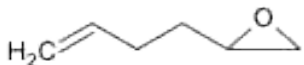
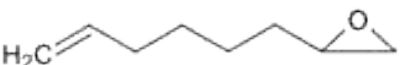
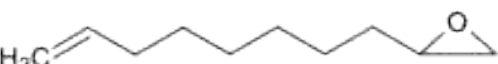
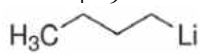
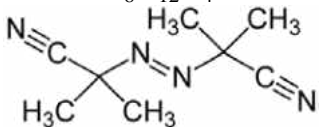
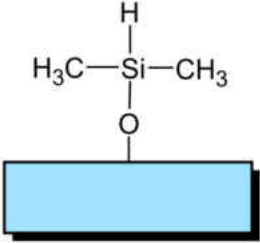
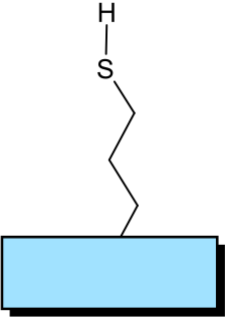
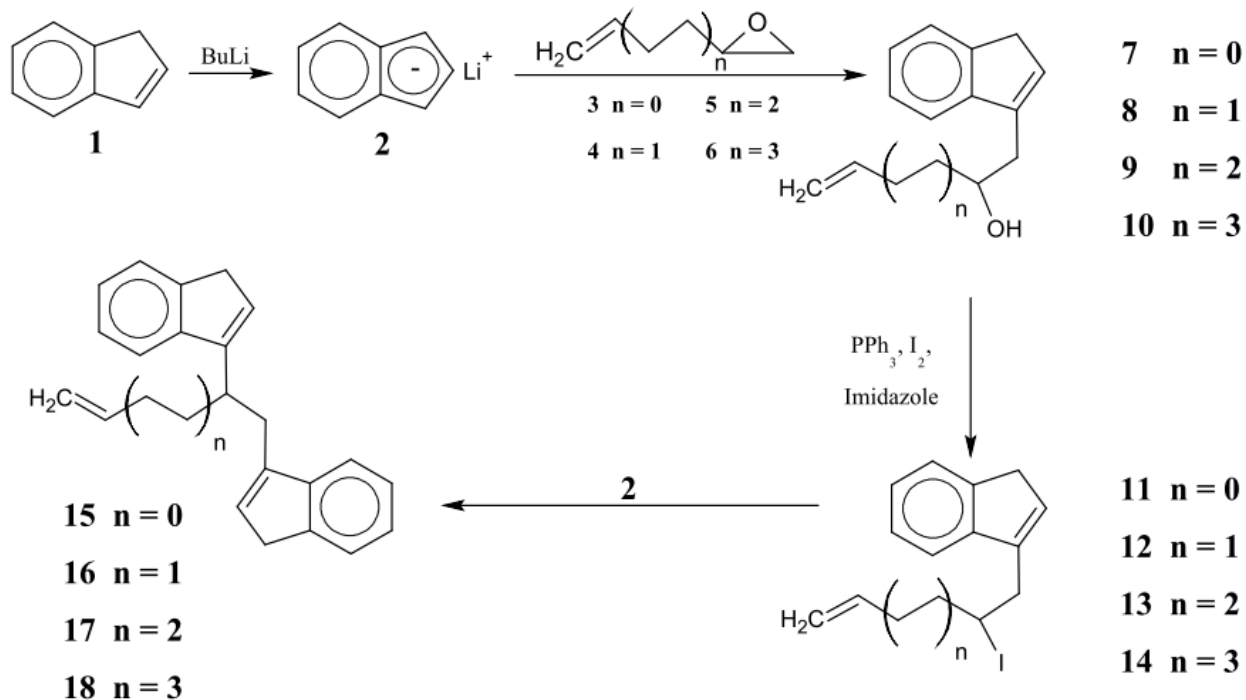
Compound Name	Molecular Formula	Purity	Manufacturer
Indene	C_9H_8 	90+%	Alfa Aesar
1,2-epoxy-3-butene	C_4H_6O 	98%	Alfa Aesar
1,2-epoxy-5-hexene	$C_6H_{10}O$ 	98%	Acros Organics
1,2-epoxy-7-octene	$C_8H_{14}O$ 	97%	Acros Organics
1,2-epoxy-9-decene	$C_{10}H_{18}O$ 	96%	Tokyo Kasei Kogyo Co. LTD
<i>n</i> -BuLi 2.5M	C_4H_9Li 	N/A	Acros Organics
Azobisisobutyronitrile (AIBN)	$C_8H_{12}N_4$ 	98%	Sigma Aldrich

Table 1. (continued)

Chloroplatinic Acid Hexahydrate	$\text{H}_2\text{PtCl}_6 \cdot 6\text{H}_2\text{O}$	99.9%	Sigma Aldrich
Copper Iodide	CuI	98%	Sigma Aldrich
Ammonium Bromide	NH_4Br	N/A	Matheson Coleman & Bell
Sodium Sulfate	Na_2SO_4	99%	Sigma Aldrich
Dimethylsiloxy-functionalized silica gel	$\text{C}_2\text{H}_7\text{OSi}^*\text{Si}$ 	N/A	Sigma Aldrich
3-Mercaptopropyl-functionalized silica gel	$\text{C}_3\text{H}_7\text{S}^*\text{Si}$ 	N/A	Sigma Aldrich
Sodium Chloride	NaCl	N/A	Flinn Scientific Inc.
Sodium Bicarbonate	NaHCO_3	99.5%	Acros Organics
Iodine	I_2	N/A	Fisher Scientific
Imidazole	$\text{C}_3\text{H}_4\text{N}_2$	99%	Alfa Aesar
Triphenylphosphine	$\text{P}(\text{C}_6\text{H}_5)_3$	99%	Sigma Aldrich

Synthesis of Bis-Indenyl Ligands

Synthesis of the *bis*-indenyl ligands involves three steps; an epoxide opening reaction and addition to indene, replacement of the hydroxyl group with iodine, and replacement of the iodine with a second molecule of indene. A complete reaction scheme displaying all three steps may be observed in Scheme 13.



Scheme 13. A complete reaction scheme of the synthesis of *bis*-indenyl ligands.

First Step: Synthesis of Indenyl Alcohols

A solution of *n*-BuLi (0.5 mL, 2.5 M, 0.074 g, 1.15 mmol) was added drop-wise to a solution of 1*H*-indene (0.122 g, 1.05 mmol) in 10 mL of dry THF at -78°C . Prior to the syntheses THF was dried on Na_2SO_4 overnight and on metallic sodium until elimination of hydrogen stopped. The syntheses involving air-sensitive compounds were carried out under dry nitrogen. The solution of indenyllithium (**2**) was added drop-wise to the solution of **3-6** (1 mmol) and CuI (0.04 g) in 10 mL of dry THF at 0°C . The reaction mixture was kept stirring at 0°C for 1.5 hrs and allowed to gradually warm to room temperature overnight. The reaction mixture was then quenched by aqueous NH_4Br and extracted by Et_2O . Organic phase was washed with water and dried over Na_2SO_4 . The solvent was removed in vacuum, and the product was purified by column chromatography on silica gel with a (5:2) mixture of hexanes/ Et_2O . Compound **7** ^1H NMR: δ 7.48-7.45 (d, 1H), 7.43-7.41 (d, 1H), 7.32-7.27 (t, 1H), 7.26-7.22 (t, 1H), 6.34 (s, 1H),

6.03-5.94 (m, 1H), 5.35-5.21 (dd, 2H), 3.96-3.94 (d, 1H), 3.84-3.83 (d, 1H), 3.41-3.37 (s, 1H), 2.63-2.62 (s, 1H), 2.10-1.65 (bs, 1H), 1.27-1.25 (s, 1H). Compound **7** ^{13}C NMR: δ 144.2, 142.9, 137.2, 129.3, 126.2, 125.1, 124.1, 119.6, 117.9, 64.5, 46.0, 38.3, 29.5. Compound **8** ^1H NMR: δ 7.49-7.46 (d, 1H), 7.39-7.36 (d, 1H), 7.33-7.29 (t, 1H), 7.24-7.20 (t, 1H), 6.34 (s, 1H), 5.89-5.83 (dq, 1H), 5.10-5.04 (dd, 2H), 4.01-3.94 (bs, 1H), 3.38-3.36 (s, 2H), 2.83-2.81 (d, 1H), 2.79-2.77 (d, 1H), 2.34-2.15 (m, 2H), 1.98-1.91 (s, 1H), 1.71-1.66 (t, 2H). Compound **8** ^{13}C NMR: δ 145.2, 142.4, 144.8, 139.8, 131.0, 126.3, 124.8, 124.0, 119.2, 115.0, 69.7, 38.1, 36.3, 31.2, 30.3. Compound **9** ^1H NMR: δ 7.49-7.46 (d, 1H), 7.42-7.39 (d, 1H), 7.29-7.25 (t, 1H), 7.22-7.18 (t, 1H), 6.34 (s, 1H), 5.85-5.74 (m, 1H), 5.03-4.93 (dd, 2H), 3.99-3.93 (bs, 1H), 3.40-3.38 (s, 2H), 2.99-2.95 (t, 2H), 2.76-2.73 (t, 1H), 2.47-2.45 (q, 2H), 2.43-2.41 (s, 1H), 2.21-2.16 (s, 1H), 2.12-2.02 (bs, 1H), 1.73-1.69 (t, 2H), 1.65-1.63 (s, 1H). Compound **9** ^{13}C NMR: δ 134.3, 132.2, 128.8, 128.2, 126.3, 125.5, 125.0, 124.7, 124.3, 123.9, 121.1, 39.3, 31.1, 30.6, 29.7, 28.9, 14.2. Compound **10** ^1H NMR: δ 7.48-7.46 (d, 1H), 7.45-7.43 (d, 1H), 7.36-7.32 (t, 1H), 7.27-7.23 (t, 1H), 6.34 (s, 1H), 5.86-5.73 (m, 1H), 5.04-4.87 (dd, 2H), 3.98-3.91 (bs, 1H), 3.38-3.36 (s, 2H), 3.12-3.10 (d, 1H), 2.98-2.95 (t, 2H), 2.93-2.88 (s, 1H), 2.76-2.73 (t, 1H), 2.48-2.45 (q, 2H), 2.09-1.94 (bs, 1H), 1.72-1.67 (t, 2H), 1.53-1.50 (t, 2H), 1.35-1.32 (s, 1H), 1.22-1.21 (s, 1H), 0.97-0.93 (t, 1H). Compound **10** ^{13}C NMR: δ 139.3, 128.7, 128.1, 127.2, 126.2, 125.4, 125.0, 124.2, 123.9, 114.4, 52.7, 47.4, 38.1, 33.7, 32.7, 29.5, 29.2, 28.1, 26.1.

Second Step: Synthesis of Iodoalkenyl Indenes

Compounds **7-10** (1 mmol) were dissolved in 15 mL of a mixture $\text{Et}_2\text{O}/\text{CH}_3\text{CN}$ (4:1) together with PPh_3 (0.288 g, 1.1 mmol), 1*H*-imidazole (0.136 g, 2 mmol) and I_2 (0.508 g, 2 mmol). After 20 min of stirring at room temperature, the reaction mixture was diluted by Et_2O and filtered. The liquid phase was washed with aqueous NaHCO_3 and NaCl , dried over Na_2SO_4 ,

and the solvent was evaporated in vacuum. The product was purified by column chromatography on silica gel using a (5:2) mixture of hexanes/Et₂O. Due to the very low stability of compounds **15-18**, they were used immediately for the next step of the synthesis. These compounds were not studied by spectroscopic methods.

Third Step: Synthesis of Alkenediyl-bis-indenes

A solution of **11-14** (1.05 mmol) in 8 mL of a (1:1) mixture of THF/hexanes was added drop-wise, while stirring, to a solution containing 0.122 g (1 mmol) of **2** in 10 mL of THF at -78°C. The reaction mixture was allowed to keep stirring and gradually warm to room temperature overnight. The reaction mixture was then quenched by aqueous NH₄Br and extracted by Et₂O. Organic phase was washed with water and dried over Na₂SO₄. The solvent was evaporated in vacuum, and the oily residue was purified by column chromatography on silica gel with a (5:2) mixture of hexanes/Et₂O. Compound **15** ¹H NMR: δ 7.52-7.49 (d, 2H), 7.47-7.42 (d, 1H), 7.37-7.29 (dd, 2H), 7.28-7.18 (m, 2H), 6.40-6.37 (d, 2H), 5.88-5.78 (dq, 1H), 5.27-5.17 (dd, 2H), 5.11-5.07 (d, 1H), 3.43-3.39 (d, 3H), 3.02-2.98 (t, 1H), 2.72-2.63 (dd, 1H), 1.97-1.94 (dd, 1H), 1.35-1.25 (d, 1H). Compound **15** ¹³C NMR: δ 143.1, 137.6, 137.0, 134.2, 132.1, 129.9, 128.8, 128.2, 127.5, 126.9, 124.7, 124.5, 123.8, 121.6, 121.1, 117.5, 115.3, 40.2, 39.2, 33.0, 29.9, 21.1. Compound **16** ¹H NMR: δ 7.50-7.46 (d, 2H), 7.39-7.36 (d, 1H), 7.33-7.28 (dd, 2H), 7.27-7.18 (m, 2H), 6.37-6.32 (s, 2H), 5.91-5.82 (dq, 1H), 5.12-4.94 (dd, 2H), 3.42-3.33 (d, 3H), 2.81-2.77 (t, 1H), 2.71-2.67 (dd, 2H), 2.67-2.62 (dd, 1H), 2.33-2.24 (m, 1H), 2.24-2.15 (m, 1H), 1.82-1.64 (q, 2H), 1.34-1.20 (d, 1H). Compound **16** ¹³C NMR: δ 145.1, 144.7, 143.4, 141.1, 138.6, 134.35, 132.1, 130.9, 126.1, 124.9, 123.9, 119.3, 115.0, 69.6, 39.2, 38.0, 36.4, 34.7, 32.1, 30.2, 29.9, 29.6, 22.9, 14.2. Compound **17** ¹H NMR: δ 7.46-7.43 (d, 2H), 7.42-7.38 (d, 1H), 7.35-7.30 (dd, 2H), 7.30-7.23 (m, 2H), 6.58-6.54 (s, 2H), 5.77-5.74 (d, 1H), 5.64-5.62 (d, 1H),

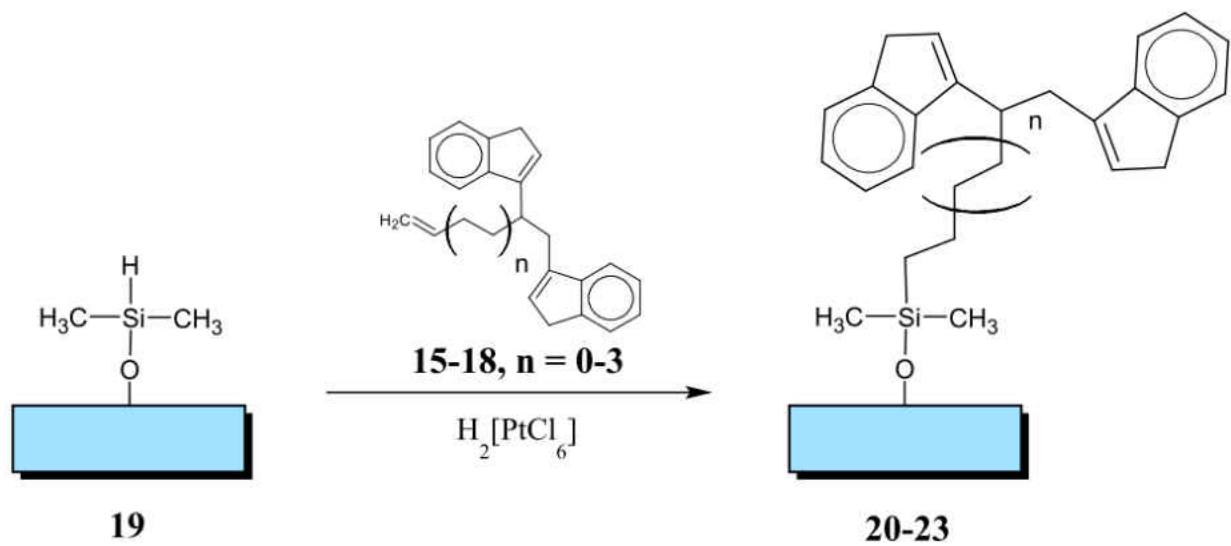
4.77-4.72 (dd, 2H), 3.93-3.90 (d, 1H), 3.54-3.52 (d, 1H), 3.39-3.36 (d, 3H), 3.12-3.10 (d, 1H), 3.00-2.92 (q, 2H), 2.90-2.88 (s, 1H), 2.86-2.78 (dd, 1H), 1.81-1.68 (m, 1H), 1.66-1.64 (s, 1H), 1.64-1.53 (m, 1H), 1.42-1.40 (s, 1H), 1.31-1.19 (d, 1H). Compound **17** ^{13}C NMR: δ 145.5, 143.4, 134.9, 134.7, 129.8, 128.1, 127.9, 127.6, 127.2, 126.9, 126.3, 126.2, 125.3, 124.4, 124.2, 75.9, 49.7, 34.7, 33.9, 32.3, 32.0, 31.0, 27.7, 24.4, 22.7, 14.2. Compound **18** ^1H NMR: δ 7.46-7.42 (d, 2H), 7.41-7.38 (d, 1H), 7.34-7.29 (dd, 2H), 7.18-7.08 (m, 2H), 6.58-6.55 (s, 2H), 5.77-5.72 (dd, 1H), 5.64-5.61 (d, 1H), 5.03-4.88 (dd, 2H), 4.76-4.71 (q, 2H), 4.23-4.15 (m, 2H), 4.06-3.98 (p, 2H), 3.38-3.34 (d, 3H), 2.85-2.77 (dd, 1H), 2.18-2.13 (s, 2H), 2.08-1.92 (m, 1H), 1.69-1.68 (s, 1H), 1.68-1.59 (dd, 2H), 1.52-1.45 (dd, 1H), 1.41-1.39 (s, 1H), 1.32-1.17 (d, 1H). Compound **18** ^{13}C NMR: δ 149.4, 147.7, 145.3, 145.1, 144.1, 143.5, 141.0, 129.8, 128.0, 126.6, 126.4, 125.1, 124.2, 123.7, 121.8, 121.3, 114.3, 72.0, 66.0, 49.8, 33.0, 32.1, 31.1, 29.9, 29.6, 27.9, 25.6, 24.4.

Immobilization of the Ligands by Hydrosilylation

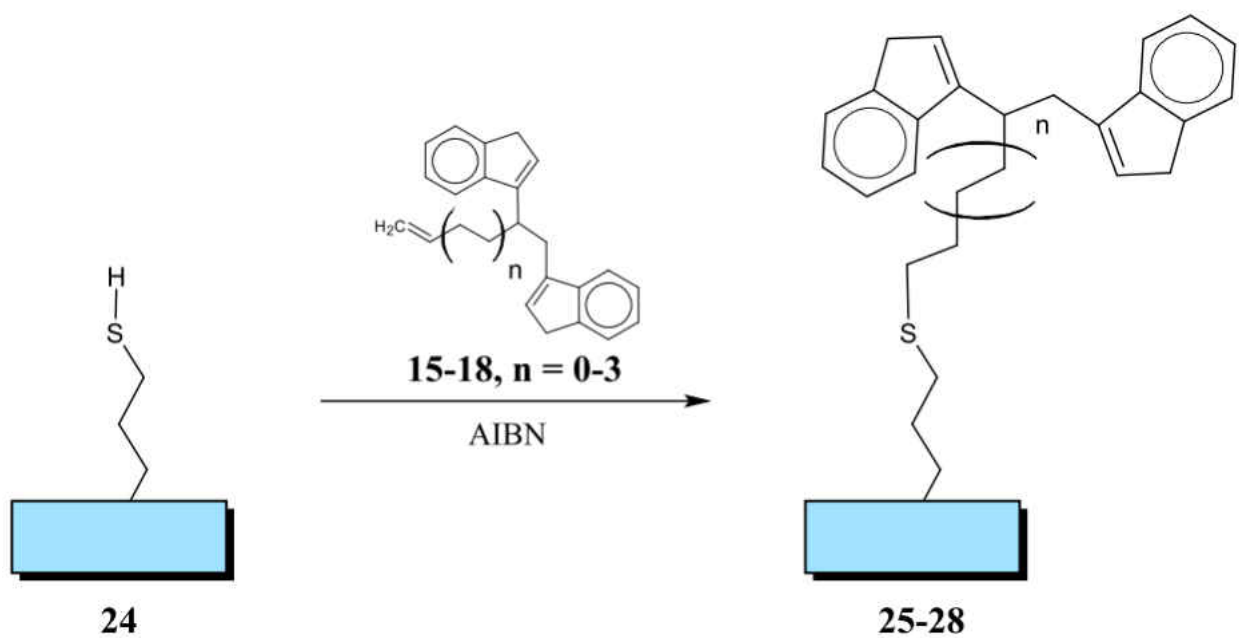
1 g of **19** was added to the solution of **15-18** (0.07 mmol) and $\text{H}_2[\text{PtCl}_6] \cdot 6\text{H}_2\text{O}$ (0.003 g) in 25 mL of isopropanol. The reaction mixture was refluxed for 12 hrs, the solid product was filtered, washed with isopropanol, water, and acetone, and allowed to air-dry overnight. A complete reaction scheme of the immobilization may be observed in Scheme 14.

Immobilization of the Ligands by Thiol-ene Coupling

1 g of **24** was added to the solution of **15-18** (0.07 mmol) and AIBN (0.08 g) in 30 mL of CHCl_3 . The reaction mixture was refluxed for 12 hrs, the solid product was filtered, washed with hexane and toluene, and allowed to air-dry overnight. A complete reaction scheme of the immobilization can be observed in Scheme 15.



Scheme 14. Reaction scheme for the immobilization of ligands by hydrosilylation.



Scheme 15. Reaction scheme for the immobilization of ligands by thiol-ene coupling.

Characterization of the Products

TLC

Thin layer chromatography of samples **7-18** was performed on silica gel-covered plates with a (9:1) mixture of hexanes/isopropanol as the solvent.

FT-IR

Spectra of **7-10** and **15-18** were obtained on a Shimadzu IR Prestige-21 (Kyoto, Japan) by directly placing the samples onto the spectrometer. Samples were obtained in the range of 600-4000 cm^{-1} for 100 scans.

Spectra of solid samples **24** and **25** were obtained on a Mattson Instruments Genesis II spectrometer (Madison, WI) by forming a KBr pellet in a (1:100) ratio of sample/KBr. Samples were obtained in the range of 600-4000 cm^{-1} for 16 scans.

LC-MS

Spectra of **7-10** and **15-18** were obtained on a Shimadzu LCMS Liquid Chromatograph/Mass Spectrometer (Kyoto, Japan) equipped with Shim-Pack XR-ODS 2.0 mm i.d. x 50 mm column at 40 °C and flow rate 0.7 mL/min. A 17:3 mixture of methanol/ethanol was used as an eluent. Samples were prepared in a concentration of 200ppm.

^1H NMR

Compounds **7-10** and **15-18** were dissolved in *d*- CDCl_3 . NMR spectra were obtained on a JEOL Oxford AS400 spectrometer at 399.8 MHz for 250 scans, using *d*- CDCl_3 as the solvent and TMS as a reference.

¹³C NMR

Compounds **7-10** and **15-18** were dissolved in *d*-CDCl₃. NMR spectra were obtained on a JEOL Oxford AS400 spectrometer at 100.5 MHz for 1500 scans, using *d*-CDCl₃ as the solvent and TMS as a reference.

Porosimetry

BET specific surface areas, average pore widths, and pore size distributions of solid samples **19-28** were measured using a Micrometrics ASAP 2020 porosimeter. Prior to the measurements, the samples were degassed at 120°C for 2 h.

Atomic Absorption (AAS)

Pt content of samples **20-23** were determined using a Shimadzu AA6300 Atomic Absorption Spectrometer (Kyoto, Japan). Standard Pt solutions were prepared from H₂[PtCl₆] • 6H₂O in concentrations of 4.708 ppm, 9.417 ppm, 18.834 ppm, 28.251 ppm, and 37.668 ppm. Solutions for the measurements were prepared by extraction of Pt from samples **20-23** by a mixture HCl/HNO₃ (3:1). After extraction, the pH was adjusted to 4-5 by addition of CH₃COONa solution.

CHAPTER 3

RESULTS

All compounds **7-18** were obtained with high yield. None of the compounds could be crystallized, and therefore appeared as oils. Their yields, appearances, and retention times in TLC are shown in Table 2.

Table 2. Yields and Properties of the Compounds

Entry	#	n	Product Appearance	Yield (%)	R _f (hexane/ isopropanol, 9:1)
1	7	0	Light brown oil	82.4	0.56
2	8	1	Brown oil	81.3	0.57
3	9	2	Brown oil	24.2	0.73
4	10	3	Brown oil	29.5	0.73
5	11	0	Brown oil	59.3	0.63
6	12	1	Brown oil	92.5	0.62
7	13	2	Brown oil	93.8	0.61
8	14	3	Dark brown oil	51.1	0.61
9	15	0	Yellow oil	67.5	0.34
10	16	1	Light orange oil	83.1	0.33
11	17	2	Yellow oil	69.4	0.56
12	18	3	Yellow oil	64.3	0.56

The structure of compounds **7-10** and **15-18** were confirmed by ¹H and ¹³C NMR.

Chemical shifts of the peaks and their characteristics are shown in Table 3.

Table 3. NMR Spectral Data

Sample	¹ H NMR (δ)	¹³ C NMR (δ)
7	7.48-7.45 (d, 1H), 7.43-7.41 (d, 1H), 7.32-7.27 (t, 1H), 7.26-7.22 (t, 1H), 6.34 (s, 1H), 6.03-5.94 (m, 1H), 5.35-5.21 (dd, 2H), 3.96-3.94 (d, 1H), 3.84-3.83 (d, 1H), 3.41-3.37 (s, 1H), 2.63-2.62 (s, 1H), 2.10-1.65 (bs, 1H), 1.27-1.25 (s, 1H)	144.2, 142.9, 137.2, 129.3, 126.2, 125.1, 124.1, 119.6, 117.9, 64.5, 46.0, 38.3, 29.5
8	7.49-7.46 (d, 1H), 7.39-7.36 (d, 1H), 7.33-7.29 (t, 1H), 7.24-7.20 (t, 1H), 6.34 (s, 1H), 5.89-5.83 (dq, 1H), 5.10-5.04 (dd, 2H), 4.01-3.94 (bs, 1H), 3.38-3.36 (s, 2H), 2.83-2.81 (d, 1H), 2.79-2.77 (d, 1H), 2.34-2.15 (m, 2H), 1.98-1.91 (s, 1H), 1.71-1.66 (t, 2H)	145.2, 142.4, 144.8, 139.8, 131.0, 126.3, 124.8, 124.0, 119.2, 115.0, 69.7, 38.1, 36.3, 31.2, 30.3
9	7.49-7.46 (d, 1H), 7.42-7.39 (d, 1H), 7.29-7.25 (t, 1H), 7.22-7.18 (t, 1H), 6.34 (s, 1H), 5.85-5.74 (m, 1H), 5.03-4.93 (dd, 2H), 3.99-3.93 (bs, 1H), 3.40-3.38 (s, 2H), 2.99-2.95 (t, 2H), 2.76-2.73 (t, 1H), 2.47-2.45 (q, 2H), 2.43-2.41 (s, 1H), 2.21-2.16 (s, 1H), 2.12-2.02 (bs, 1H), 1.73-1.69 (t, 2H), 1.65-1.63 (s, 1H)	134.3, 132.2, 128.8, 128.2, 126.3, 125.5, 125.0, 124.7, 124.3, 123.9, 121.1, 39.3, 31.1, 30.6, 29.7, 28.9, 14.2

Table 3. (continued)

10	7.48-7.46 (d, 1H), 7.45-7.43 (d, 1H), 7.36-7.32 (t, 1H), 7.27-7.23 (t, 1H), 6.34 (s, 1H), 5.86-5.73 (m, 1H), 5.04-4.87 (dd, 2H), 3.98-3.91 (bs, 1H), 3.38-3.36 (s, 2H), 3.12-3.10 (d, 1H), 2.98-2.95 (t, 2H), 2.93-2.88 (s, 1H), 2.76-2.73 (t, 1H), 2.48-2.45 (q, 2H), 2.09-1.94 (bs, 1H), 1.72-1.67 (t, 2H), 1.53-1.50 (t, 2H), 1.35-1.32 (s, 1H), 1.22-1.21 (s, 1H), 0.97-0.93 (t, 1H)	139.3, 128.7, 128.1, 127.2, 126.2, 125.4, 125.0, 124.2, 123.9, 114.4, 52.7, 47.4, 38.1, 33.7, 32.7, 29.5, 29.2, 28.1, 26.1
15	7.52-7.49 (d, 2H), 7.47-7.42 (d, 1H), 7.37-7.29 (dd, 2H), 7.28-7.18 (m, 2H), 6.40-6.37 (d, 2H), 5.88-5.78 (dq, 1H), 5.27-5.17 (dd, 2H), 5.11-5.07 (d, 1H), 3.43- 3.39 (d, 3H), 3.02-2.98 (t, 1H), 2.72-2.63 (dd, 1H), 1.97-1.94 (dd, 1H), 1.35-1.25 (d, 1H)	143.1, 137.6, 137.0, 134.2, 132.1, 129.9, 128.8, 128.2, 127.5, 126.9, 124.7, 124.5, 123.8, 121.6, 121.1, 117.5, 115.3, 40.2, 39.2, 33.0, 29.9, 21.1
16	7.50-7.46 (d, 2H), 7.39-7.36 (d, 1H), 7.33-7.28 (dd, 2H), 7.27-7.18 (m, 2H), 6.37-6.32 (s, 2H), 5.91-5.82 (dq, 1H), 5.12-4.94 (dd, 2H), 3.42-3.33 (d, 3H), 2.81- 2.77 (t, 1H), 2.71-2.67 (dd, 2H), 2.67-2.62 (dd, 1H), 2.33-2.24 (m, 1H), 2.24-2.15 (m, 1H), 1.82-1.64 (q, 2H), 1.34-1.20 (d, 1H)	145.1, 144.7, 143.4, 141.1, 138.6, 134.35, 132.1, 130.9, 126.1, 124.9, 123.9, 119.3, 115.0, 69.6, 39.2, 38.0, 36.4, 34.7, 32.1, 30.2, 29.9, 29.6, 22.9, 14.2

Table 3. (continued)

17	7.46-7.43 (d, 2H), 7.42-7.38 (d, 1H), 7.35-7.30 (dd, 2H), 7.30-7.23 (m, 2H), 6.58-6.54 (s, 2H), 5.77-5.74 (d, 1H), 5.64-5.62 (d, 1H), 4.77-4.72 (dd, 2H), 3.93-3.90 (d, 1H), 3.54-3.52 (d, 1H), 3.39-3.36 (d, 3H), 3.12-3.10 (d, 1H), 3.00-2.92 (q, 2H), 2.90-2.88 (s, 1H), 2.86-2.78 (dd, 1H), 1.81-1.68 (m, 1H), 1.66-1.64 (s, 1H), 1.64-1.53 (m, 1H), 1.42-1.40 (s, 1H), 1.31-1.19 (d, 1H)	145.5, 143.4, 134.9, 134.7, 129.8, 128.1, 127.9, 127.6, 127.2, 126.9, 126.3, 126.2, 125.3, 124.4, 124.2, 75.9, 49.7, 34.7, 33.9, 32.3, 32.0, 31.0, 27.7, 24.4, 22.7, 14.2
18	7.46-7.42 (d, 2H), 7.41-7.38 (d, 1H), 7.34-7.29 (dd, 2H), 7.18-7.08 (m, 2H), 6.58-6.55 (s, 2H), 5.77-5.72 (dd, 1H), 5.64-5.61 (d, 1H), 5.03-4.88 (dd, 2H), 4.76-4.71 (q, 2H), 4.23-4.15 (m, 2H), 4.06-3.98 (p, 2H), 3.38-3.34 (d, 3H), 2.85-2.77 (dd, 1H), 2.18-2.13 (s, 2H), 2.08-1.92 (m, 1H), 1.69-1.68 (s, 1H), 1.68-1.59 (dd, 2H), 1.52-1.45 (dd, 1H), 1.41-1.39 (s, 1H), 1.32-1.17 (d, 1H)	149.4, 147.7, 145.3, 145.1, 144.1, 143.5, 141.0, 129.8, 128.0, 126.6, 126.4, 125.1, 124.2, 123.7, 121.8, 121.3, 114.3, 72.0, 66.0, 49.8, 33.0, 32.1, 31.1, 29.9, 29.6, 27.9, 25.6, 24.4

Study of compounds **7-10** and **15-18** by FT-IR spectroscopy showed the presence of functional groups in their structures. The position of the peaks and the corresponding functional groups are shown in Table 4. Confirmation of immobilization of the ligands **15-18** on 3-Mercaptopropyl-functionalized silica gel may be observed by the appearance of bands seen in the FT-IR spectra of the ligands **15-18**. The FT-IR of compounds **24** and **25** may be observed in Figure 6.

Table 4. FT-IR Spectral Data

Sample	ν_{\max} , cm^{-1}
7	623, 719, 768, 916, 966, 991, 1020, 1045, 1204, 1288, 1327, 1393, 1460 (Ar), 1605 (C=C), 1636 (C=C), 1701, 2880 (CH), 2926 (CH), 3071 (CH=), 3389 (OH)
8	642, 721, 756, 910, 993, 1018, 1063, 1119, 1155, 1207, 1285, 1393, 1460 (Ar), 1603 (C=C), 1639 (C=C), 1711, 2928 (CH), 3071 (CH=), 3408 (OH)
9	719, 750, 860, 914, 941, 1018, 1153, 1207, 1261, 1288, 1325, 1369, 1393, 1460, 1603 (C=C), 1709, 2926 (CH), 3065 (CH=), 3435 (OH)
10	646, 729, 908, 993, 1018, 1083, 1153, 1207, 1288, 1325, 1369, 1462, 1603 (C=C), 1639 (C=C), 1708, 2247, 2855 (CH), 2926 (CH), 3067 (CH=), 3435 (OH)
15	629, 691, 719, 752, 768, 866, 905, 947, 989, 1018, 1094, 1153, 1198, 1225, 1260, 1366, 1456, 1605 (C=C), 1634 (C=C), 1711, 2855 (CH), 2924 (CH), 2957 (CH), 3069 (CH=)
16	629, 719, 756, 910, 964, 1018, 1067, 1153, 1204, 1260, 1288, 1364, 1395, 1458, 1603 (C=C), 1639 (C=C), 1709, 2924 (CH), 3069 (CH=)
17	619, 752, 835, 878, 937, 1020, 1084, 1155, 1273, 1288, 1319, 1364, 1460, 1605 (C=C), 1643 (C=C), 1709, 2868 (CH), 2924 (CH), 2961 (CH), 3065 (CH=)
18	627, 721, 750, 797, 835, 878, 903, 968, 1020, 1042, 1076, 1092, 1113, 1155, 1198, 1260, 1327, 1371, 1447, 1460, 1570, 1607 (C=C), 1643 (C=C), 1713, 2342, 2855 (CH), 2924 (CH), 2965 (CH), 3065 (CH=)
24	2855, 2933, 2960
25	1459, 1499, 1638, 1719, 2855, 2926, 2957

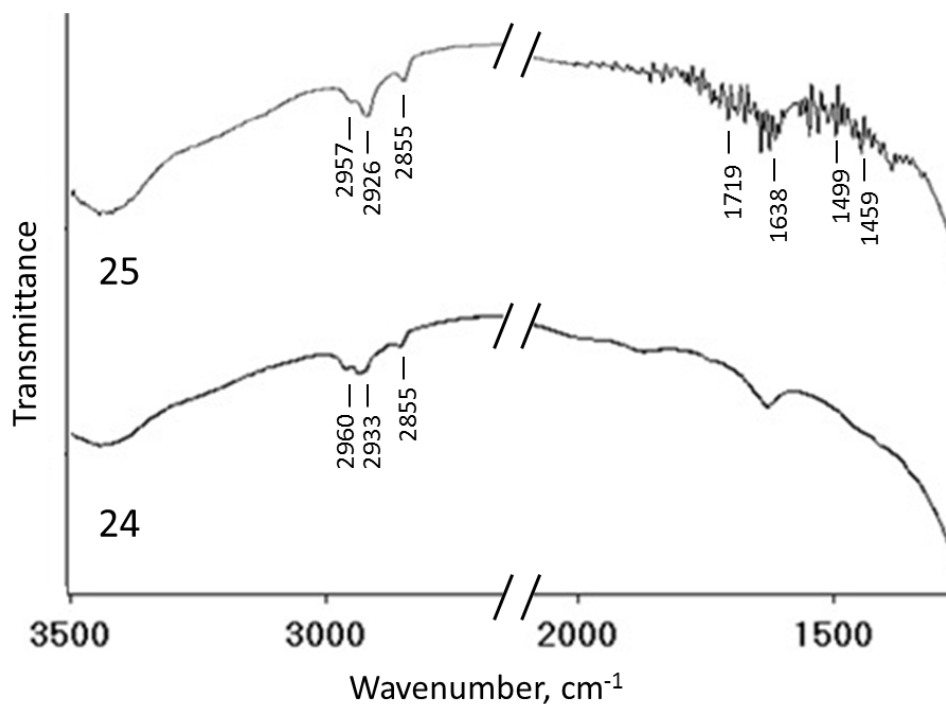


Figure 6. FT-IR Spectra of Samples **24** and **25**.

Study of compounds **7-10** and **15-18** by MS spectroscopy showed the presence of fragmented ions that are characteristic of the proposed structures. This can be observed in Table 5.

Table 5. MS Spectral Data

Sample	m/z
7	186 (M) ⁺ , 168 (Ind-CH(CH)-CH=CH ₂) ⁺ , 157 (Ind-CH(CH ₂)CH ₃) ⁺ , 115 (Ind) ⁺
8	213 (M-1) ⁺ , 197 (Ind-CH(CH)-(CH ₂) ₄) ⁺ , 131 (Ar-(CH ₂)(CH-CH ₂) ⁺ , 115 (Ind) ⁺ , 102 (Ar-CH ₂ -C) ⁺
9	243 (M+1) ⁺ , 225 (Ind-CH(CH ₂)-(CH ₂) ₄ -CH=CH ₂) ⁺ , 173 (Ind-C ₄ H ₉) ⁺ , 131 (Ar-(CH ₂ -CH ₂)-CH-CH ₂) ⁺ , 102 (Ar-CH ₂ -C) ⁺
10	261, 245, 202, 155 (Ind-CH(CH)-CH ₂) ⁺ , 102 (Ar-CH ₂ -C) ⁺

Table 5. (continued)

15	261, 245, 219, 209 (Ind-CH(CH=CH ₂)-CH ₂ -CH=CH-CH ₂) ⁺ , 168 (Ind-CH(CH)-CH=CH ₂) ⁺ , 157 (Ind-CH(CH ₂)CH ₃) ⁺ , 102 (Ar-CH ₂ -C) ⁺
16	311 (M-1) ⁺ , 293, 279, 245, 219, 197 (Ind-CH(CH)-(CH ₂) ₄) ⁺ , 131 (Ar-(CH ₂)(CH-CH ₂) ⁺ , 115 (Ind) ⁺
17	341 (M+1) ⁺ , 307, 279, 261, 245, 219, 173 (Ind-C ₄ H ₉) ⁺ , 159 (Ind-C ₃ H ₇) ⁺
18	279, 271 (Ind-CH ₂ -CH(CH ₂)-Ind) ⁺ , 261, 245, 219, 173 (Ind-C ₄ H ₉) ⁺ , 155 (Ind-CH(CH)-CH ₂) ⁺ , 115 (Ind) ⁺

Immobilization of ligands **15-18** on Dimethylsiloxy-functionalized silica gel was unsuccessful as can be observed in Table 6. In contrast, immobilization of ligands **15-18** on 3-Mercaptopropyl-functionalized silica gel was successful; the loading of the ligands was much higher.

Table 6. Loading of the Ligands on the Silica Surface and Porous Characteristics of Products

Entry	#	n	Loading of ligands		Fraction of surface functional groups reacted (%)	BET surface area, m ² /g	Total pore volume cm ³ /g	Average pore width, nm
			mmol/g	molecules/nm ²				
1	19	-	-	-	-	362	0.57	6.3
2	20	0	0.03	0.05	0.07	404	0.61	6.1
3	21	1	0.03	0.05	0.07	363	0.54	6.0
4	22	2	0.01	0.02	0.03	399	0.63	6.3

Table 6. (continued)

5	23	3	0.03	0.05	0.07	392	0.61	6.2
6	24	-	-	-	-	248	0.50	8.0
7	25	0	0.16	0.39	0.48	251	0.45	7.1
8	26	1	0.14	0.34	0.42	239	0.41	6.9
9	27	2	0.13	0.31	0.39	244	0.45	7.4
10	28	3	0.08	0.19	0.24	247	0.45	7.3

Study of the products porosity showed the BET surface areas and total pore volumes. The BET surface areas and total pore volumes were higher for products **20-23** than the corresponding data for **19**. The opposite was observed for compounds **25-28**; their BET surface areas and total pore volumes were lower than the corresponding data for **24**. The comparisons of **19** and **20**, and **24** and **25** may be observed in Figures 7 and 8.

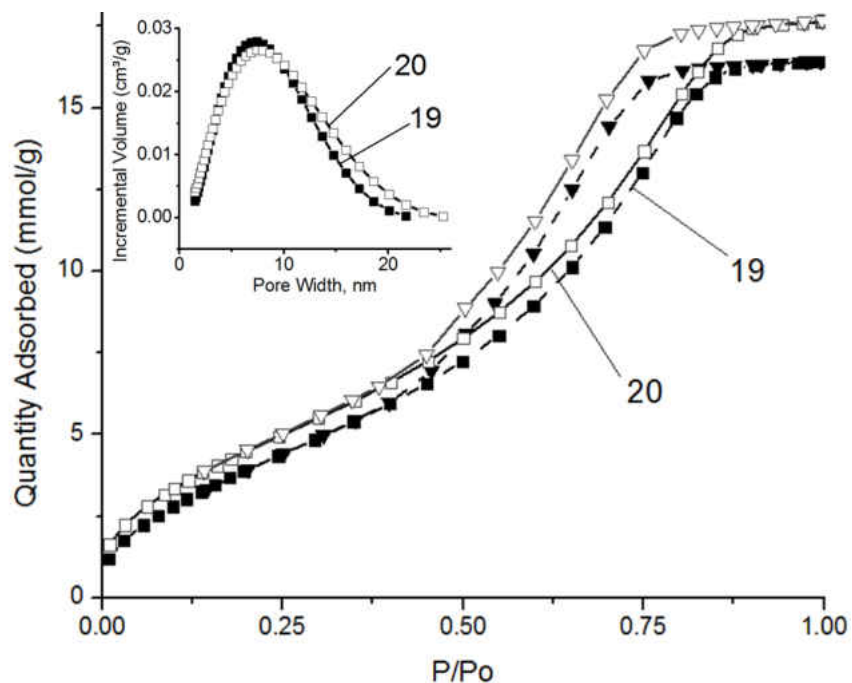


Figure 7. Adsorption/Desorption Isotherms and Pore Size Distributions of **19** and **20**.

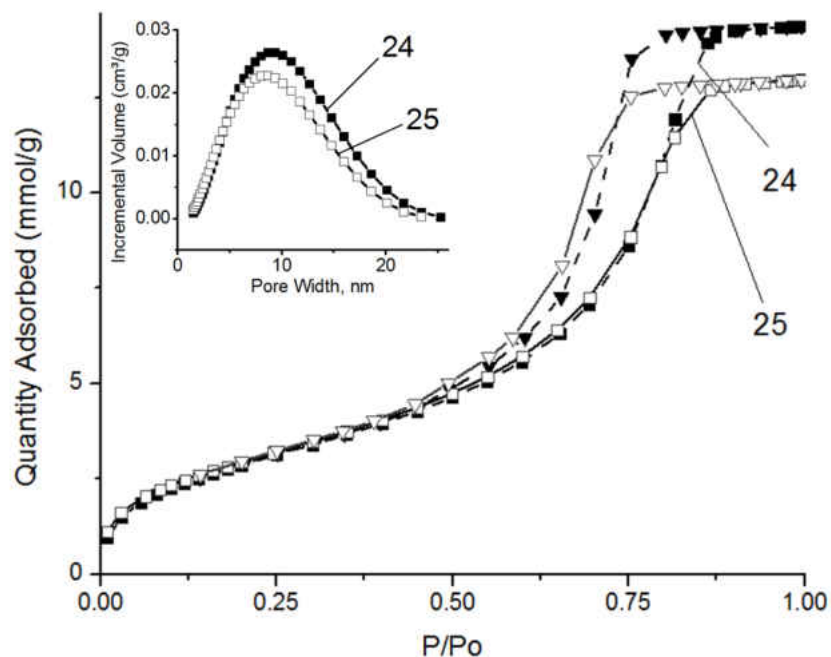


Figure 8. Adsorption/Desorption Isotherms and Pore Size Distributions of **24** and **25**.

At attempts of immobilization of the ligands **15-18** on Dimethylsiloxy-functionalized silica gel a side reaction of the catalyst decomposition resulted in the precipitation of metallic Pt. The amounts of Pt deposited on the silica gel are shown in Table 7.

Table 7. Contents of Metallic Pt on Silica Samples **20-23** After Hydrosilylation

Sample	Amount of Pt, mg/g
20	2.26
21	2.17
22	1.68
23	2.38

CHAPTER 4

DISCUSSION

Synthesis of *Bis*-indenyl Ligands

EBI ligands containing functionalized tethers of various lengths were synthesized using a slightly modified procedure described by Panarello *et al.* [86]. A general strategy of the synthesis is shown in Scheme 1. First, 1*H*-indene (**1**) was converted to its lithium salt (**2**) in dry THF. On the next step, compound **2** was applied in a regioselective ring-opening reaction of alkene-substituted epoxides **3-6** containing terminal double bonds.

In accordance with Abramson *et al.*, the reaction of 1,2-epoxy-5-hexene with indenyl lithium resulted in the formation of 2-(1*H*-inden-3'-yl)hex-5-en-1-ol [87]. However, the structure of the product is unusual due to regioselectivity of the base catalyzed opening of the epoxide ring, which favors nucleophilic attack on the less sterically hindered carbon atom of the ring. In contrast, Gruber-Woelfler *et al.* [108] in a similar reaction of 1,2-epoxy-9-decene reported formation of 1-(1*H*-inden-3'-yl)dec-9-en-2-ol as an expected product of the CH₂-O bond cleavage. Our study of all indenyl-substituted alcohols by ¹H NMR showed the presence of only one hydrogen atom with a signal at 3.91-4.01 ppm (CH-OH) that proves the conventional mechanism of this reaction.

NMR spectra of the indenyl alcohols (**7-10**) indicated the formation of their isomers. In addition to the preferred secondary alcohols, a very small amount of primary alcohols was formed. The formation of the primary alcohols is not preferred due to steric hindrance of the epoxides containing the terminal alkene group. Also, the location of the double bond in the 5-

member ring of the indenyl group can differ. The preferred isomer, the tri-substituted alkene, is produced in excess to the non-preferred, di-substituted alkene. Only four protons were observed in the alkene region of ^1H NMR instead of five protons that proves the formation of the tri-substituted isomers as major products. This can be explained by the energy of the molecule as well. Alkene energy decreases with substitution degree, which results in an increase in stability; this is common knowledge in organic chemistry. Due to the higher stability, formation of the tri-substituted alkene is more preferred. The presence of minor isomers results in appearance of additional small peaks in the ^1H and ^{13}C NMR spectra of compounds **7-10**. In some cases, the splittings of peaks in the ^1H NMR spectra were difficult to determine due to their complexity. However, the primary alcohols were successfully iodinated and alkylated with a second molecule of indene, producing the expected alkenediyl-*bis*-indenyl ligands (**15-18**), as confirmed by ^1H and ^{13}C NMR. The structure of each compound was confirmed in accordance with data reported by Gruber-Woelfler *et al.* [106]. In particular, it was confirmed by integration data, proving the correct amount of protons for each structure. In each structure, the correct amount of protons was detected in the saturated alkyl region (δ 0.0-4.0 ppm), the alkene region (δ 4.0-7.0 ppm), and the aromatic region (δ 6.5-8.0 ppm). In each indenyl alcohol structure, an alcohol group (CH-OH) was observed in the expected region of δ 2.5-5.0 ppm.

Study of compounds **7-10** and **15-18** by FT-IR confirmed the expected structures for the indenyl alcohols and alkenediyl-*bis*-indenyl ligands. The presence of alkene groups was detected by vibrations of C=C bonds at 1603-1605 cm^{-1} and 1634-1639 cm^{-1} , and =CH bonds at 3065-3071 cm^{-1} . The aromatic region was detected by bands at 1460-1462 cm^{-1} . Saturated CH vibrations were detected at 2880-2928 cm^{-1} . Lastly, hydroxyl group vibrations were detected for the indenyl alcohols at 3389-3435 cm^{-1} . The presence of the alkene groups, aromatic groups,

saturated alkyl groups, and hydroxyl groups confirmed the expected structures of the indenyl alcohols and alkenediyl-*bis*-indenyl ligands.

Immobilization of the Ligands on Porous Support

The first attempt to immobilize the ligands was based on the catalytic hydrosilylation of the terminal double bond. This approach was successfully used earlier for such immobilizations on H-terminated Si(111) surfaces using UV-mediated alkene hydrosilylation [95]. However, the silicon support used in these studies was not porous. Its low surface area limited the amount of immobilized ligand making it impractical for synthesis of heterogeneous catalysts. In addition, this method is applicable only to oxide-free surfaces while most of porous supports are simple or mixed oxides.

For immobilization of the ligands on porous silica support, functionalized silica gel containing surface dimethylsiloxy groups was chosen first [109]. Ligands **15-18** reacted with surface Si-H groups of a silane-functionalized support **19** in the presence of Speier catalyst ($\text{H}_2[\text{PtCl}_6] \cdot 6\text{H}_2\text{O}$ in isopropanol) as shown in Scheme 14. However, in accordance with the data in Table 2, only a small fraction of the Si-H groups reacted with the terminal alkene group of the ligands. At the same time, the absorption band at 2143 cm^{-1} ($\nu_{\text{Si-H}}$) in the FT-IR spectra of products **20-23** completely disappeared. Study of the products porosity showed that their BET surface areas and total pore volumes were higher than corresponding data for **19** (Figure 7). Usually, immobilization of bulky molecules reduces these parameters of a porous support. The observed effects may be interpreted as evidence of defunctionalization of the silica surface rather than ligand immobilization. Similar phenomena was observed earlier on H-terminated silicon and explained by side reactions of alcohol with silane groups [110, 138].

In addition, the Speier catalyst decomposed upon interaction with the dimethylsiloxy-functionalized silica surface. During immobilization, platinum was reduced to metallic form and precipitated on silica gel. The amount of metallic platinum that precipitated on the silica gel was measured by Atomic Absorption Spectrometry (AAS). It was found that products **20-23** contain 1.7-2.4 mg of platinum. Considering the total amount of Pt in the Speier catalyst used in the syntheses (3 mg), it is clear that most of the catalyst decomposed during the reaction.

Observed precipitation of platinum can be explained by the mechanism of hydrosilylation where the catalytically active species are colloidal Pt nanoparticles formed at the reduction of $\text{H}_2[\text{PtCl}_6]$ by silane groups [111]. As a result, a prospective catalyst support was contaminated by Pt nanoparticles, which might affect its original catalytic properties. Thus, this method was not effective in the ligand immobilizations.

An alternative strategy of immobilization (Scheme 15) was based on a thiol-ene coupling reaction [112, 113]. This reaction proceeds on a radical mechanism and requires an initiator such as AIBN. In contrast to moderately acidic ($\text{pK}_a=4.9-8.5$) and highly reactive silanol groups, thiol groups have much lower acidity ($\text{pK}_a=10-11$) and reactivity. As it was shown earlier by Yu and Jones [114], thiol-ene coupling can be carried out in presence of some organometallic complexes without risk of their destruction.

Results of immobilization experiments gave successful immobilization of the EBI ligands on the thiol-functionalized silica gel (Table 6). The obtained hybrid organic/inorganic materials were highly porous. However, immobilization slightly reduced BET surface area and pore volume (Figure 8). As it may be seen from pore size distribution, immobilization of the ligands affects mostly pores of larger width (8-20 nm), while their effect on small pores is insignificant.

Immobilization of the ligands was confirmed by FT-IR spectroscopy. The spectrum of **24** contains weak bands of CH₃ groups at 2855-2960 cm⁻¹ (Figure 6). The intensity of this band increased after immobilization, which proves an increase in the contents of organic phase on the surface. In addition, several bands appeared in the region 1400-1800 cm⁻¹. Some of these bands (marked on the spectrum of product **25**) correspond to the bands observed in the FT-IR spectra of the ligands **15-18**.

The amounts of immobilized ligands **15-18** depended on their tether lengths. The ligands with longer tethers demonstrated lower loading on the surface. The volumes of the ligand molecules (calculated using Spartan '08 software) fall in the range of 0.33-0.44 nm³ [113]; this can be observed in Figure 9. As shown by the data on the ligand loading, this value strongly depended on the molecular size; this can be observed in Figure 10. In particular, the size of **18** is 33% higher than **15**, while its loading on the silica surface was half as much. It is evident that a significant part of the surface thiol groups are located in small pores inaccessible for ligands of larger size. Thus, the use of the ligand with the shortest tether provides the highest loading on the silica gel.

Summary

A simple and efficient method of immobilization of EBI ligands containing tethers of various lengths on porous silica gel was described. Two methods were investigated; hydrosilylation and thiol-ene coupling. Hydrosilylation was found to be ineffective. Destruction of functional groups on the surface of functionalized silica gel was observed; average pore size increased in contrast to decreasing upon immobilization. In addition, decomposition of the Speier catalyst results in the contamination of the immobilized product by metallic platinum. Thiol-ene coupling was found to be a more appropriate method for the immobilization of EBI ligands.

Destruction of functional groups and contamination from the AIBN catalyst were not observed. In contrast to most of the reported methods, the immobilization by thiol-ene coupling does not require the presence of acidic and highly reactive silanol groups on the silica surface. The thiol-ene coupling method may be used for immobilization of catalytically active *bis-indenyl ansa*-metallocenes.

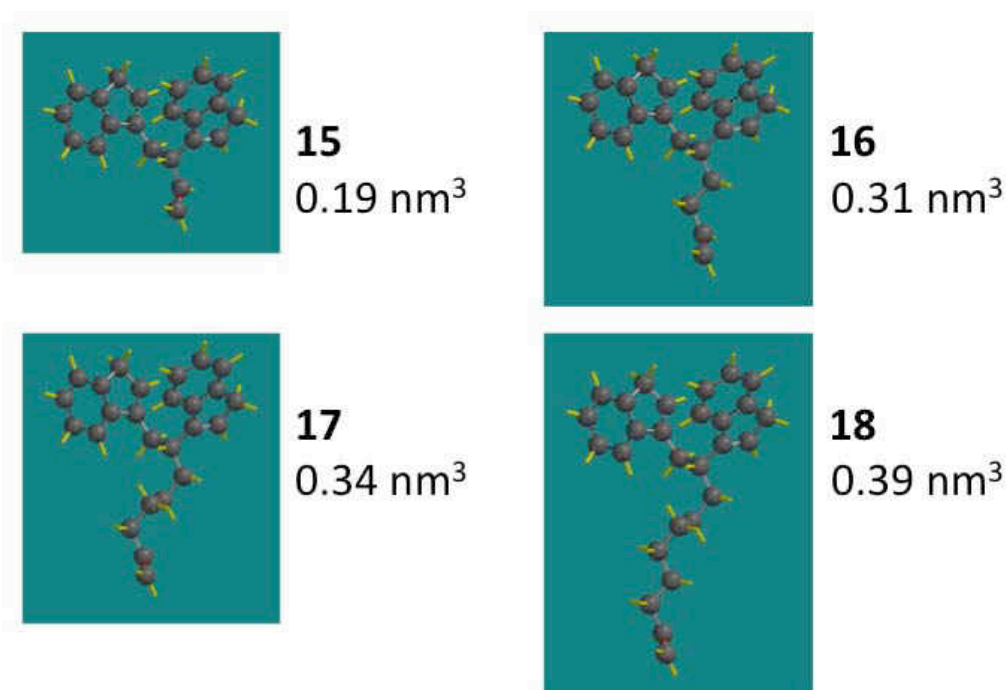


Figure 9. The Volumes of the Ligand Molecules.

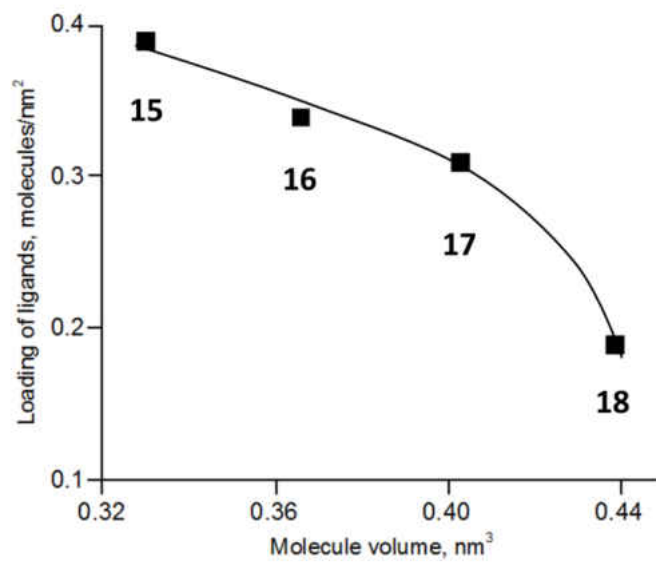


Figure 10. Dependence of the Ligand Loading on the Molecular Size.

BIBLIOGRAPHY

1. Vassilyev, O; Panarello, A.; Khinast, J. Development of Heterogeneous Titanocene Catalysts for Stereo-Selective Reductions. Rutgers University, New Brunswick, NJ. Grant Proposal, 2005.
2. Panarello, A. Ethylene-Bis(Indenyl) Catalytic Complexes: Efficient Synthesis, Introduction of the Active Metal Species and Immobilization. Ph.D. Dissertation, Rutgers, The State University of New Jersey, New Brunswick, NJ, 2005.
3. Jang, Y.; Wang, J.; Kim, J.; Kwon, H.; Yeo, N.; Lee, B. Levocetirizine Inhibits Rhinovirus-Induced ICAM-1 and Cytokine Expression and Viral Replication in Airway Epithelial Cells. *Antiviral. Res.* **2009**, *81*, 226-233.
4. Shankar, S.; Dube, M.; Gorski, J.; Klaunig, J.; Steinberg, H. Indinavir Impairs Endothelial Function in Healthy HIV-Negative Men. *Am. Heart J.* **2005**, *150*, 933.
5. Teo, S.; Colburn, W.; Tracewell, W.; Kook, K.; Stirling, D.; Iaworsky, M.; Scheffler, M.; Thomas, S.; Laskin, O. Clinical Pharmacokinetics of Thalidomide. *Clin. Pharmacokinet.* **2004**, *43*, 311-327.
6. Sinnema, P. Carbon-Bridged Cyclopentadienyl Amido Group 4 Metal Complexes, Ligand Tuning and Olefin Polymerization. Ph.D. Dissertation, University of Groningen, Groningen, The Netherlands, 1999.
7. Duthaler, R.; Hafner, A. Chiral Titanium Complexes for Enantioselective Addition of Nucleophiles to Carbonyl Groups. *Chem. Rev.* **1992**, *92*, 807-832.
8. Halterman, R. Synthesis and Applications of Chiral Cyclopentadienylmetal Complexes. *Chem. Rev.* **1992**, *92*, 965-994.

9. Paquette, L.; Sivik, M.; Bzowej, E.; Stanton, K. Catalytic Enantioselective Hydrogenation of 1,1-Disubstituted Alkenes with Optically Active Titanocene and Zirconocene Complexes Containing either Identical or Different Ligands. *Organometallics*. **1995**, *14*, 4865-4878.
10. Troutman, M.; Appella, D.; Buchwald, S. Asymmetric Hydrogenation of Unfunctionalized Tetrasubstituted Olefins with a Cationic Zirconocene Catalyst. *J. Am. Chem. Soc.* **1999**, *121*, 4916-4917.
11. Noyori, R. *Asymmetric Catalysis in Organic Synthesis*; Wiley: New York, 1994; pp 16-94.
12. Seyden-Penne, J. *Chiral Auxiliaries and Ligands in Asymmetric Synthesis*; Wiley: New York, 1995; pp 367-388.
13. Broene, R.; Buchwald, S. Asymmetric Hydrogenation of Unfunctionalized Trisubstituted Olefins with a Chiral Titanocene Catalyst. *J. Am. Chem. Soc.* **1993**, *115*, 12569-12570.
14. Jordan, R.; Bajgur, C.; Dasher, W.; Rheingold, A. Hydrogenation of Cationic Dicyclopentadienylzirconium(IV) Alkyl Complexes. Characterization of Cationic Zirconium(IV) Hydrides. *Organometallics* **1987**, *6*, 1041-1051.
15. Waymouth, R.; Pino, P. Enantioselective Hydrogenation of Olefins with Homogeneous Ziegler-Natta Catalysts. *J. Am. Chem. Soc.* **1990**, *112*, 4911-4914.
16. Grossman, R.; Doyle, R.; Buchwald, S. Syntheses of [Ethylene-1,2-Bis(η -5-4,5,6,7-tetrahydro-1-indenyl)]Zirconium and -Hafnium Hydride Complexes. Improved Syntheses of the Corresponding Dichlorides. *Organometallics* **1991**, *10*, 1501-1505.
17. Halterman, R.; Ramsey, T. Asymmetric Synthesis of a Sterically Rigid Binaphthyl-Bridged Chiral Metallocene: Asymmetric Catalytic Epoxidation of Unfunctionalized Alkenes. *Organometallics* **1993**, *12*, 2879-2880.

18. Vassilyev, O.; Panarello, A.; Khinast, J. Enantioselective Hydrogenations with Chiral Titanocenes. *Molecules* **2005**, *10*, 587-619.
19. Horton, A.; Frijns, J. BPh₄⁻ as a Ligand in Cationic Zirconium Complexes: Novel Bonding Mode and Fluxionality. *Angew. Chem. Int. Ed. Engl.* **1991**, *30*, 1152-1154.
20. Willoughby, C.; Buchwald, S. Catalytic Asymmetric Hydrogenation of Imines with a Chiral Titanocene Catalyst: Scope and Limitations. *J. Am. Chem. Soc.* **1994**, *116*, 8952-8965.
21. Willoughby, C.; Buchwald, S. Synthesis of Highly Enantiomerically Enriched Cyclic Amines by the Catalytic Asymmetric Hydrogenation of Cyclic Imines. *J. Org. Chem.* **1993**, *58*, 7627-7629.
22. Bakos, J.; Orosz, A.; Heil, B.; Laghmari, M.; Lhoste, P.; Sinou, D. Rhodium(I)-Sulfonated-BDPP Catalysed Asymmetric of Imines in Aqueous-Organic Two-Phase Solvent Systems. *J. Chem. Soc., Chem. Commun.* **1991**, *23*, 1684-1685.
23. Spindler, F.; Pugin, B.; Blaser, H. Novel Diphosphinoiridium Catalysts for the Enantioselective Hydrogenation of N-Arylketimines. *Angew. Chem. Int. Ed. Engl.* **1990**, *29*, 558-559.
24. Chan, Y.; Osborn, J. Iridium(III) Hydride Complexes for the Catalytic Enantioselective Hydrogenation of Imines. *J. Am. Chem. Soc.* **1990**, *112*, 9400-9401.
25. Oppolzer, W.; Wills, M.; Starkeman, C.; Bernardinelli, G. Chiral Toluene-2,α-Sultam Auxillaries: Preparation and Structure of Enantiomerically Pure (2R) and (S)-Ethyl-2,1'-Sultam. *Tetrahedron Lett.* **1990**, *31*, 4117-4120.
26. Kang, G.; Cullen, W.; Fryzuk, M.; James, B.; Kutney, J. Rhodium(I)-Catalysed Asymmetric Hydrogenation of Imines. *J. Chem. Soc., Chem. Commun.* **1988**, *22*, 1466-1467.

27. Becker, R.; Brunner, H.; Mahboobi, S.; Wiegrebe, W. Enantioselective Hydrosilylation of Prochiral 3,4-Dihydro-2H-Pyrrole Derivatives. *Angew. Chem. Int. Ed. Engl.* **1985**, *24*, 995-996.
28. Kagan, H.; Langlois, N.; Dang, T. Asymmetric Reduction Catalyzed by Complexes of Transition Metals IV. Synthesis of Chiral Amines by Means of a Rhodium Complex and Isopropylidene Dihydroxy-2,3-Bis(diphenylphosphino)-1,4-butane(diop). *J. Organomet. Chem.* **1975**, *90*, 353-365.
29. Burk, M.; Feaster, J. Enantioselective Hydrogenation of the C:N Group: A Catalytic Asymmetric Reductive Amination Procedure. *J. Am. Chem. Soc.* **1992**, *114*, 6266-6267.
30. Becalski, A.; Cullen, W.; Fryzuk, M.; James, B.; Kang, G.; Rettig, S. Catalytic Asymmetric Hydrogenation of Imines. Use of Rhodium(I)/Phosphine Complexes and Characterization of Rhodium(I)/Imine Complexes. *J. Inorg. Chem.* **1991**, *30*, 5002-5008.
31. Bercaw, J.; Brintzinger, H. Di- μ -Hydrido-Bis(Cyclopentadienyltitanium(III)), a Transition Metal Complex with a Diborane-Like Double Hydrogen Bridge. *J. Am. Chem. Soc.* **1969**, *91*, 7301-7306.
32. Bercaw, J.; Marvich, R.; Bell, L.; Brintzinger, H. Titanocene as an Intermediate in Reactions Involving Molecular Hydrogen and Nitrogen. *J. Am. Chem. Soc.* **1972**, *94*, 1219-1238.
33. Pattiasina, J.; Bolhuis, F.; Teuben, J. Titanium Hydride Formation through Hydrogen Transfer from 2-Methylpyridine to a Titanium Fulvene Compound; the First Structurally Characterized Terminal Titanium Hydride. *Angew. Chem. Int. Ed. Engl.* **1987**, *26*, 330-331.
34. Wild, F.; Zsolnai, J.; Huttner, G.; Brintzinger, H. Ansa-Metallocene Derivatives: IV. Synthesis and Molecular Structures of Chiral Ansa-Titanocene Derivatives with Bridged Tetrahydroindenyl Ligands. *J. Organomet. Chem.* **1982**, *232*, 233-247.

35. Willoughby, C.; Buchwald, S. Asymmetric Titanocene-Catalyzed Hydrogenation of Imines. *J. Am. Chem. Soc.* **1992**, *114*, 7562-7564.
36. Harada, K. In *Chemistry of the Carbon-Nitrogen Double Bond*; Patai, S., Ed.; Interscience: London, 1970; pp 364-383.
37. Spaltenstein, E.; Palma, P.; Kreutzer, K.; Willoughby, C.; Davis, W.; Buchwald, S. Preparation and X-Ray Structure of Cp₂Ti(Ph₂SiH₂)(PMe₃). *J. Am. Chem. Soc.* **1994**, *116*, 10308-10309.
38. Xin, S.; Harrod, J.; Samuel, E. Synthesis and Structure of Rac-Bis{[1,2-Bis(Tetrahydroindenyl)ethane](.mu.-Hydrido)Titanium(III)}: An Antiferromagnetic Ti(III) Hydride Dimer. *J. Am. Chem. Soc.* **1994**, *116*, 11562-11563.
39. Aitken, C.; Harrod, J.; Samuel, E. Identification of some Intermediates in the Titanocene-Catalyzed Dehydrogenative Coupling of Primary Organosilanes. *J. Am. Chem. Soc.* **1986**, *108*, 4059-4066.
40. Carter, M.; Schiott, B.; Gutierrez, A.; Buchwald, S. Enantioselective Hydrosilylation of Ketones with a Chiral Titanocene Catalyst. *J. Am. Chem. Soc.* **1994**, *116*, 11667-11670.
41. Kaminsky, W.; Kulper, K.; Wild, F.; Brintzinger, H. Polymerization of Propene and Butene with a Chiral Zirconocene and Methylaluminumoxane as Cocatalyst. *Angew. Chem. Int. Ed. Engl.* **1985**, *24*, 507-508.
42. Mallin, D.; Rausch, M.; Chien, J.; Rieger, B.; Mu, X. Degree of Stereochemical Control of Racemic Ethylenebis(indenyl)zirconium Dichlorides/Methyl Aluminumoxane Catalyst and Properties of Anisotactic Polypropylenes. *Macromolecules* **1990**, *23*, 3559-3568.

43. Spaleck, W.; Kuber, F.; Bachmann, B.; Antberg, M.; Dolle, V.; Rohrmann, J.; Winter, A.; Paulus, E. The Influence of Aromatic Substituents on the Polymerization Behavior of Bridged Zirconocene Catalysts. *Organometallics* **1994**, *13*, 954-963.
44. Ewen, J.; Jones, R.; Razavi, A.; Ferrara J. Syndiospecific Propylene Polymerizations with Group IVB Metallocenes. *J. Am. Chem. Soc.* **1988**, *110*, 6255-6256.
45. Ewen, J.; Elder, M.; Jones, R.; Curtis, S.; Cheng, H. In *Catalytic Olefin Polymerization: Proceedings of the International Symposium on Recent Developments in Olefin Polymerization Catalysts*, Keii, T.; Soga, K. Eds., Elsevier, Amsterdam, 1989, 439.
46. Razavi, J.; Atwood, J. Preparation and Structures of the Complexes (η^5 -C₅H₄CPh₂- η^5 -C₁₃H₈) MCl₂ (M = Zr, Hf) *J. Organomet. Chem.* **1993**, *459*, 117-123.
47. Ewen, J.; Elder, M. *Eur. Pat. Appl.* 1993, EP-A 0537130.
48. Hlatky, G.; Turner, H.; Eckman, R. Ionic, Base-Free Zirconocene Catalysts for Ethylene Polymerization. *J. Am. Chem. Soc.* **1989**, *111*, 2728-2729.
49. Chien, J.; Tsai, W.; Rausch, M. Isospecific Polymerization of Propylene Catalyzed by Rac-Ethylenebis(indenyl)methylzirconium Cation. *J. Am. Chem. Soc.* **1991**, *113*, 8570-8571.
50. Jordan, R. Chemistry of Cationic Dicyclopentadienyl Group 4 Metal-Alky I Complexes. *Adv. Organomet. Chem.* **1991**, *32*, 325-387.
51. Marks, T. Surface-Bound Metal Hydrocarbyls. Organometallic Connections Between Heterogeneous and Homogeneous Catalysis. *J. Acc. Chem. Res.* **1992**, *25*, 57-65.
52. Kesti, M.; Coates, G.; Waymouth, R. Homogeneous Ziegler-Natta Polymerization of Functionalized Monomers Catalyzed by Cationic Group IV Metallocenes. *J. Am. Chem. Soc.* **1992**, *114*, 9679-9680.

53. Bochmann, M. Cationic Group 4 Metallocene Complexes and Their Role in Polymerisation Catalysis: The Chemistry of Well-Defined Ziegler Catalysts. *J. Chem. Soc. Dalton Trans.* 1996, 3, 255-270.
54. Fink, G.; Schnell, D.; Elementary Processes of the Ziegler Catalysis. II. Molecular Weight Distribution and Reaction Scheme. *Angew. Makromol. Chem.* **1982**, 105, 15-30.
55. Fink, G.; Fenzi, W.; Mynott, R. Ethylene Insertion with Soluble Ziegler Catalysts: Direct Insight into the Reaction Using Enriched Ethylene-¹³C and Carbon-13 NMR Spectroscopy. II. The System Cp₂TiMeCl/AlMeCl₂/¹³C₂H₄. *Z. Naturforsch.* **1985**, 40b, 158-166.
56. Mynott, R.; Fink, G.; Fenzl, W. Ethylene Insertion with Soluble Ziegler Catalysts. III. The System Cp₂TiMeCl/AlMe₂Cl/¹³C₂H₄ Studied by ¹³C-NMR Spectroscopy. The Time-Development of Chain Propagation and Oligomer Distribution. *Angew. Makromol. Chem.* **1987**, 154, 1-21.
57. Dyachkovski, F.; Shilova, A.; Silov, A. The Role of Free Ions in Reactions of Olefins with Soluble Complex Catalysts. *J. Polym. Sci., Part C* **1967**, 16, 2333-2339.
58. Eisch, J.; Plotrowsky, A.; Brownstein, S.; Gabe, E.; Lee, F. Organometallic Compounds of Group III. Part 41. Direct Observation of the Initial Insertion of an Unsaturated Hydrocarbon into the Titanium-Carbon Bond of the Soluble Ziegler Polymerization Catalyst Cp₂TiCl₂-MeAlCl₂. *J. Am. Chem. Soc.* **1985**, 107, 7410-7221.
59. Jordan, R.; Bajgur, C.; Willett, R.; Scott, B. Ethylene Polymerization by a Cationic Dicyclopentadienyl Zirconium(IV) Alkyl Complex. *J. Am. Chem. Soc.* **1986**, 108, 7410-7411.
60. Cossee, P. Ziegler-Natta Catalysis I. Mechanism of Polymerization of α -Olefins with Ziegler-Natta Catalysts. *J. Catal.* **1964**, 3, 80-88.

61. Arlman, E.; Cossee, P. Ziegler-Natta Catalysis III. Stereospecific Polymerization of Propene with the Catalyst System $\text{TiCl}_3 \cdot \text{AlEt}_3$. *J. Catal.* **1964**, *3*, 99-104.
62. Watson, P. Ziegler-Natta Polymerization: The Lanthanide Model. *J. Am. Chem. Soc.* **1982**, *104*, 337-339.
63. Watson, P.; Roe, D. Beta-Alkyl Transfer in a Lanthanide Model for Chain Termination. *J. Am. Chem. Soc.* **1982**, *104*, 6471-6473.
64. Watson, P.; Parshall, G. Organolanthanides in Catalysis. *Acc. Chem. Res.* **1985**, *18*, 51-56.
65. Jeske, G.; Lauke, H.; Mauermann, H.; Swepton, P.; Schumann, H.; Marks, T. Highly Reactive Organolanthanides. A Mechanistic Study of Catalytic Olefin Hydrogenation by Bis(pentamethylcyclopentadienyl) and Related 4f Complexes. *J. Am. Chem. Soc.* **1985**, *107*, 8111-8118.
66. Thompson, M.; Baxter, S.; Bulls, A.; Burger, B.; Nolan, M.; Santarsiero, B.; Schaefer, W.; Bercaw, J. Sigma-Bond Metathesis for Carbon-Hydrogen Bonds of Hydrocarbons and Sc-R (R = H, Alkyl, Aryl) Bonds of Permethylscandocene Derivatives. Evidence for Noninvolvement of the Pi-System in Electrophilic Activation of Aromatic and Vinylic C-H Bonds. *J. Am. Chem. Soc.* **1987**, *109*, 203-219.
67. Bunel, E.; Burger, B.; Bercaw, J. Carbon-Carbon Bond Activation Via Beta-Alkyl Elimination. Reversible Branching of 1,4-Pentadienes Catalyzed by Scandocene Hydride Derivatives. *J. Am. Chem. Soc.* **1988**, *110*, 976-978.
68. Burger, B.; Thompson, M.; Cotter, W.; Bercaw, J. Ethylene Insertion and Beta-Hydrogen Elimination for Permethylscandocene Alkyl Complexes. A Study of the Chain Propagation and Termination Steps in Ziegler-Natta Polymerization of Ethylene. *J. Am. Chem. Soc.* **1990**, *112*, 1566-1577.

69. Corey, E.; Jones, G. Enantioselective Route to α -Hydroxy Aldehyde and Acid Derivatives. *Tetrahedron Lett.* **1991**, *32*, 5713-5716.
70. Corey, E.; Cimprich, K. Highly Enantioselective Alkynylation of Aldehydes Promoted by Chiral Oxazaborolidines. *J. Am. Chem. Soc.* **1994**, *116*, 3151-3152.
71. Keck, G.; Krishnamurthy, D.; Chen, X. Asymmetric Synthesis of Homopropargylic Alcohols from Aldehydes and Allenyltri-*n*-butylstannane. *Tetrahedron Lett.* **1994**, *35*, 8323-8324.
72. Rodewald, S.; Jordan, R. Stereoselective Olefin Insertion Reactions of Chiral (EBI)Zr(.eta.2-pyrid-2-yl)⁺ and (EBTHI)Zr(.eta.2-pyrid-2-yl)⁺ Complexes. *J. Am. Chem. Soc.* **1994**, *116*, 4491-4492.
73. Coates, G.; Waymouth, R. Enantioselective Cyclopolymerization: Optically Active Poly(methylene-1,3-cyclopentane). *J. Am. Chem. Soc.* **1991**, *113*, 6270-6271.
74. Coates, G.; Waymouth, R. Enantioselective Cyclopolymerization of 1,5-Hexadiene Catalyzed by Chiral Zirconocenes: A Novel Strategy for the Synthesis of Optically Active Polymers with Chirality in the Main Chain. *J. Am. Chem. Soc.* **1993**, *115*, 91-98.
75. Hong, Y.; Kuntz, B.; Collins, S. Asymmetric Induction in the Diels-Alder Reaction Using Chiral Metallocene Catalysts. *Organometallics* **1993**, *12*, 964-969.
76. Jaquith, J.; Guan, J.; Wang, S.; Collins, S. Asymmetric Induction in the Diels-Alder Reaction Catalyzed by Chiral Metallocene Triflate Complexes: Dramatic Effect of Solvent Polarity. *Organometallics* **1995**, *14*, 1079-1081.
77. Morken, J.; Didiuk, M.; Hoveyda, A. Zirconium-Catalyzed Asymmetric Carbomagnesation. *J. Am. Chem. Soc.* **1993**, *113*, 6997-6998.
78. Morken, J.; Didiuk, M.; Visser, M.; Hoveyda, A. Zirconium-Catalyzed Kinetic Resolution of Pyrans. *J. Am. Chem. Soc.* **1994**, *116*, 3123-3124.

79. Lee, N.; Buchwald, S. Asymmetric Hydrogenation of Enamines with a Chiral Titanocene Catalyst. *J. Am. Chem. Soc.* **1994**, *116*, 5985-5986.
80. Kesti, M.; Waymouth, R. Group 4 Metallocene Olefin Hydrosilylation Catalysts. *Organometallics* **1992**, *11*, 1095-1103.
81. Verdaguer, X.; Lange, U.; Reading, M.; Buchwald, S. Highly Enantioselective Imine Hydrosilylation Using (*S,S*)-Ethylenebis(η^5 -tetrahydroindenyl)titanium Difluoride. *J. Am. Chem. Soc.* **1996**, *118*, 6784-6785.
82. Grossmann, R.; Davis, W.; Buchwald, S. Enantioselective, Zirconium-Mediated Synthesis of Allylic Amines. *J. Am. Chem. Soc.* **1991**, *113*, 2321-2322.
83. Coletti, S.; Halterman, R. Asymmetric Epoxidation of Unfunctionalized Alkenes Using the New C_2 -Symmetrical 1,1'-Binaphthyl-2,2'-Dimethylene Bridged Ansa-Bis(1-Indenyl)Titanium Dichloride Catalyst. *Tetrahedron Lett.* **1992**, *33*, 1005-1008.
84. Halterman, R.; Ramsey, T.; Pailes, N.; Khan, M. Application of the Double Pauson-Khand Cyclization to the Synthesis of Bis(cyclopentadienes): Preparation of Phenyl-Bridged Bis(tetrahydroindenyl)Titanium and Zirconium Dichlorides. *J. Organomet. Chem.* **1995**, *497*, 45-53.
85. Halterman, R.; Schumann, H.; Dubner, F. Synthesis and Structure of Ansa-Metallocene Complexes (M = ZrCl₂, TiCl₂, YCl, and LuCl) Containing the Bis(2-methyl-4,5,6,7-tetrahydroinden-yl)dimethylsilane Ligand. *J. Organomet. Chem.* **2000**, *604*, 12-19.
86. Panarello, A.; Vassilyev, O.; Khinast, J. Use of Oxirane Ring-Opening Reactions for Synthesis of Ethylene-Bis(indenyl) Ligands Containing Alkene Tethers. *Synlett* **2005**, *5*, 797-800.

87. Abramson, S.; Baiker, A.; Bayston, D.; Bellocq, N.; Bergbreiter, D.; Blaser, H.; Brunel, D.; Cocu, F.; De Bruyn, M.; De Vos, D.; Hanson, B.; Jacobs, P.; Lasperas, M.; Mandoli, A.; Moreau, P.; Parvulescu, V.; Petri, A.; Pini, D.; Polywka, M.; Pugin, B.; Rasor, P.; Salvadori, P.; Studer, M.; Sugimura, T.; Tai, A.; Vankelecom, I.; Wells, P.; Wells, R. In *Chiral Catalyst Immobilization and Recycling*; De Vos, D.; Vankelecom, I.; Jacobs, P., Eds.; Wiley: Weinheim, 2000.
88. Haag, M.; Dupont, J.; Stedile, F.; Dos Santos, J. Metallocene Catalyst Supported on Chemically Modified Silica for Production of Ethylene–Propylene Copolymers. *J. Mol. Catal. A: Chem.* **2003**, *197*, 223-232.
89. Marques, M.; Pombo, C.; Silva, R.; Conte, A. Binary Metallocene Supported Catalyst for Propylene Polymerization. *Eur. Polym. J.* **2003**, *39*, 561-567.
90. Herrmann, W.; Cornils, B. *Appl. Homogen. Catal. With Organomet. Comp.* **1996**, *2*, 1167-1197.
91. Pomogailo, A. Catalysis by Heterogenized Metal Polymers: Advances and Prospects. *Kinet. Catal.* **2004**, *45*, 61-104.
92. Abbenhuis, H. Heterogenization of Metallocene Catalysts for Alkene Polymerization. *Angew. Chem. Int. Ed. Engl.* **1999**, *38*, 1058-1060.
93. Carnahan, E.; Jacobsen, G. Supported Metallocene Catalysts. *CATTECH* **2000**, *4*, 74-88.
94. Severn, J.; Chadwick, J.; Duchateau, R.; Friedericks, N. Bound but Not Gagged – Immobilizing Single-Site α -Olefin Polymerization Catalysts. *Chem. Rev.* **2005**, *105*, 4073-4147.

95. Langner, A.; Panarello, A.; Rivillon, S.; Vassilyev, O.; Khinast, J.; Chabal, Y. Controlled Silicon Surface Functionalization by Alkene Hydrosilylation. *J. Am. Chem. Soc.* **2005**, *127*, 12798-12799.
96. Cicero, R.; Linford, M.; Chidsey, C. Photoreactivity of Unsaturated Compounds with Hydrogen-Terminated Silicon(111). *Langmuir* **2000**, *16*, 5688-5695.
97. Buriak, J. Organometallic Chemistry on Silicon and Germanium Surfaces. *Chem. Rev.* **2002**, *102*, 1271-1308.
98. Tertykh, V.; Dabrowski, A. *Adsorption on New and Modified Inorganic Sorbents*; Elsevier: New York, 1996: Vol. 99.
99. Terry, J.; Linford, M.; Wigren, C.; Cao, R.; Pianetta, P.; Chidsey, C. Determination of the Bonding of Alkyl Monolayers to the Si(111) Surface Using Chemical-Shift, Scanned-Energy Photoelectron Diffraction. *Appl. Phys. Lett.* **1997**, *71*, 1056-1058.
100. Terry, J.; Linford, M.; Wigren, C.; Cao, R.; Pianetta, P.; Chidsey, C. Alkyl-Terminated Si(111) Surfaces: A High-Resolution, Core Level Photoelectron Spectroscopy Study. *J. Appl. Phys.* **1999**, *85*, 213-221.
101. Stewart, M.; Buriak, J. Chemical and Biological Applications of Porous Silicon Technology. *Adv. Mater.* **2000**, *12*, 859-869.
102. Stewart, M.; Buriak, J. Exciton-Mediated Hydrosilylation on Photoluminescent Nanocrystalline Silicon. *J. Am. Chem. Soc.* **2001**, *123*, 7821-7830.
103. Panarello, A.; Khinast, J. Synthesis of a Novel Ethylene-Bis(tetrahydroindenyl) Ligand Containing a Functionalized Four-Carbon Tether. *Tetrahedron Lett.* **2003**, *44*, 4095-4098.

104. Panarello, A.; Vassilyev, O.; Khinast, J. Selective Alkylation and Suzuki Coupling as an Efficient Strategy for Introducing Functional Anchors to the Ethylene-Bis(indenyl) Ligand. *Tetrahedron Lett.* **2005**, *46*, 1353-1356.
105. Ofunne, G.; Booth, B.; Tait, P. Characterization and Polymerization Studies on Silica-Supported Titanium (IV) Complexes. *Ind. J. Chem.* **1988**, *27A*, 1040-1046.
106. Gruber-Woelfler, H.; Rivillon Amy, S.; Chabal, Y.; Schitter, G.; Polo, E.; Ringwald, M.; Khinast, J. UV-Induced Immobilization of Tethered Zirconocenes on H-Terminated Silicon Surfaces. *Chem. Commun.* **2008**, 1329-1331.
107. Hayashi, T. In *Hydrosilylation: A Comprehensive Review on Recent Advances*, Marciniak, B., Ed.; Springer, Berlin, 2009, pp. 319-333.
108. Bateman, J.; Eagling, R.; Horrocks, B.; Houlton, A. A Deuterium Labeling, FTIR, and Ab Initio Investigation of the Solution-Phase Thermal Reactions of Alcohols and Alkenes with Hydrogen-Terminated Silicon Surfaces. *J. Phys. Chem. B* **2000**, *104*, 5557-5565.
109. Stein, J.; Lewis, L.; Gao, Y.; Scott, R. In Situ Determination of the Active Catalyst in Hydrosilylation Reactions Using Highly Reactive Pt(0) Catalyst Precursors. *J. Am. Chem. Soc.* **1999**, *121*, 3693-3703.
110. Hoyle, C.; Lee, T.; Roper, T. Thiol-enes: Chemistry of the Past with Promise for the Future. *J. Polym. Sci. A* **2004**, *42*, 5301-5338.
111. Kade, M.; Burke, D.; Hawker, C. The Power of Thiol-ene Chemistry. *J. Polym. Sci. A* **2010**, *48*, 743-750.
112. Yu, K.; Jones, C. Silica-Immobilized Zinc β -Diimine Catalysts for the Copolymerization of Epoxides and Carbon Dioxide. *Organometallics* **2003**, *22*, 2571-2580.
113. Spartan '08. Wavefunction Inc., Irvine, CA.

APPENDICES
APPENDIX A
NMR Spectrums

75

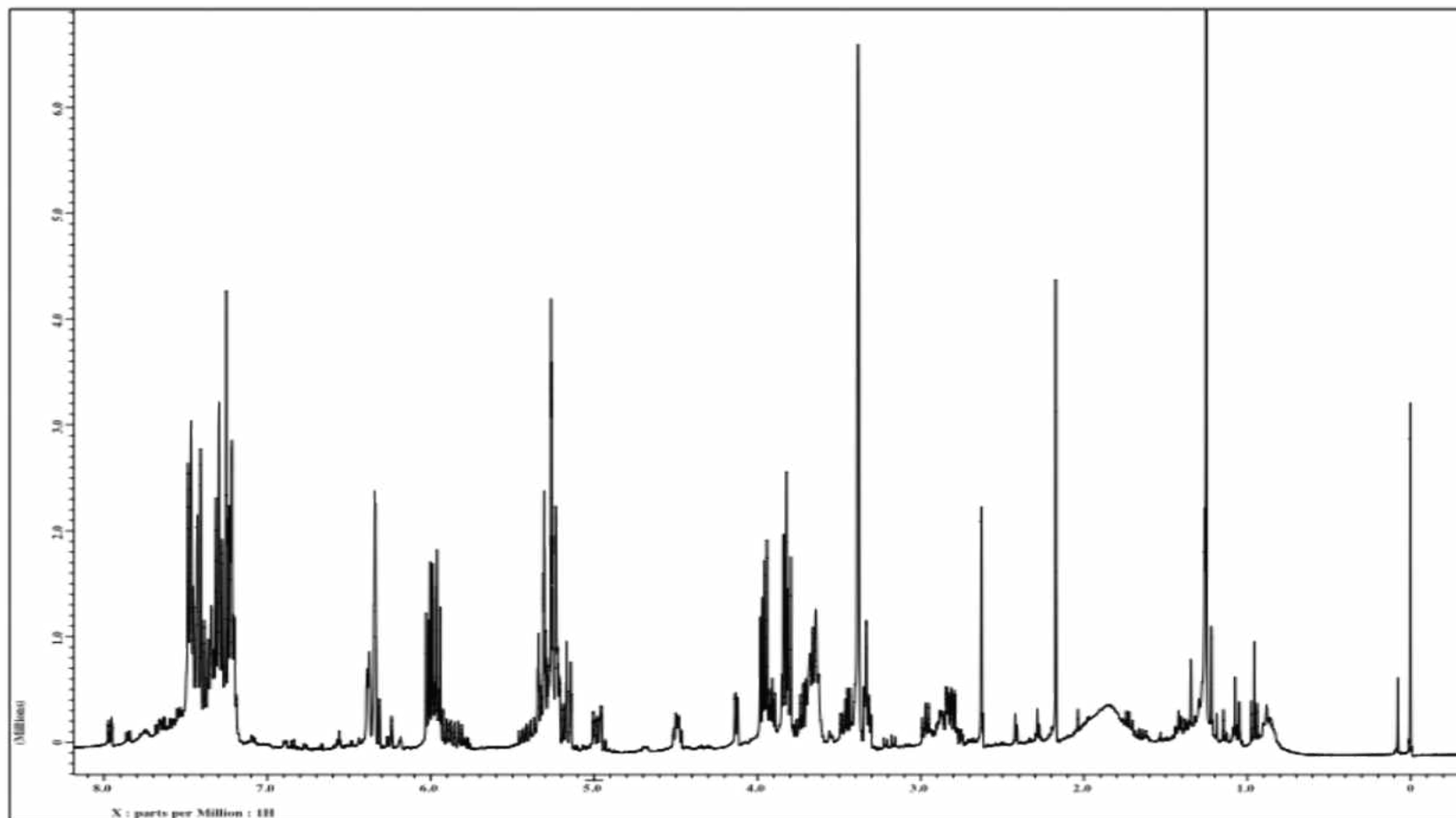


Figure 11. ^1H NMR Spectrum of 7.

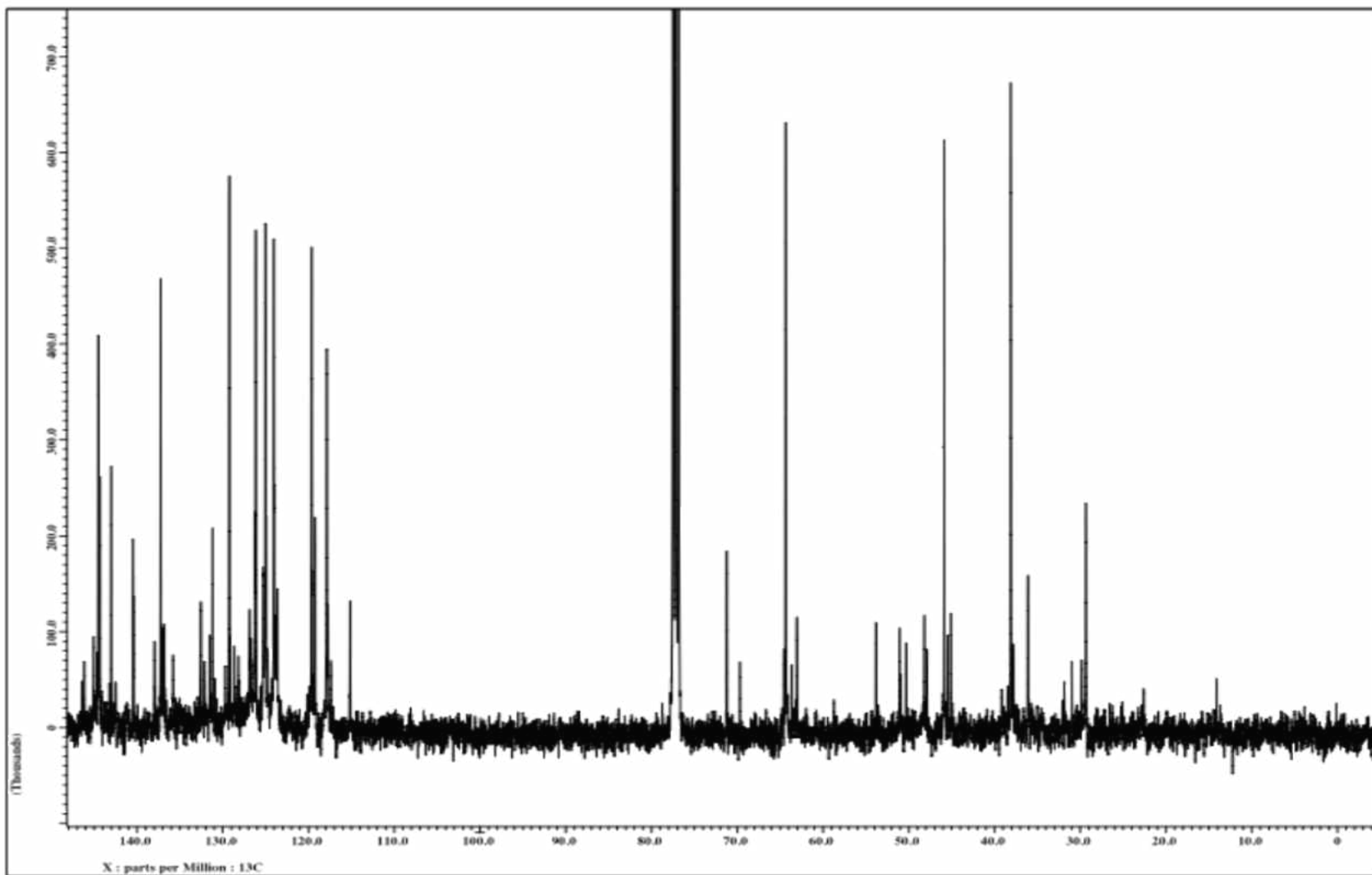


Figure 12. ^{13}C NMR Spectrum of 7.

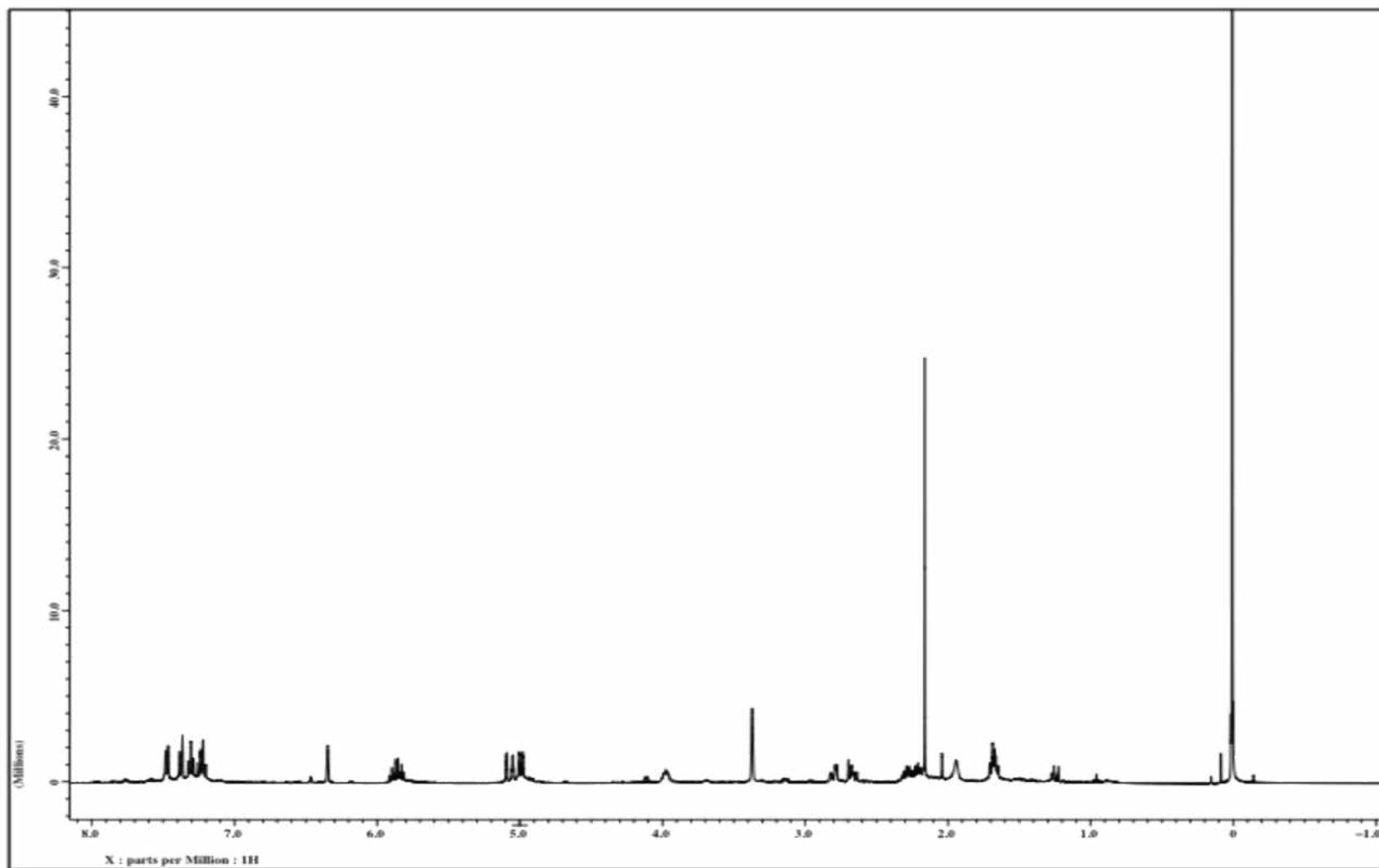


Figure 13. ^1H NMR Spectrum of **8**.

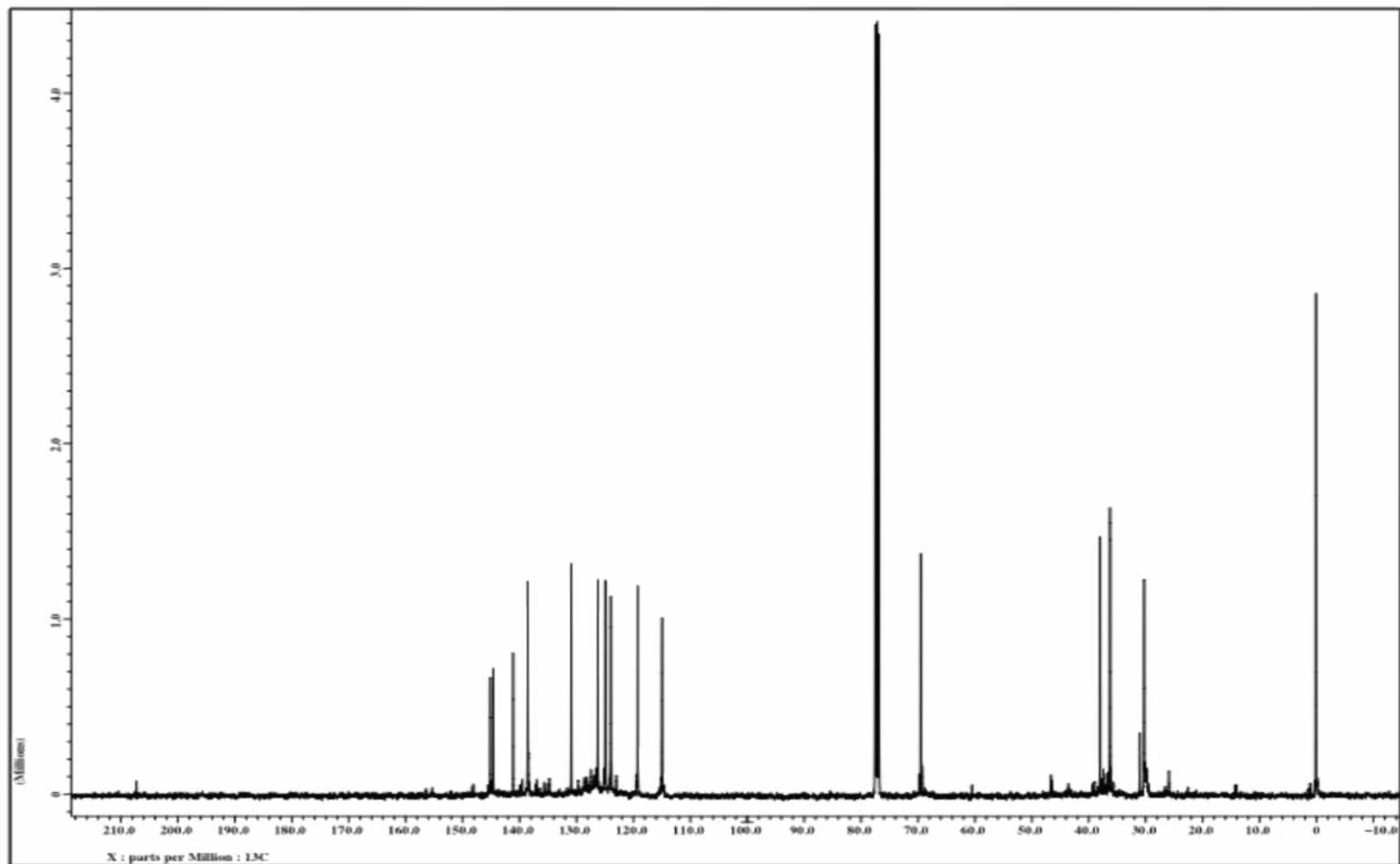


Figure 14. ^{13}C NMR Spectrum of **8**.

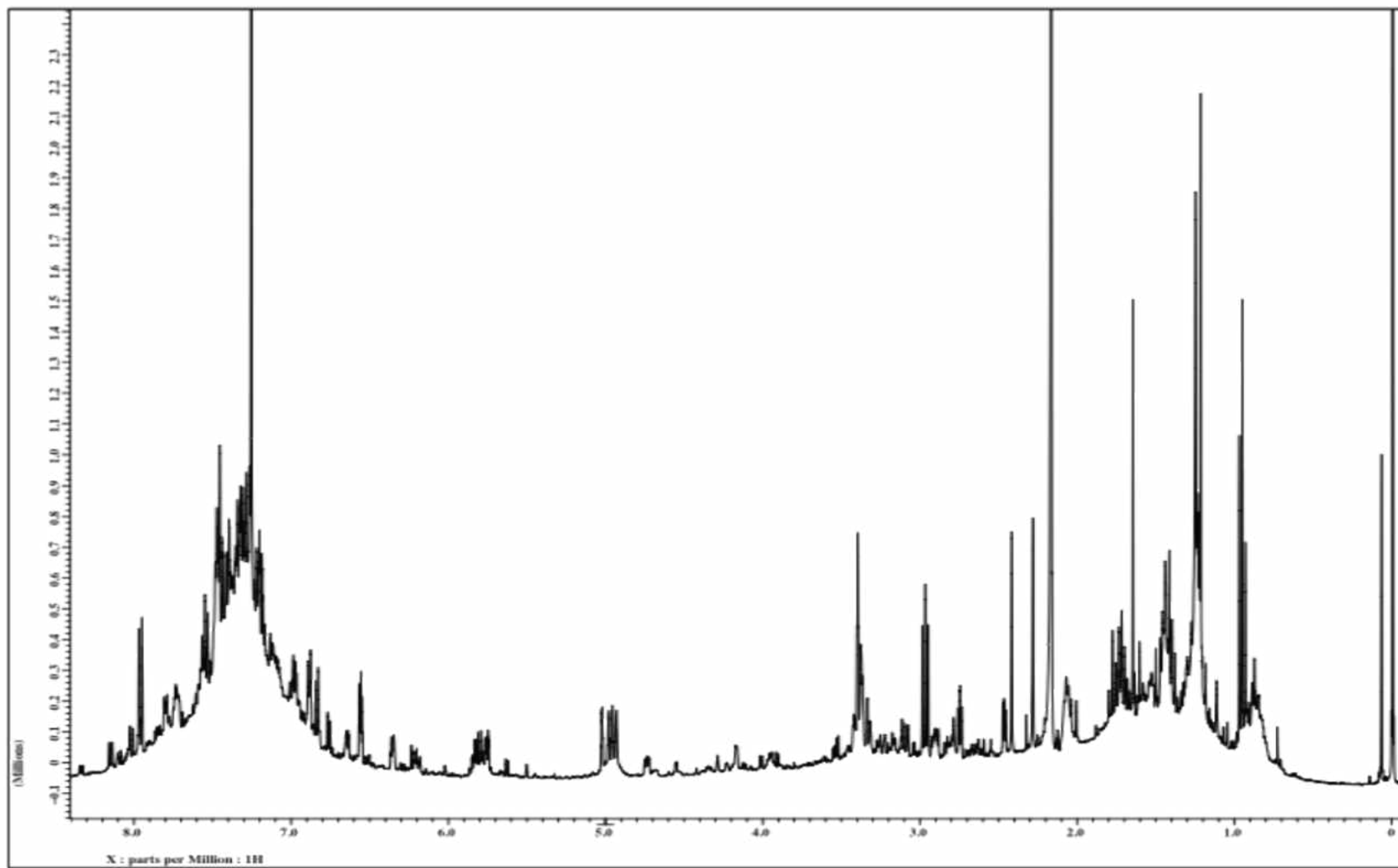


Figure 15. ^1H NMR Spectrum of **9**.

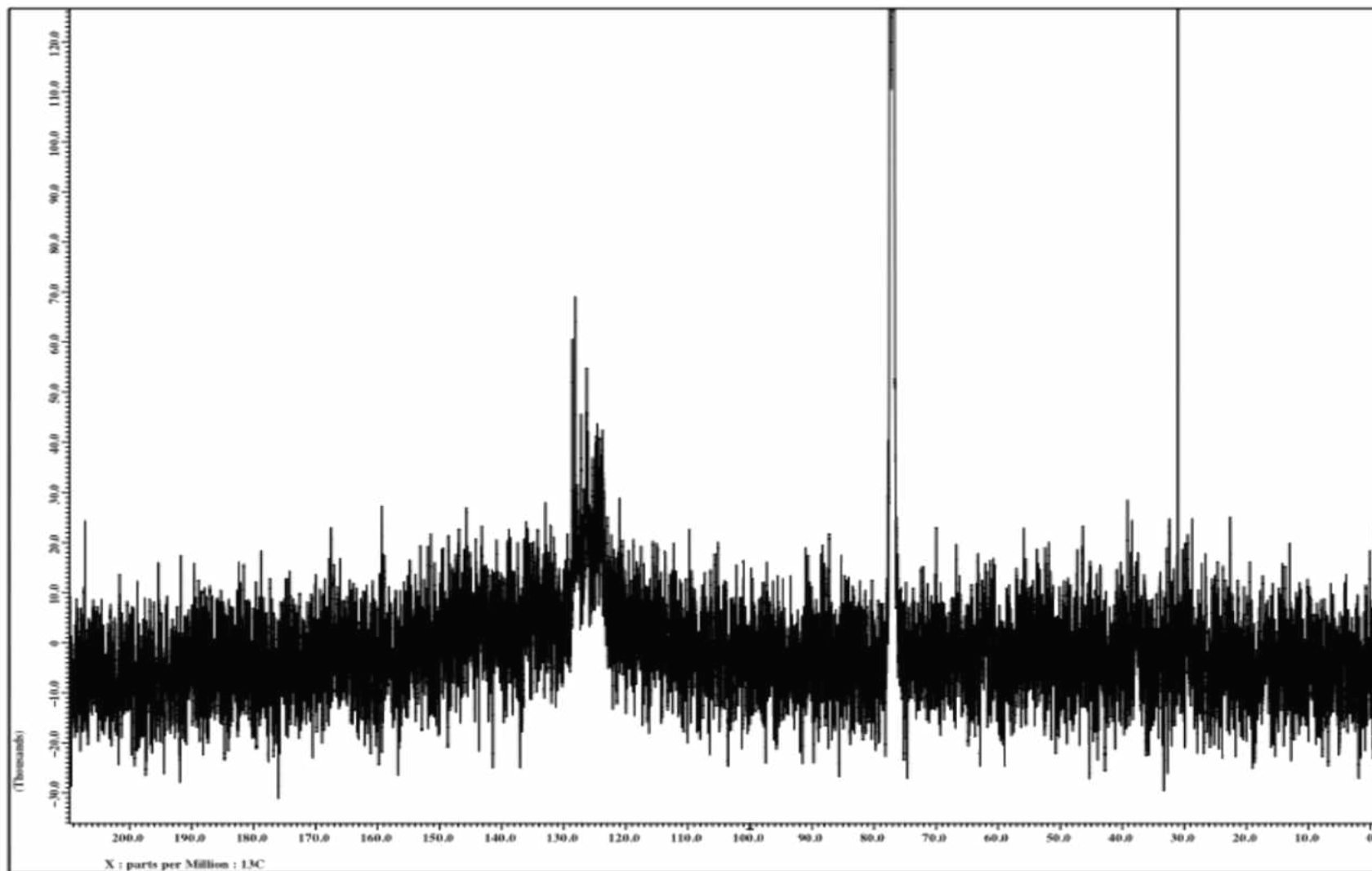


Figure 16. ^{13}C NMR Spectrum of **9**.

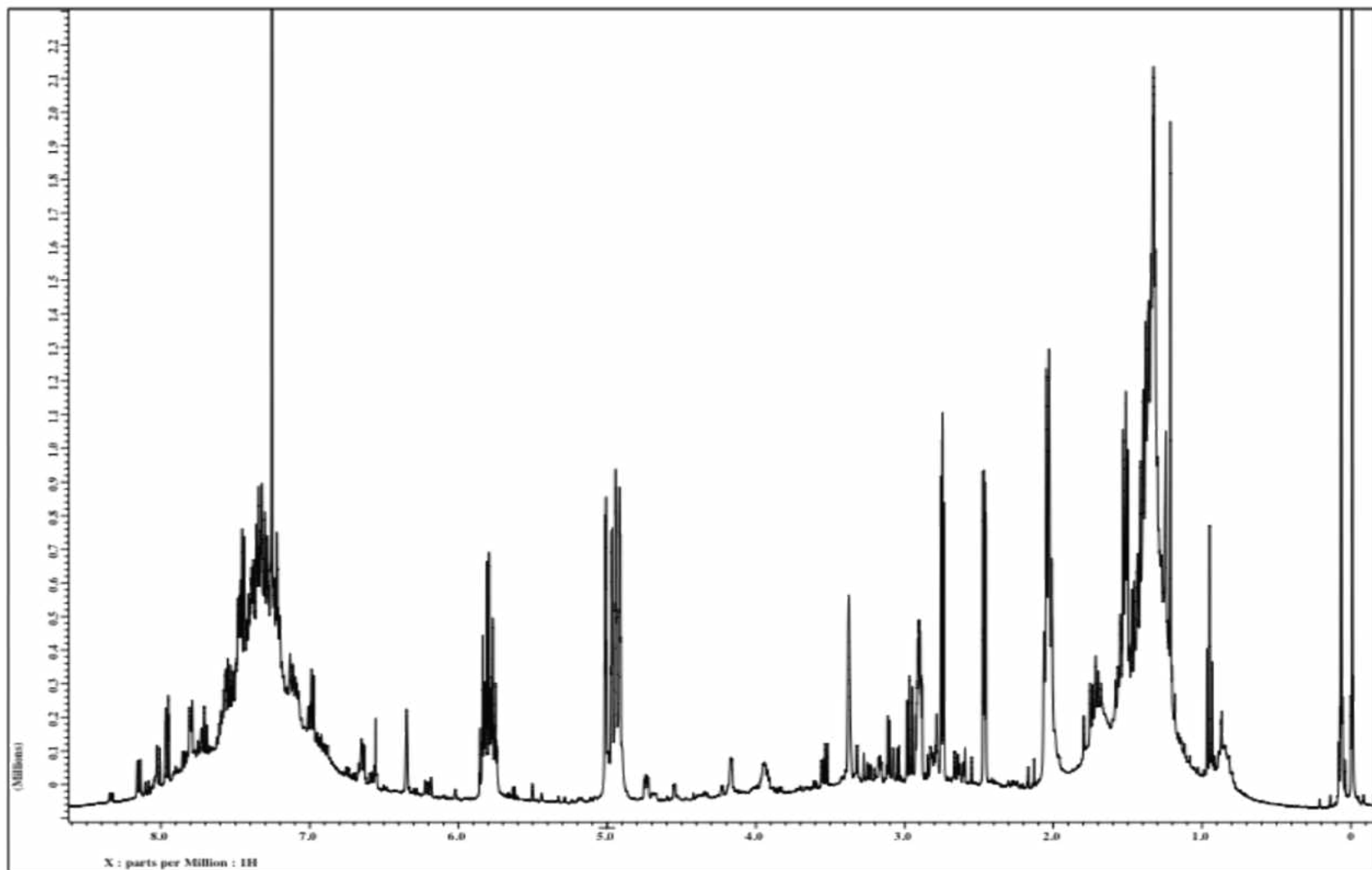


Figure 17. ^1H NMR Spectrum of 10.

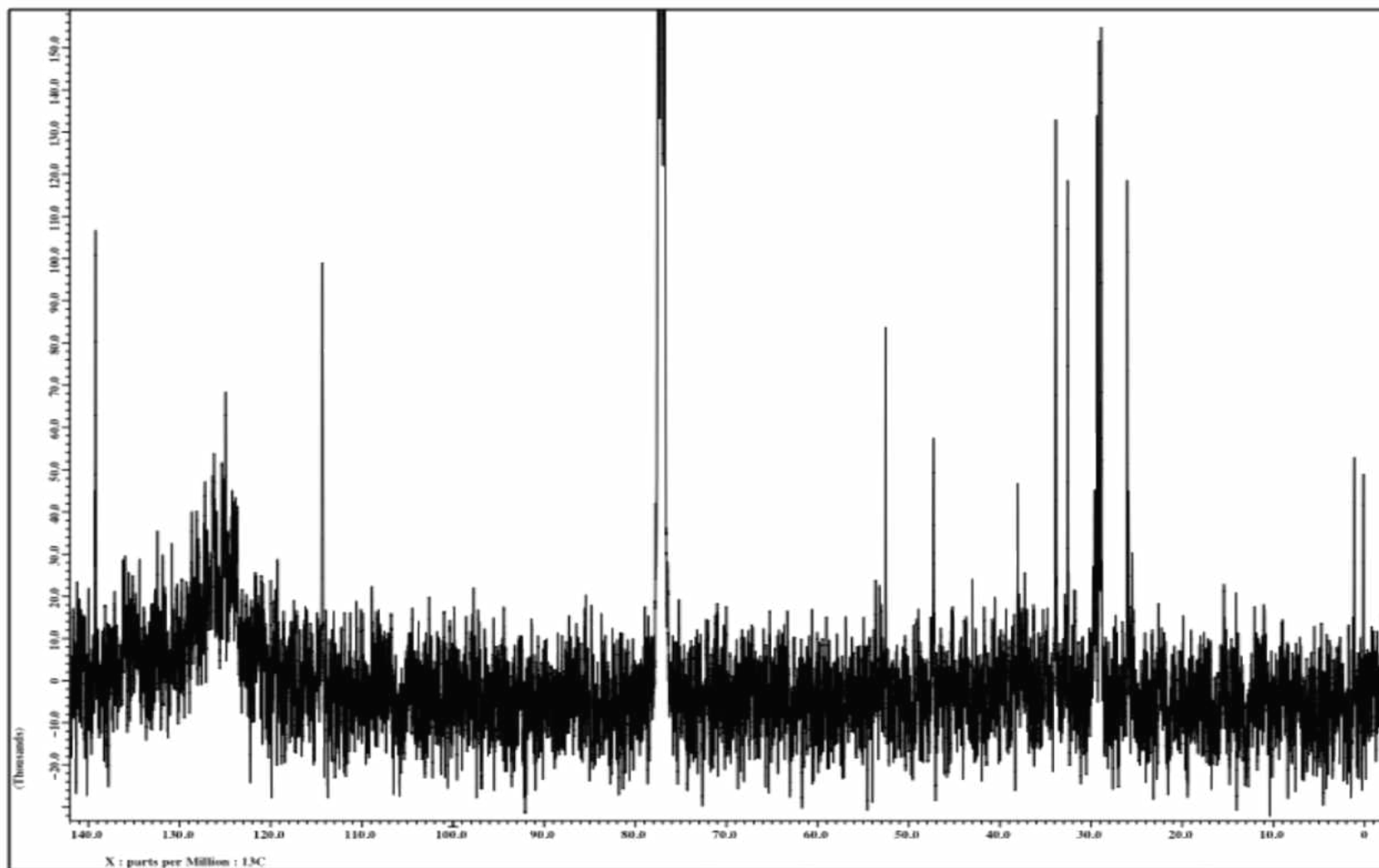


Figure 18. ^{13}C NMR Spectrum of **10**.

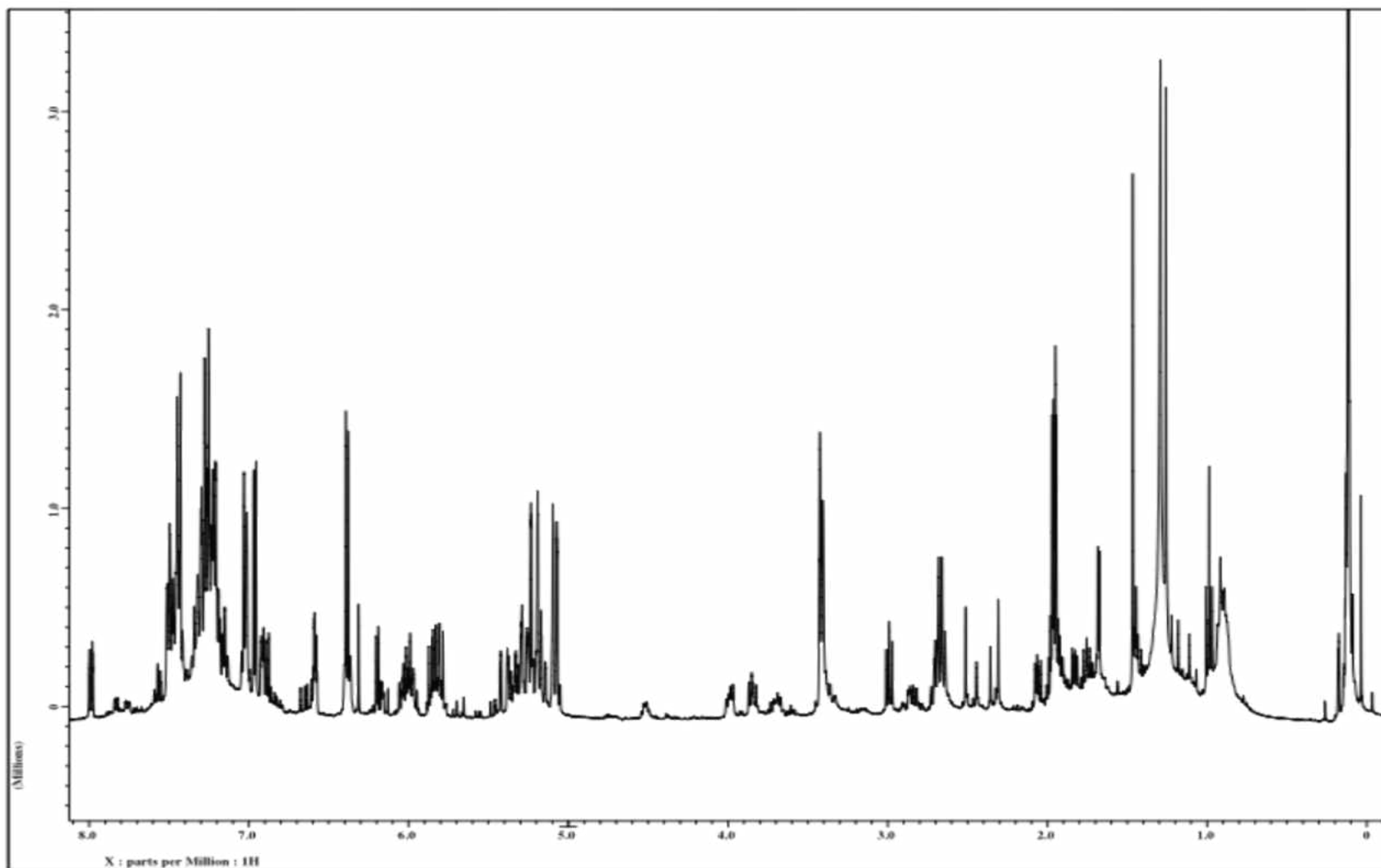


Figure 19. ^1H NMR Spectrum of **15**.

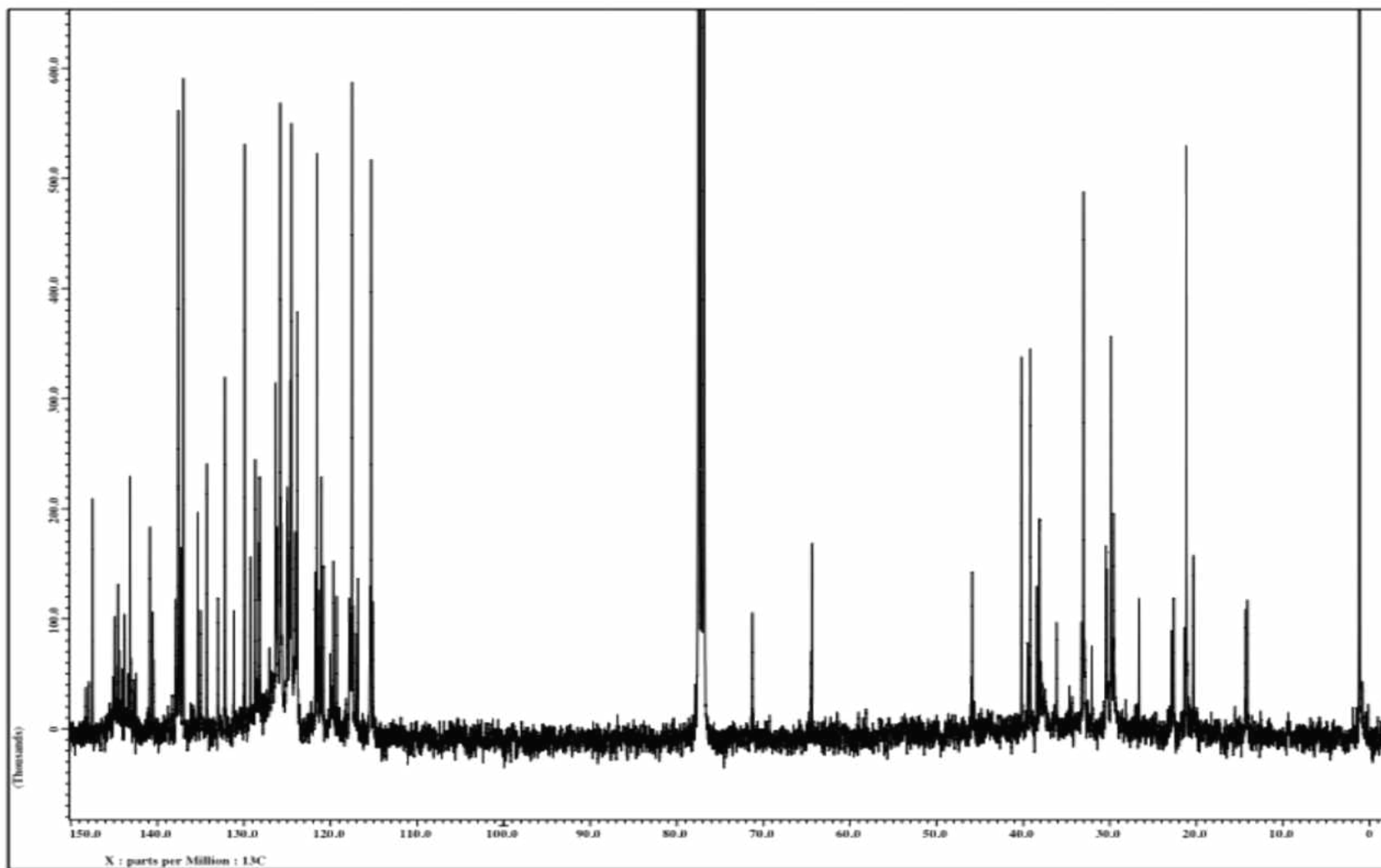


Figure 20. ^{13}C NMR Spectrum of **15**.

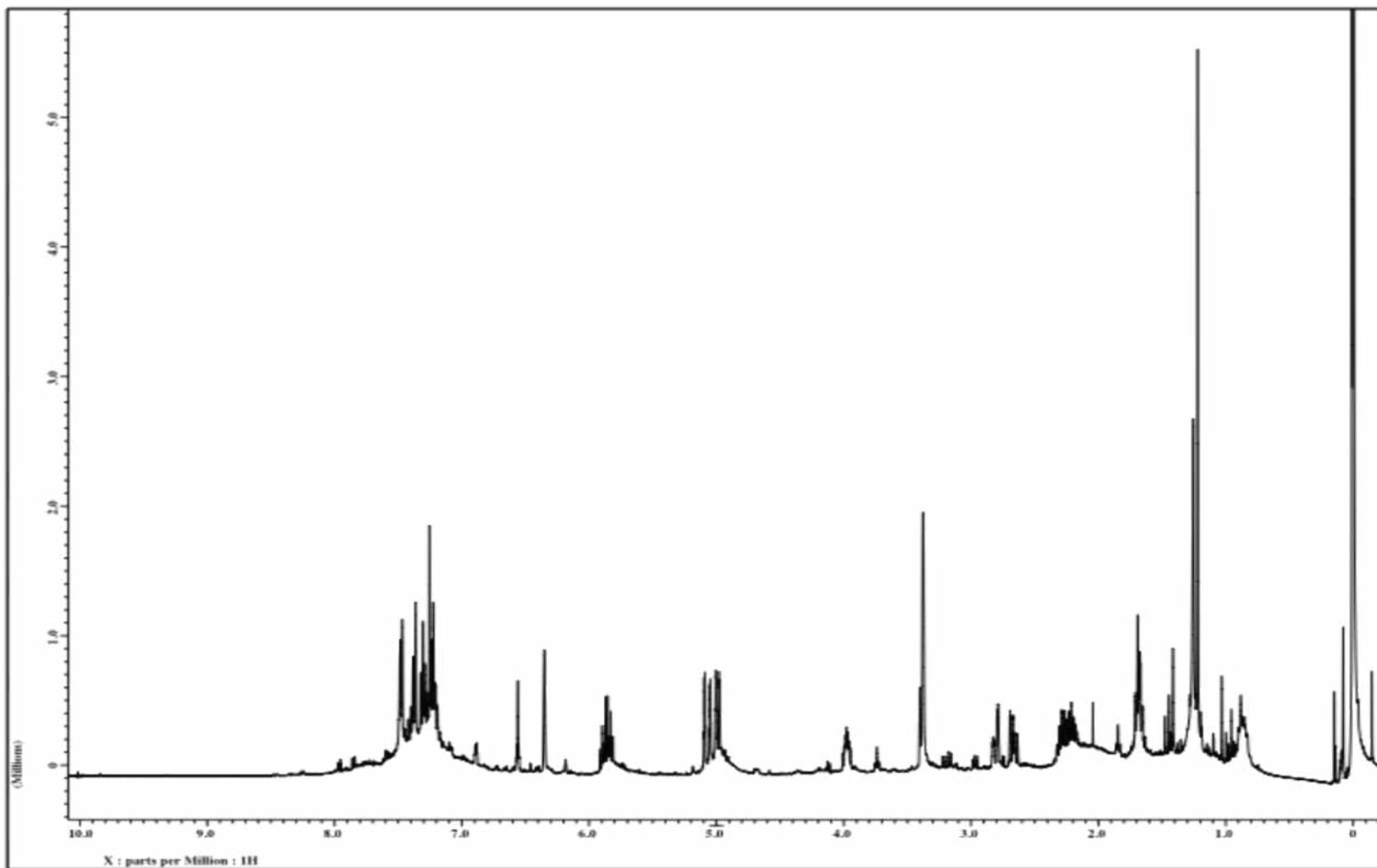


Figure 21. ^1H NMR Spectrum of **16**.

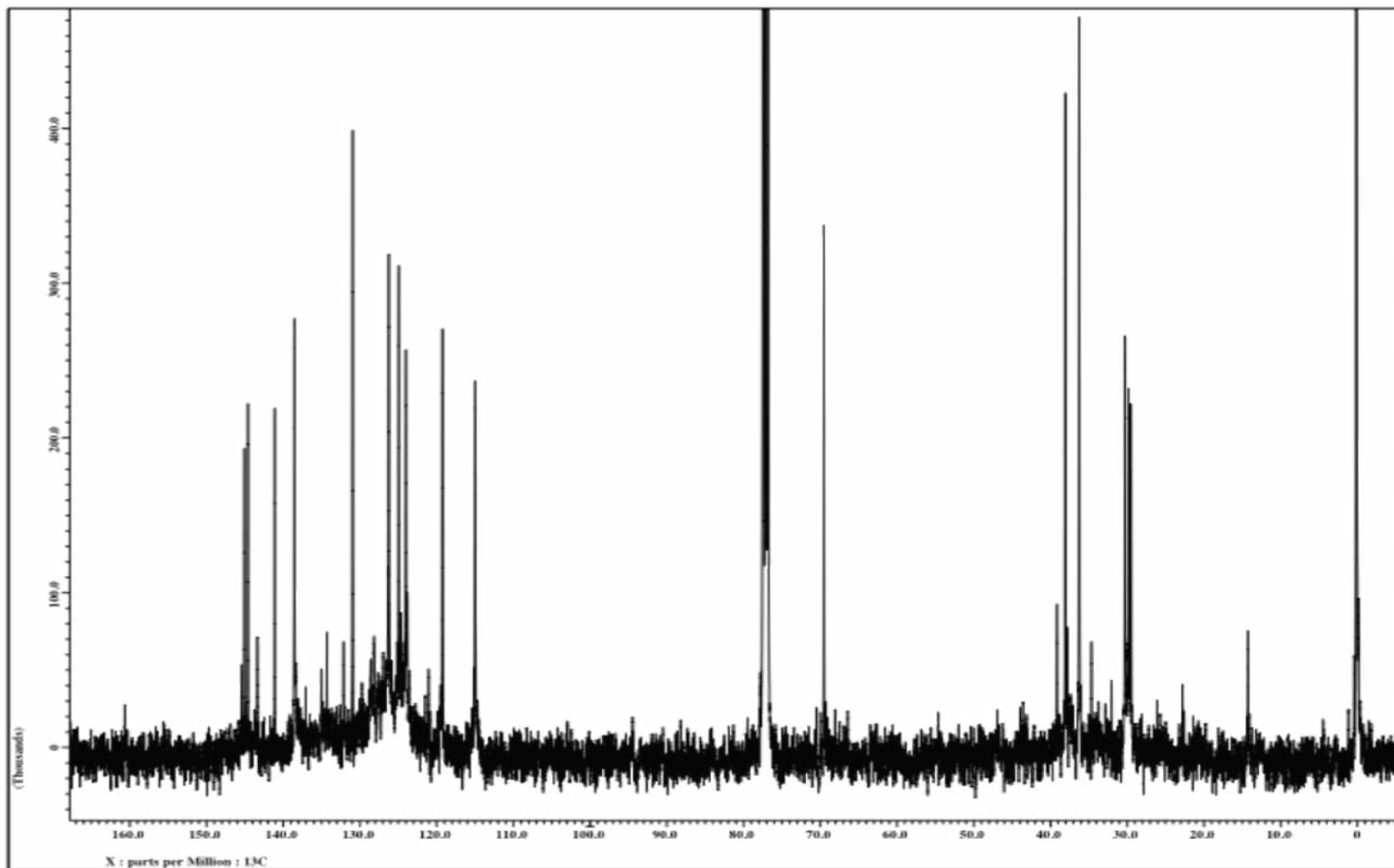


Figure 22. ^{13}C NMR Spectrum of **16**.

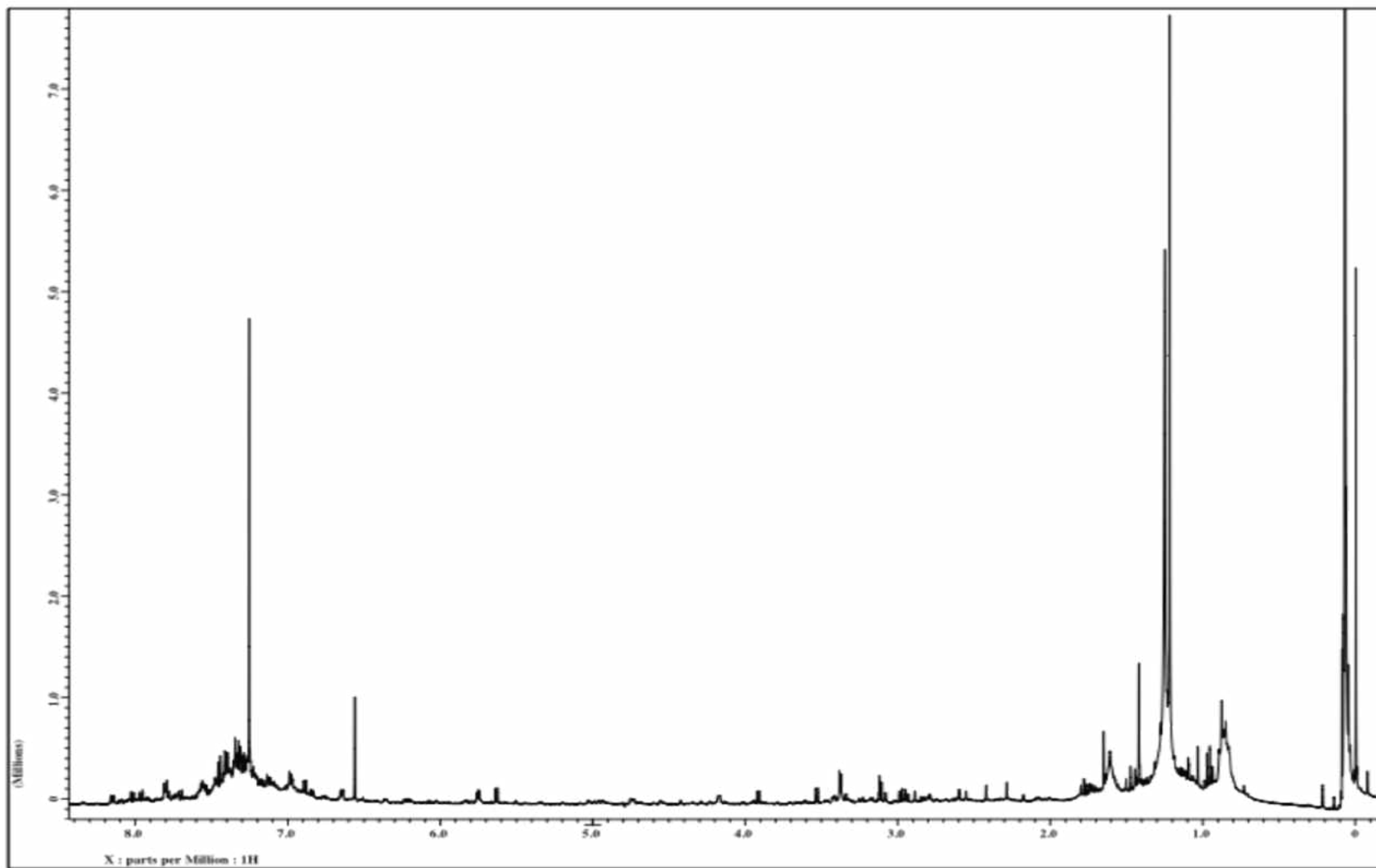


Figure 23. ^1H NMR Spectrum of 17.

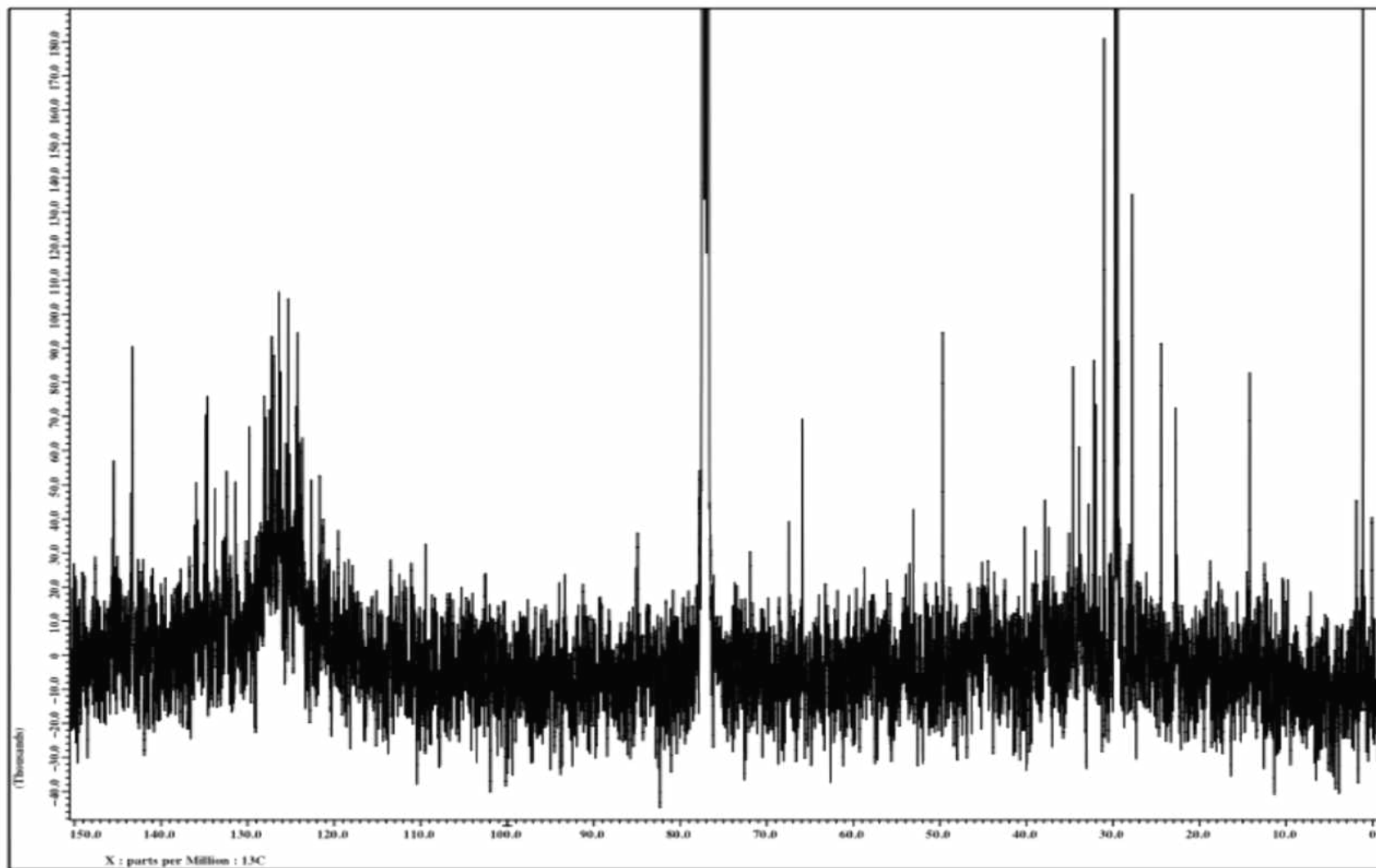
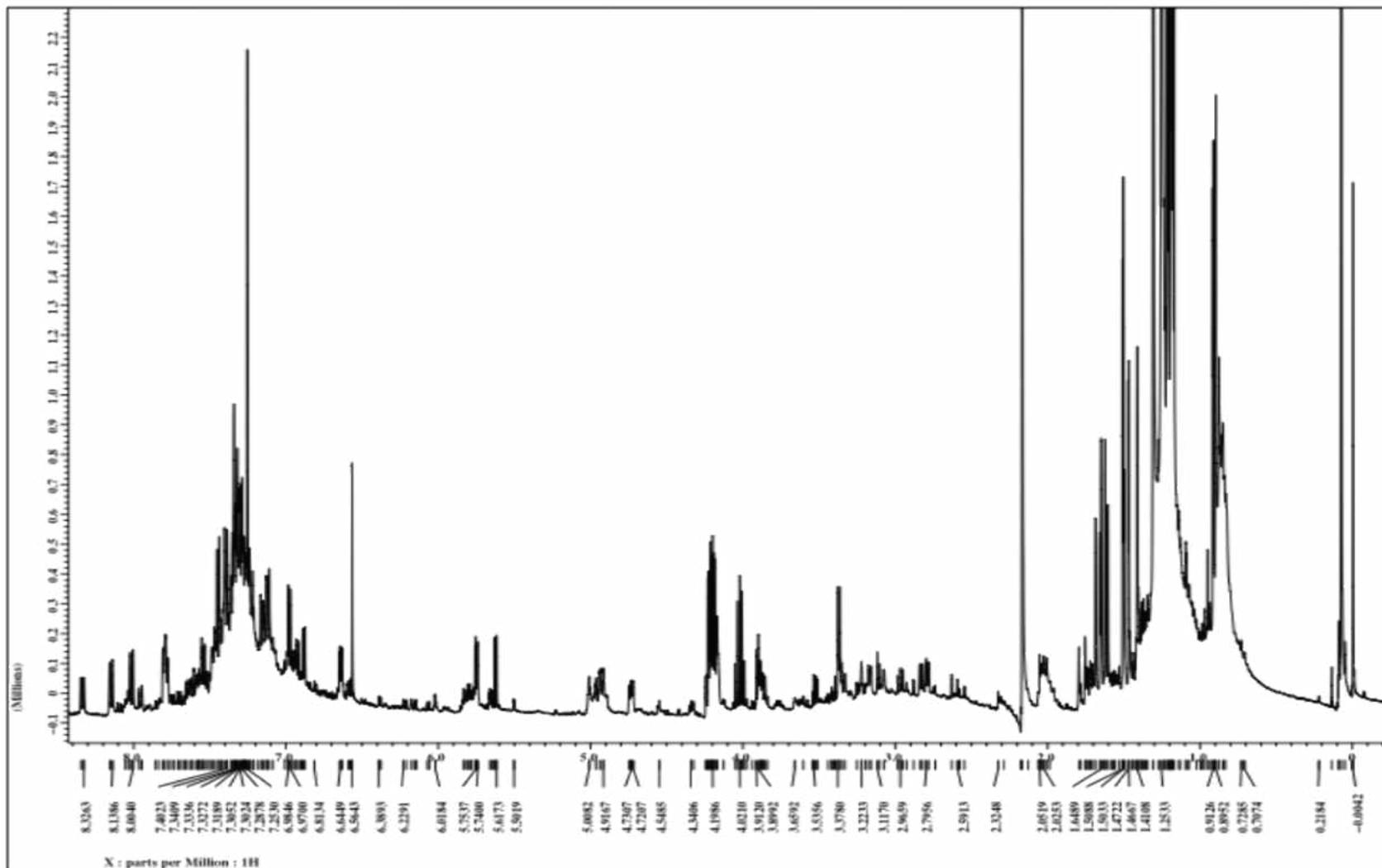


Figure 24. ^{13}C NMR Spectrum of **17**.

Figure 25. ^1H NMR Spectrum of **18**.

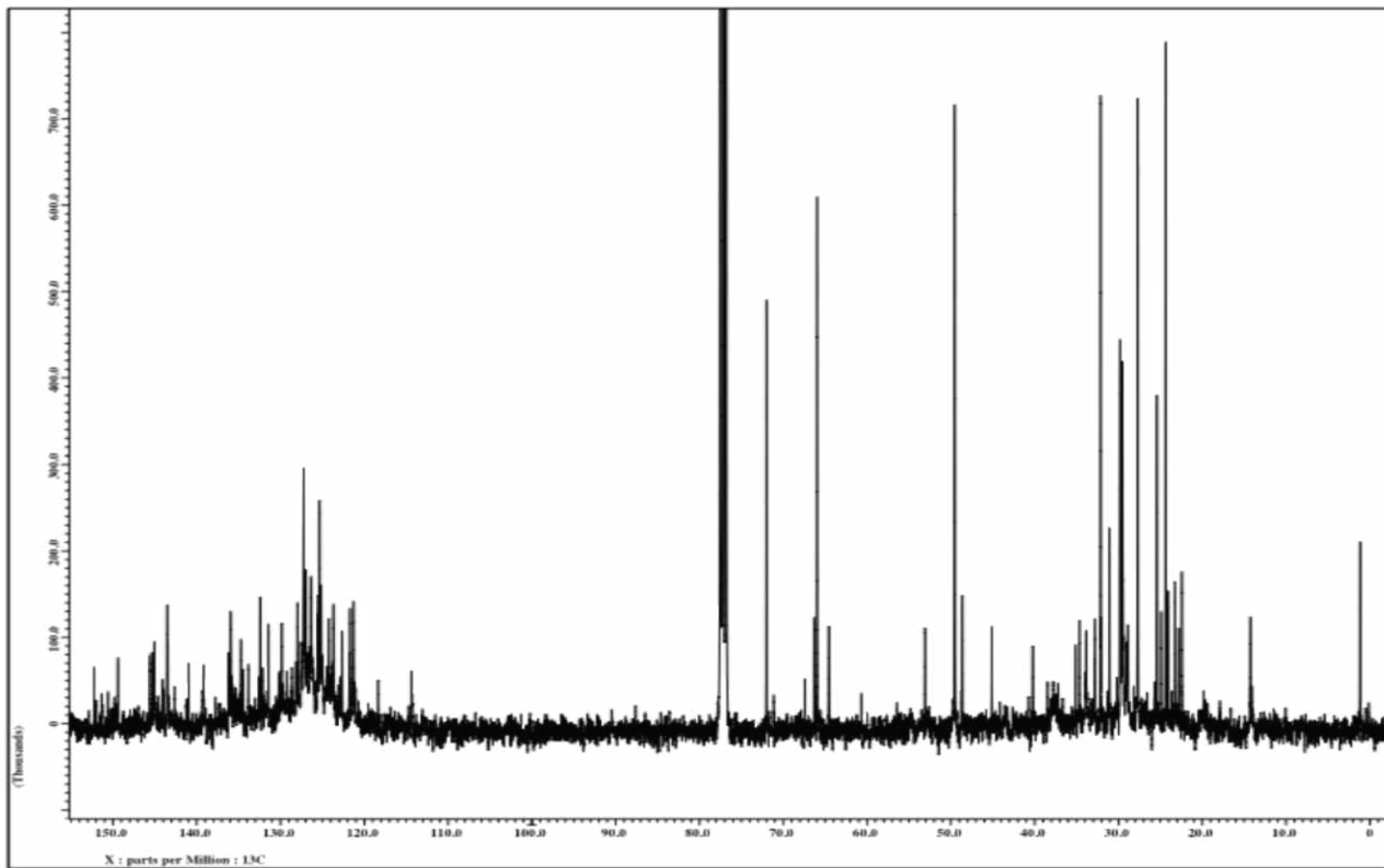


Figure 26. ^{13}C NMR Spectrum of **18**.

APPENDIX B
FT-IR Spectrums

16

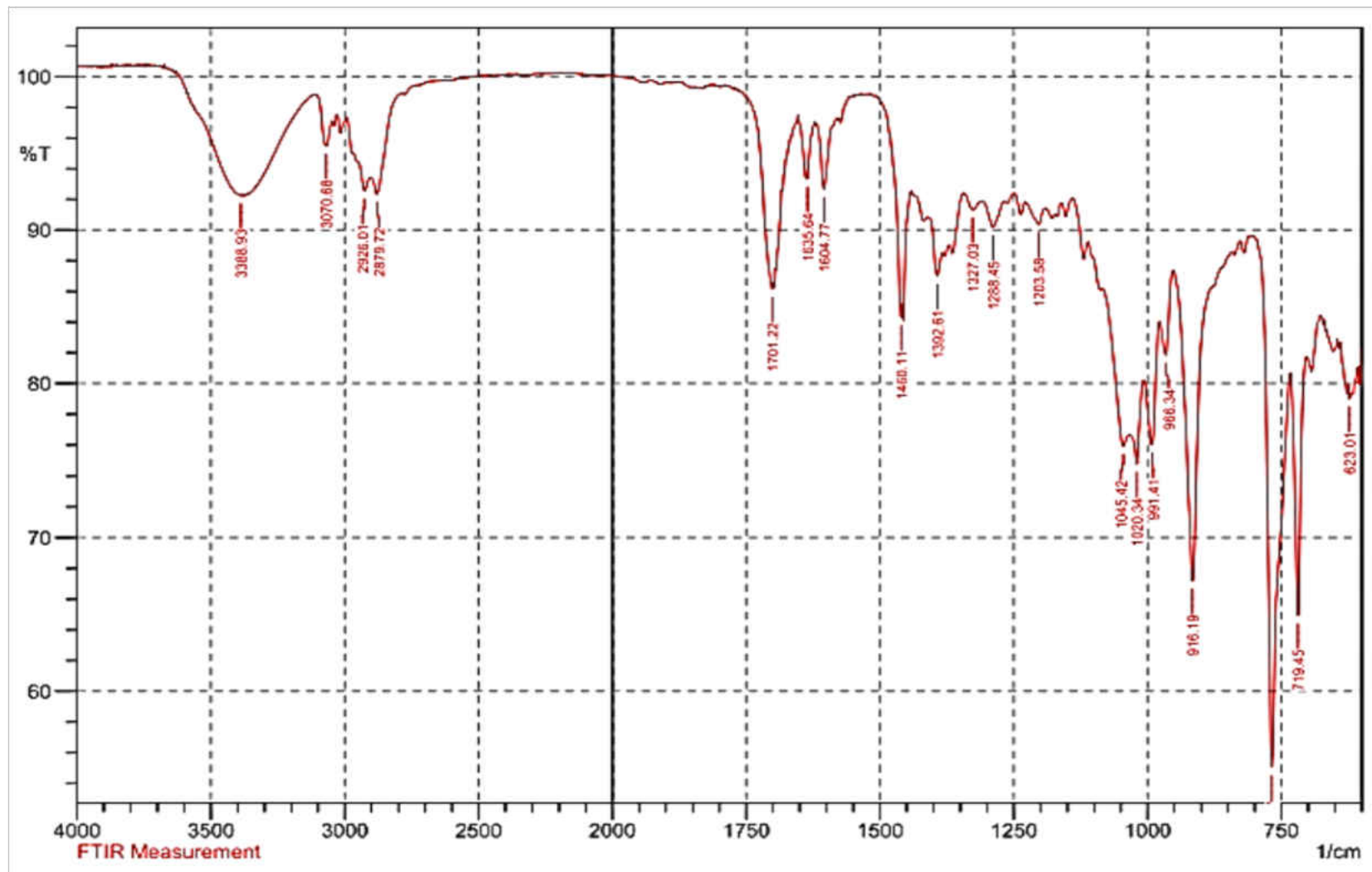


Figure 27. FT-IR of 7.

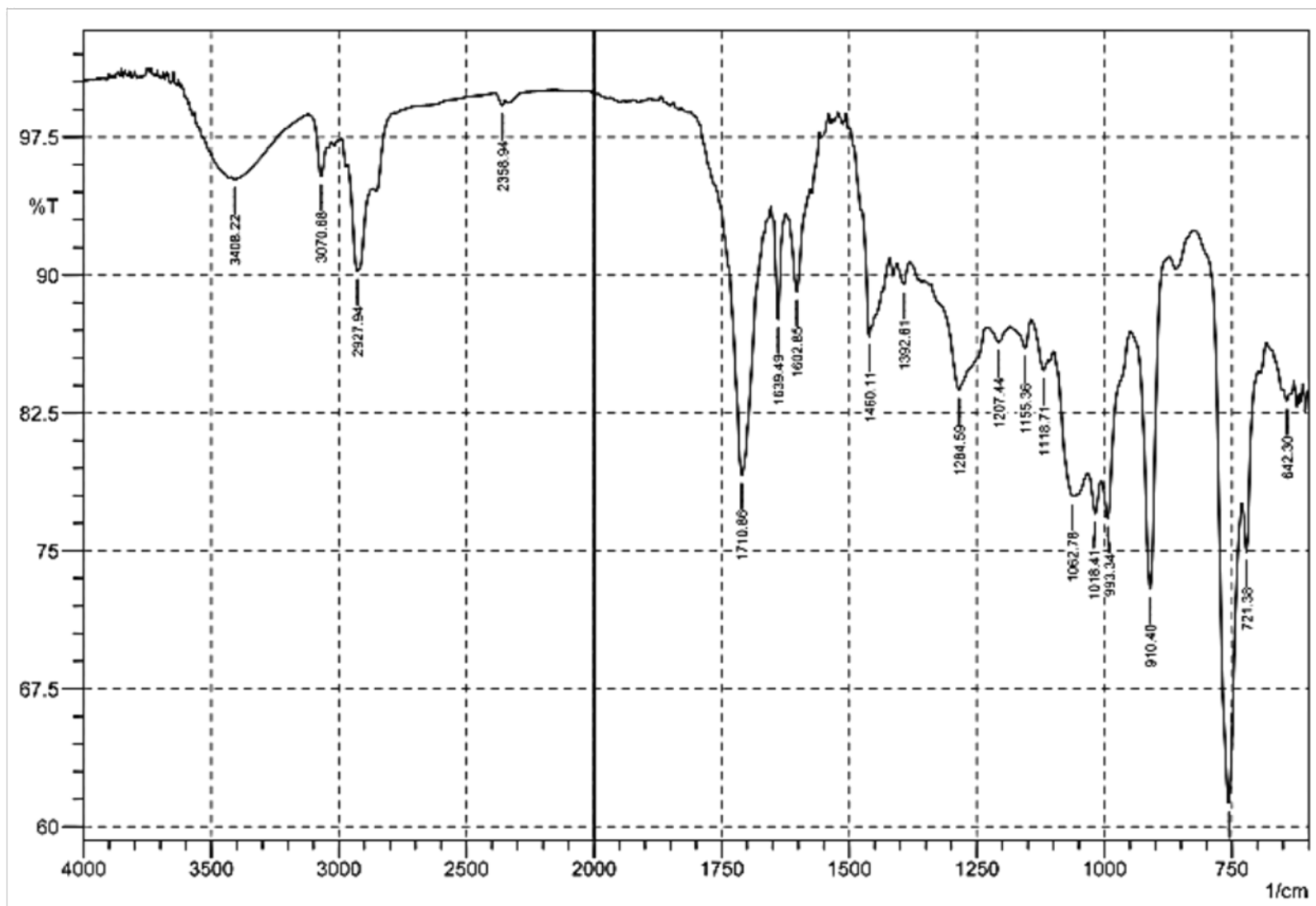


Figure 28. FT-IR of 8.

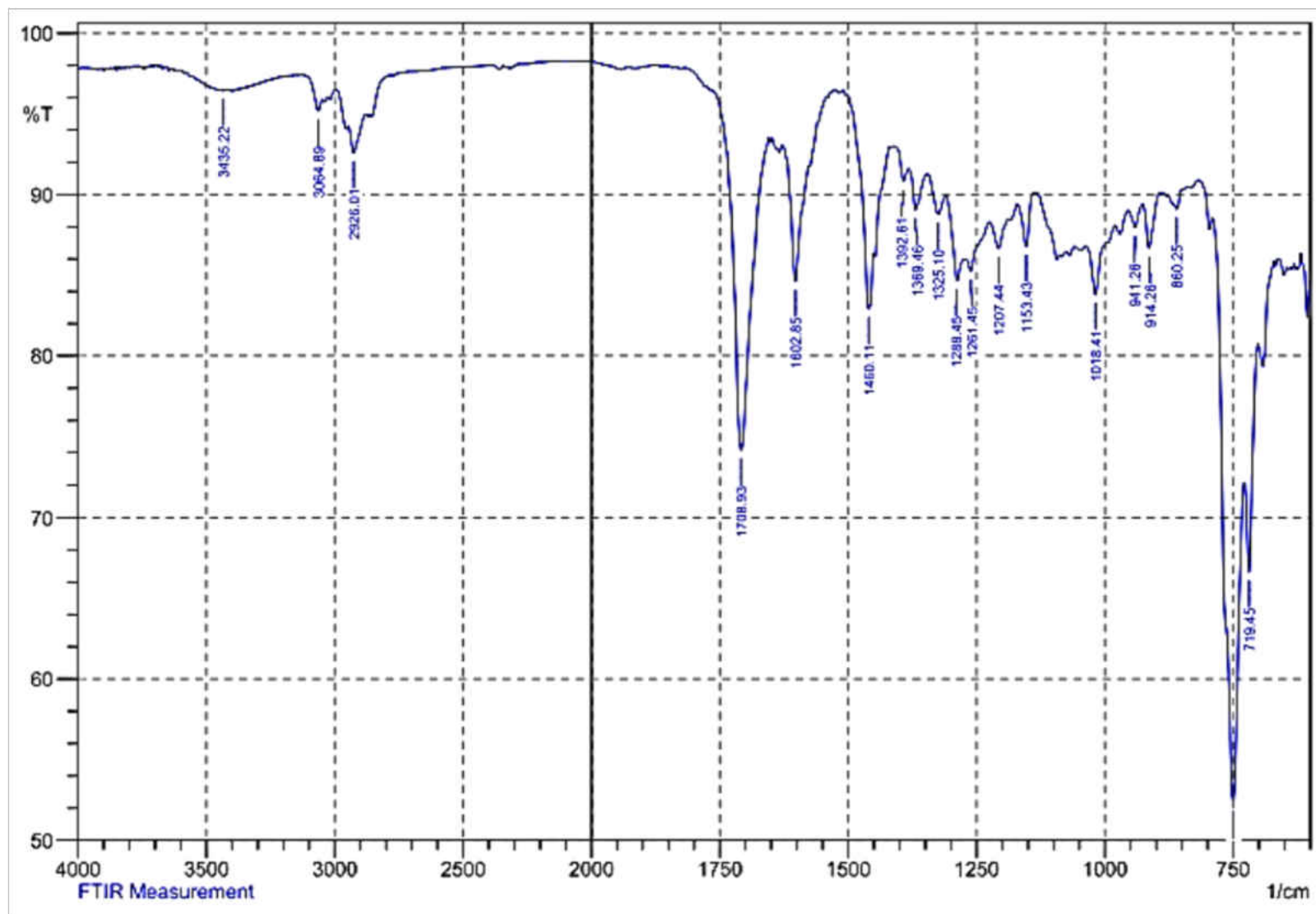


Figure 29. FT-IR of 9.

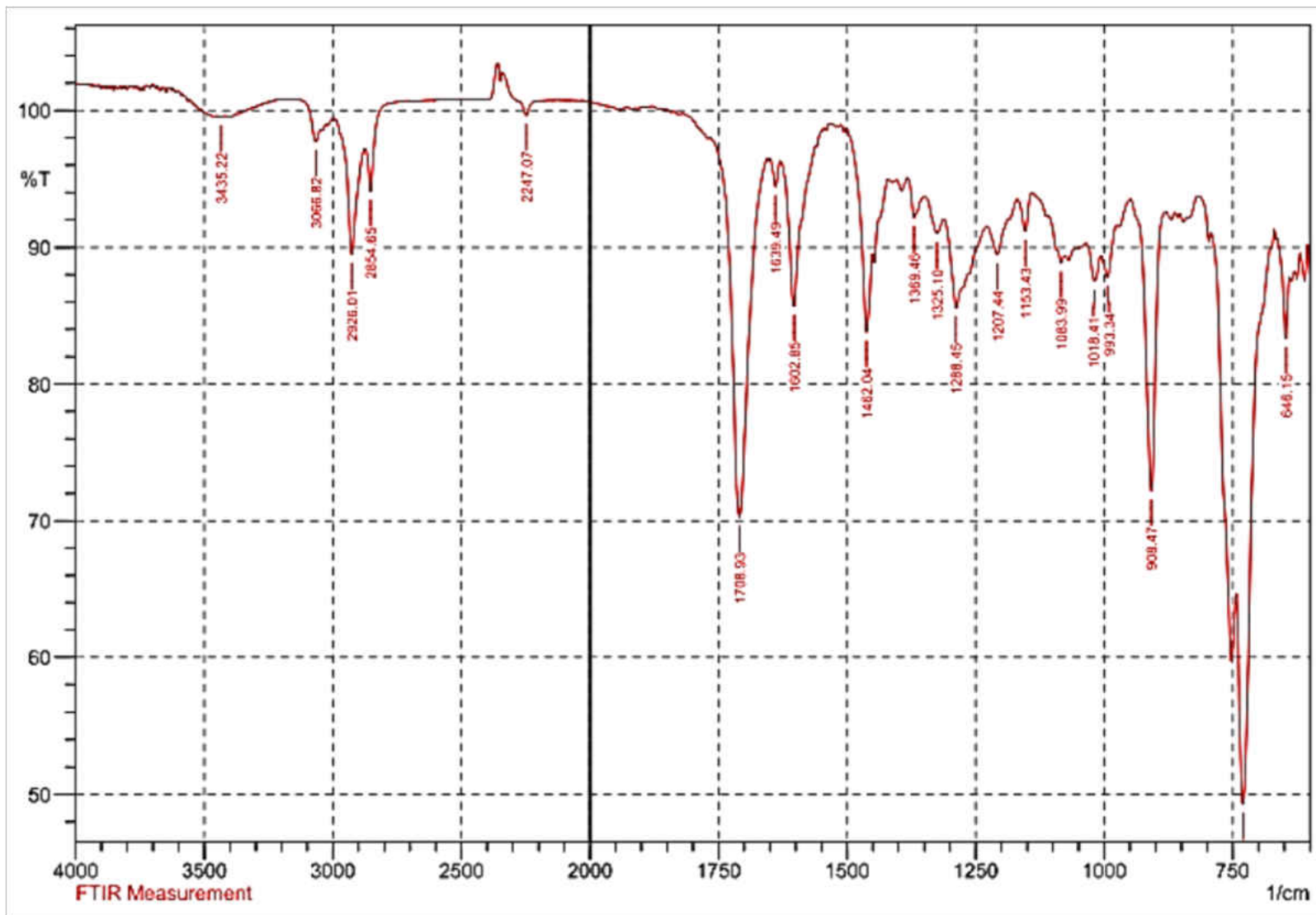


Figure 30. FT-IR of 10.

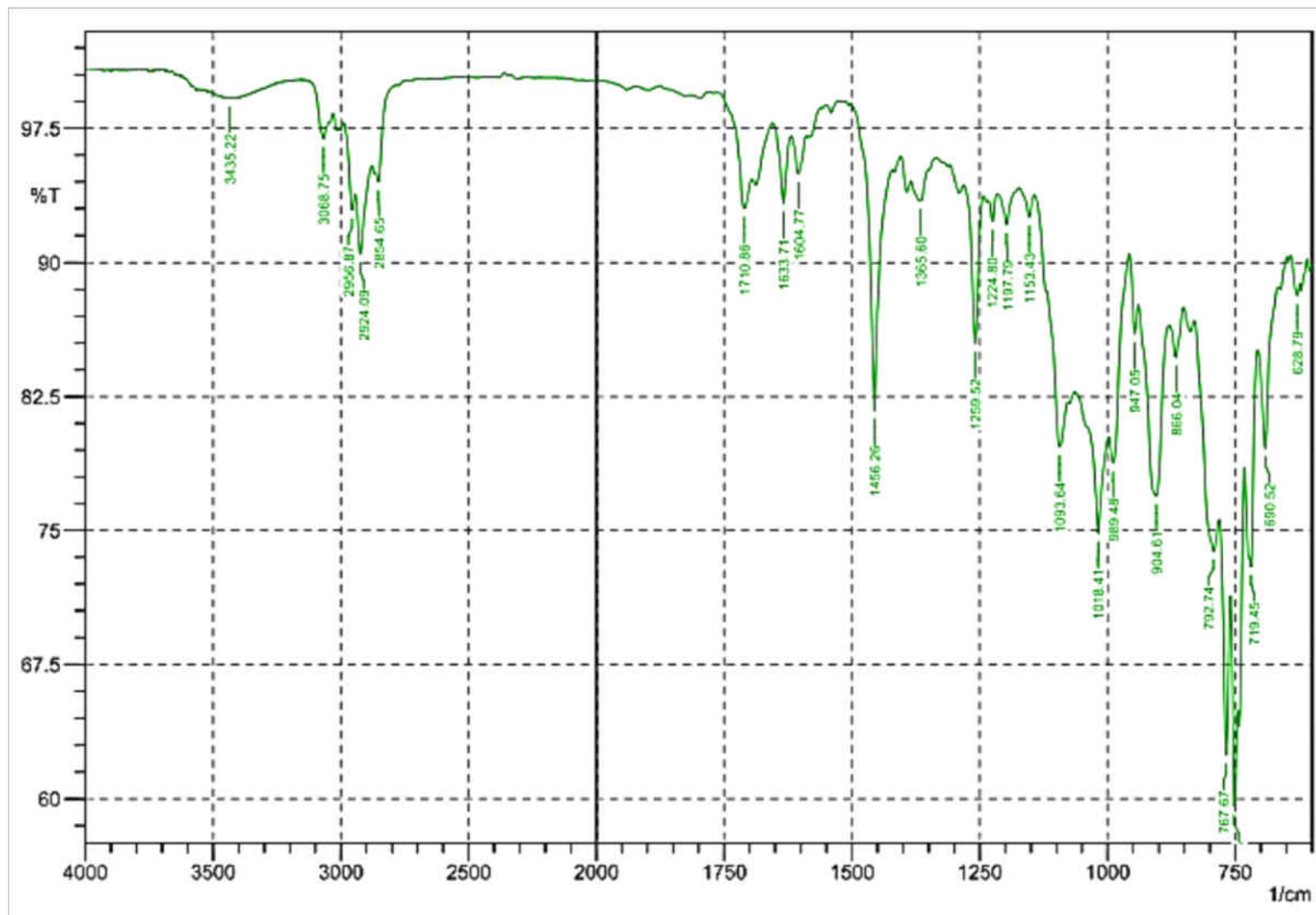


Figure 31. FT-IR of 15.

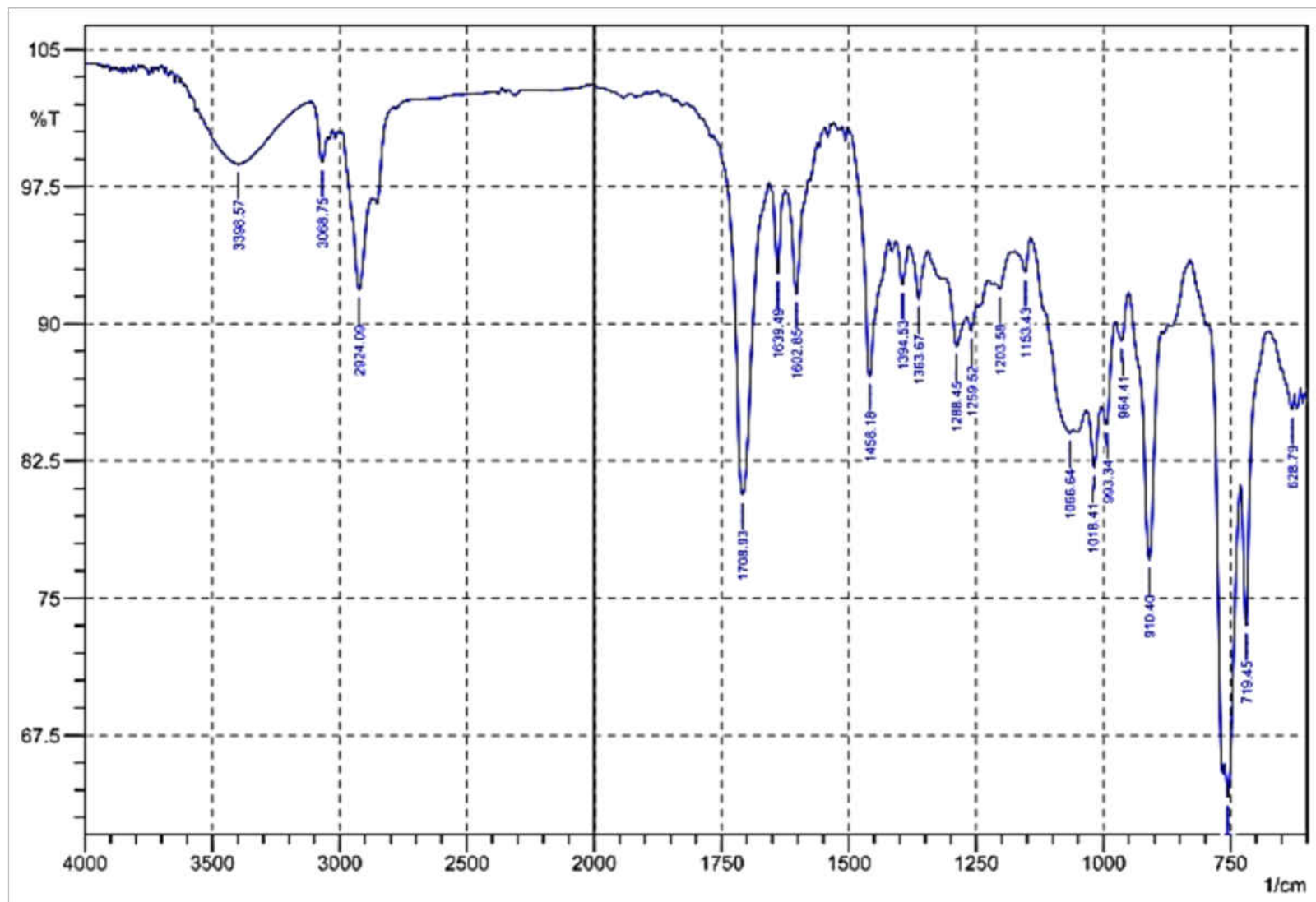


Figure 32. FT-IR of 16.

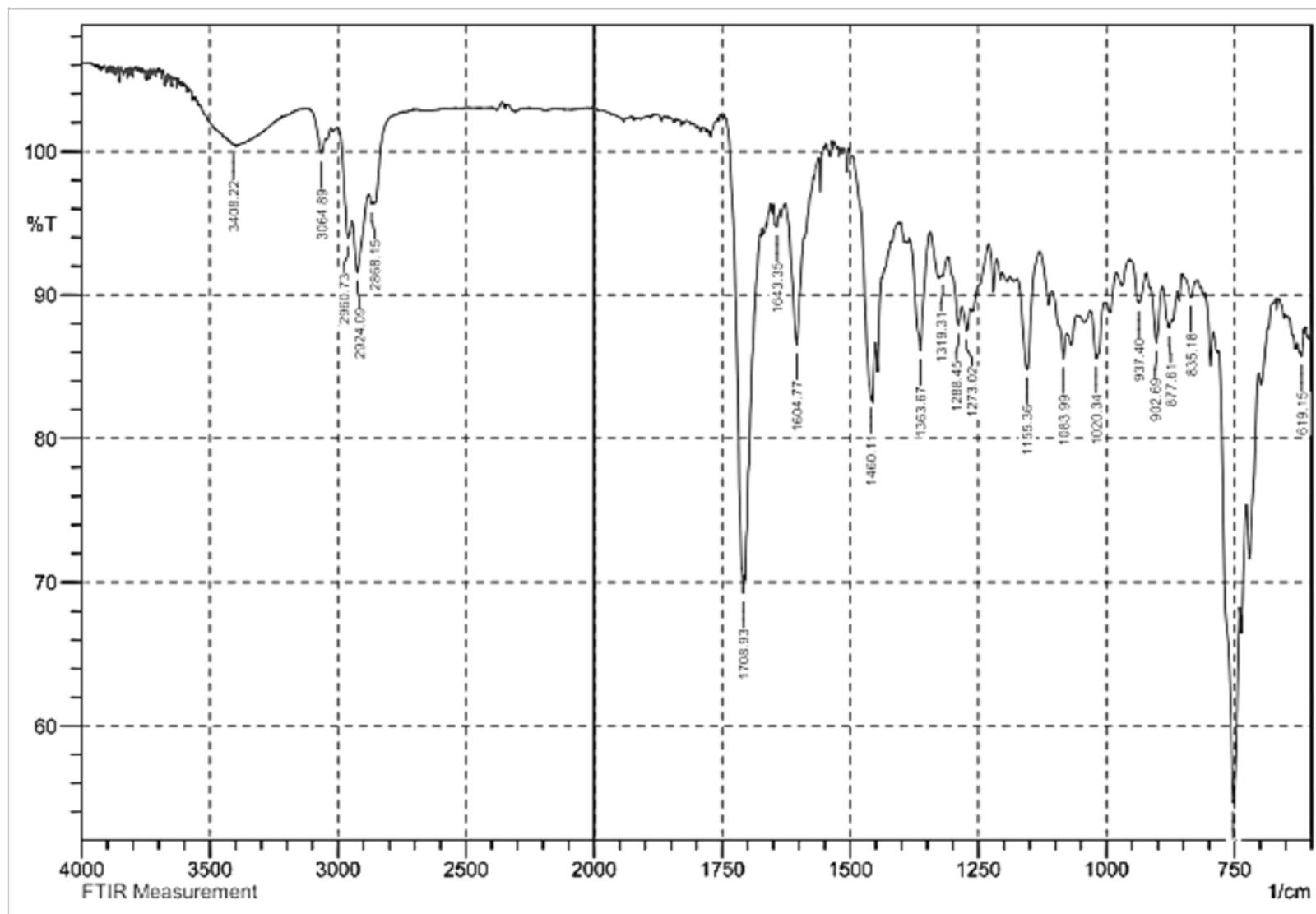


Figure 33. FT-IR of 17.

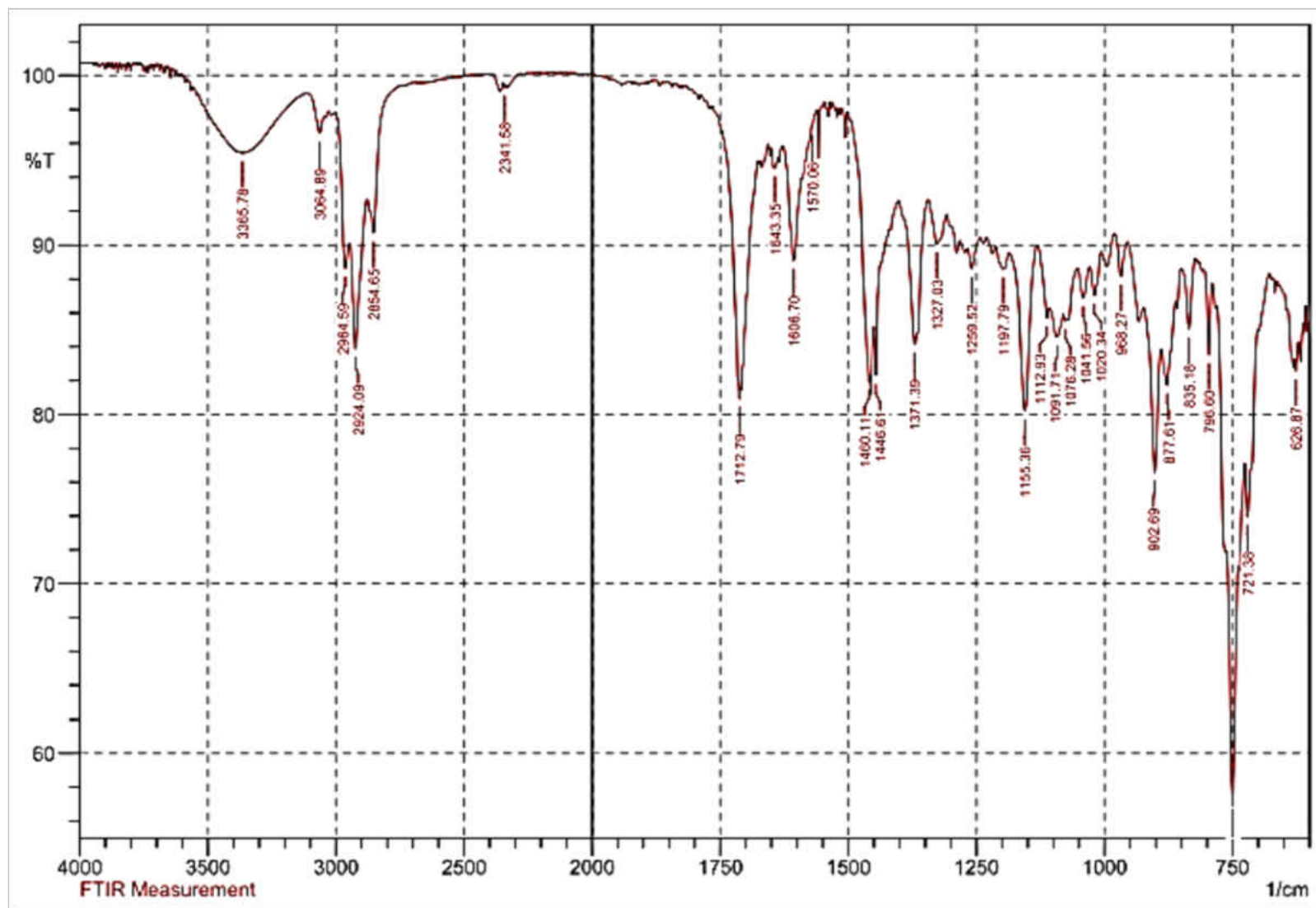


Figure 34. FT-IR of 18.

APPENDIX C

Porosimetry Graphs

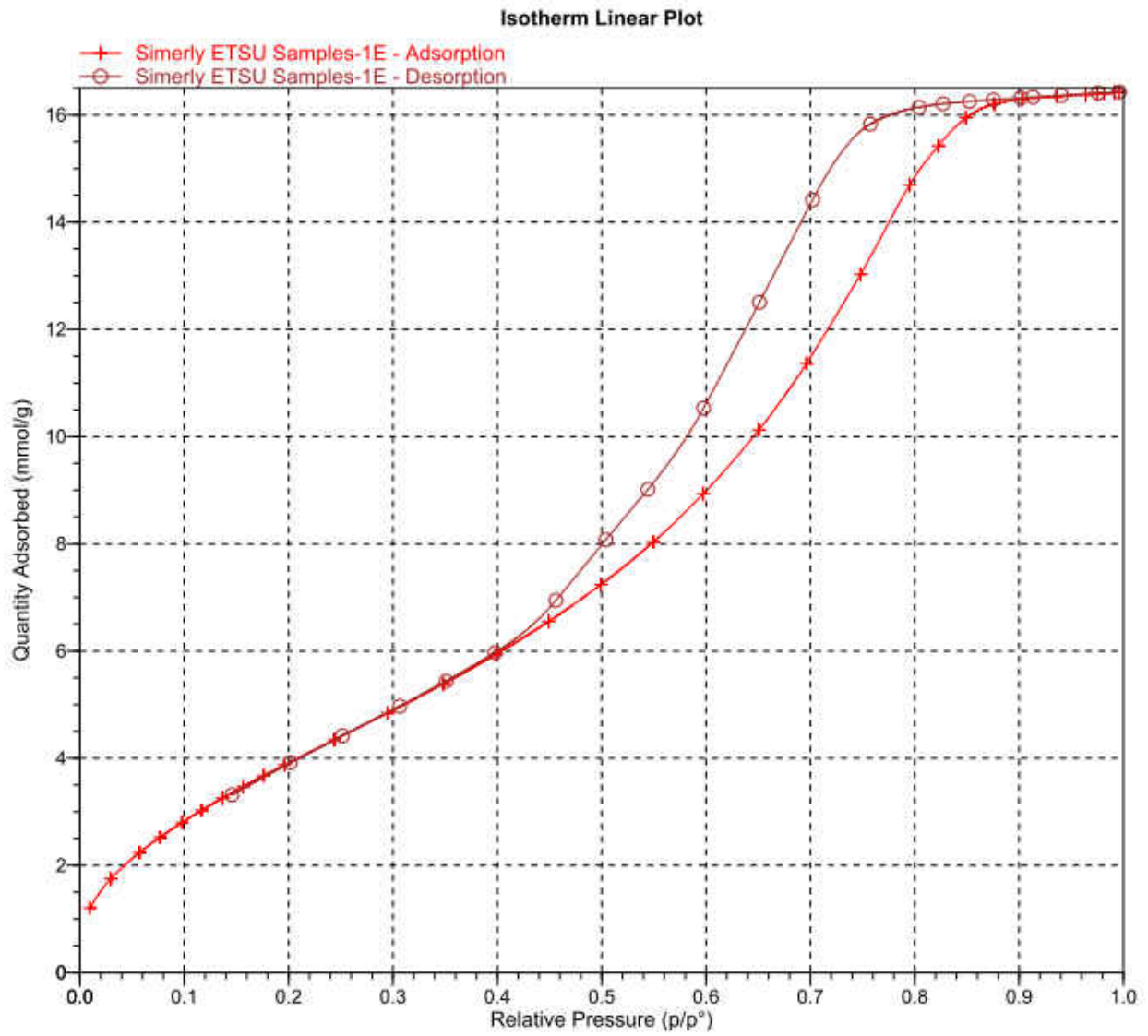


Figure 35. Adsorption/Desorption Isotherm of 19.

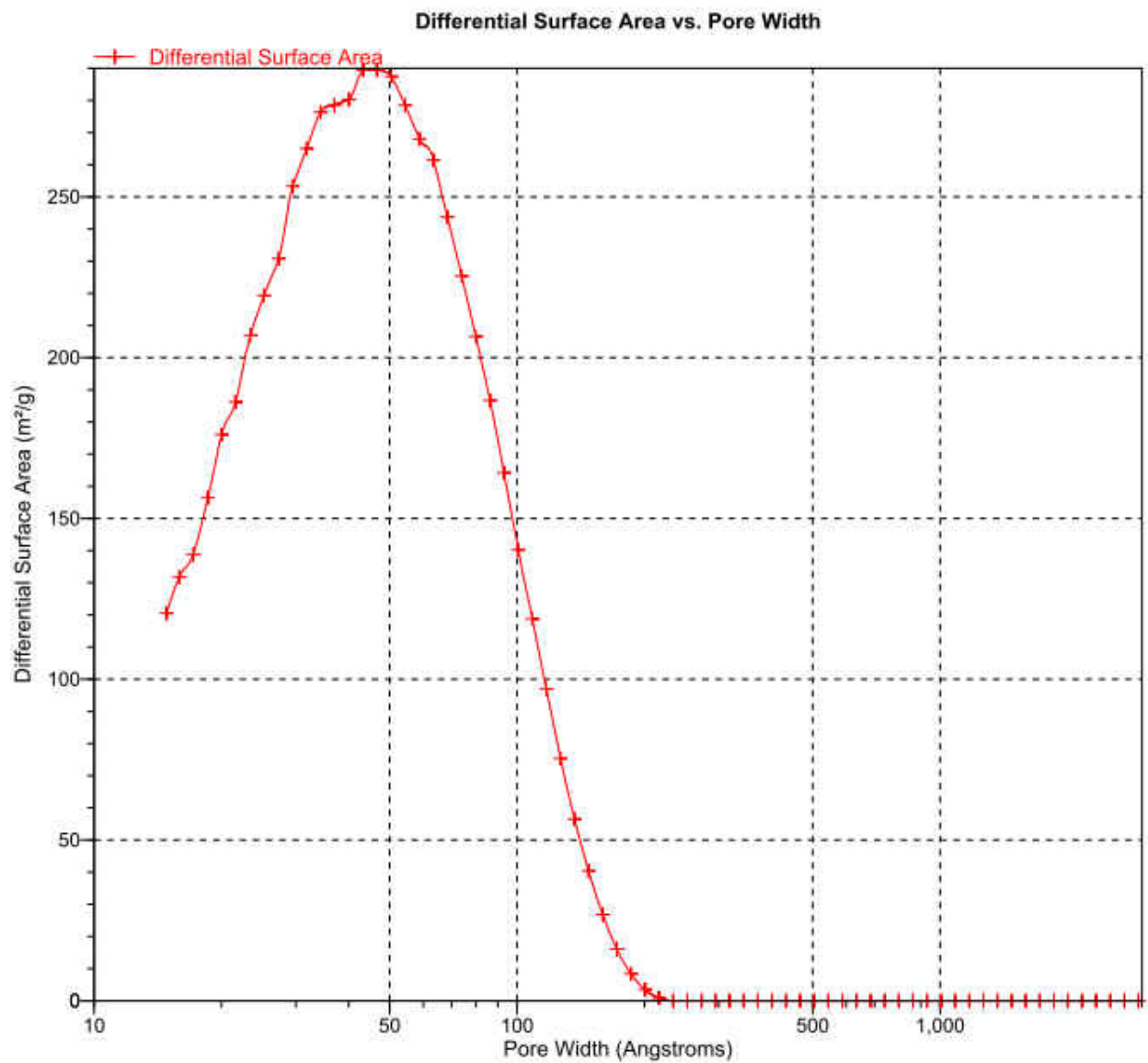


Figure 36. Pore Size Distribution of **19**.

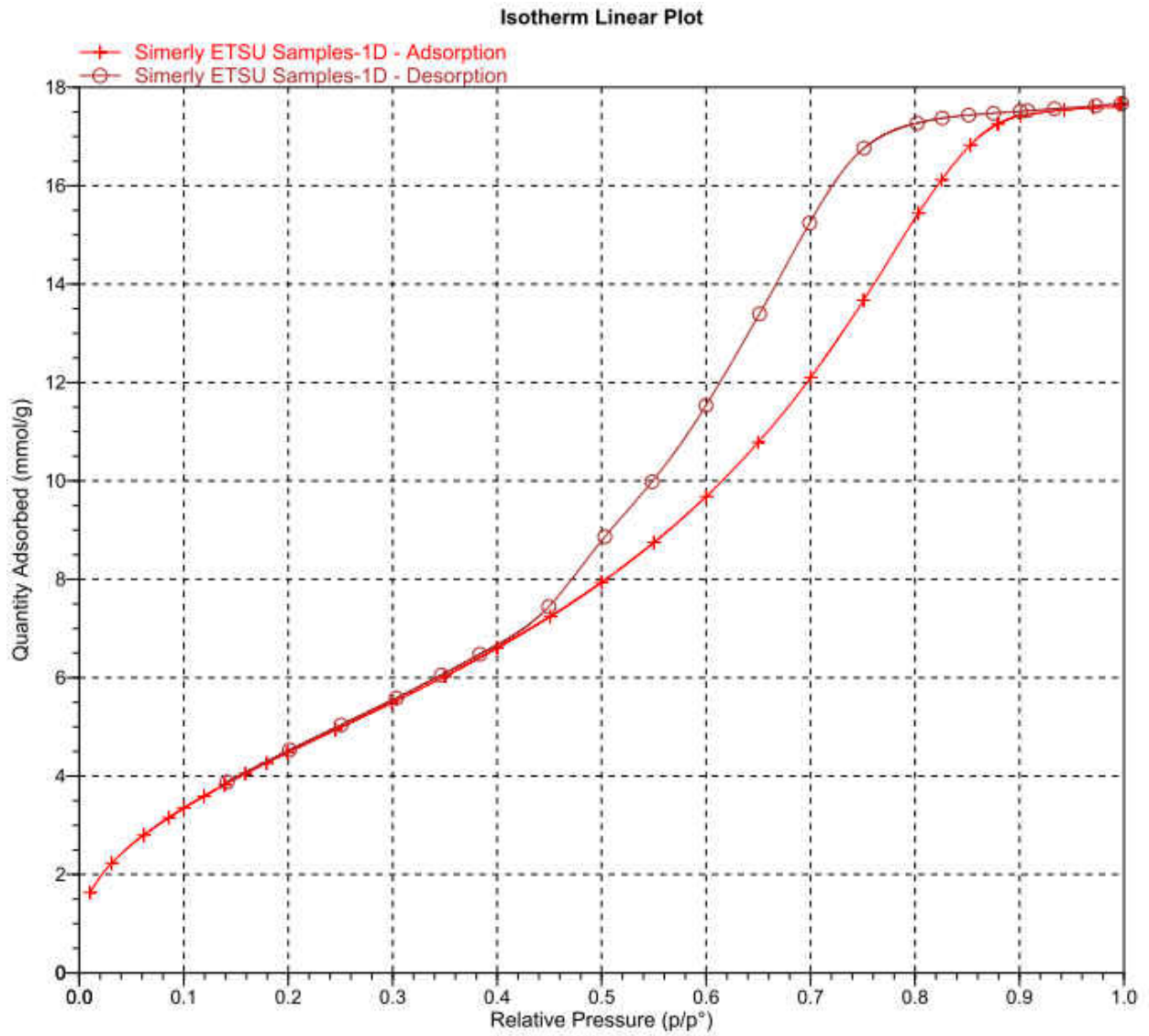


Figure 37. Adsorption/Desorption Isotherm of 20.

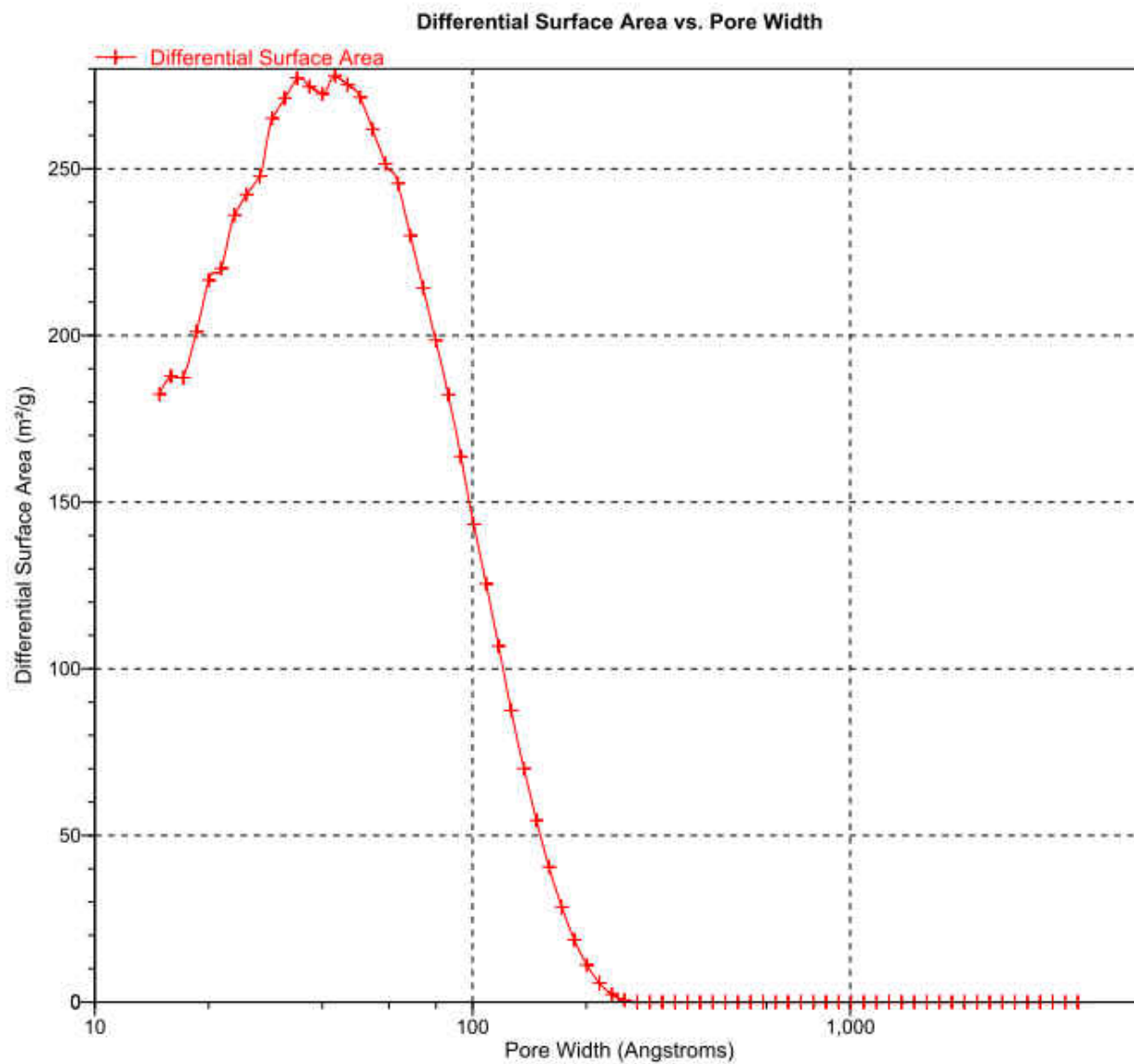


Figure 38. Pore Size Distribution of **20**.

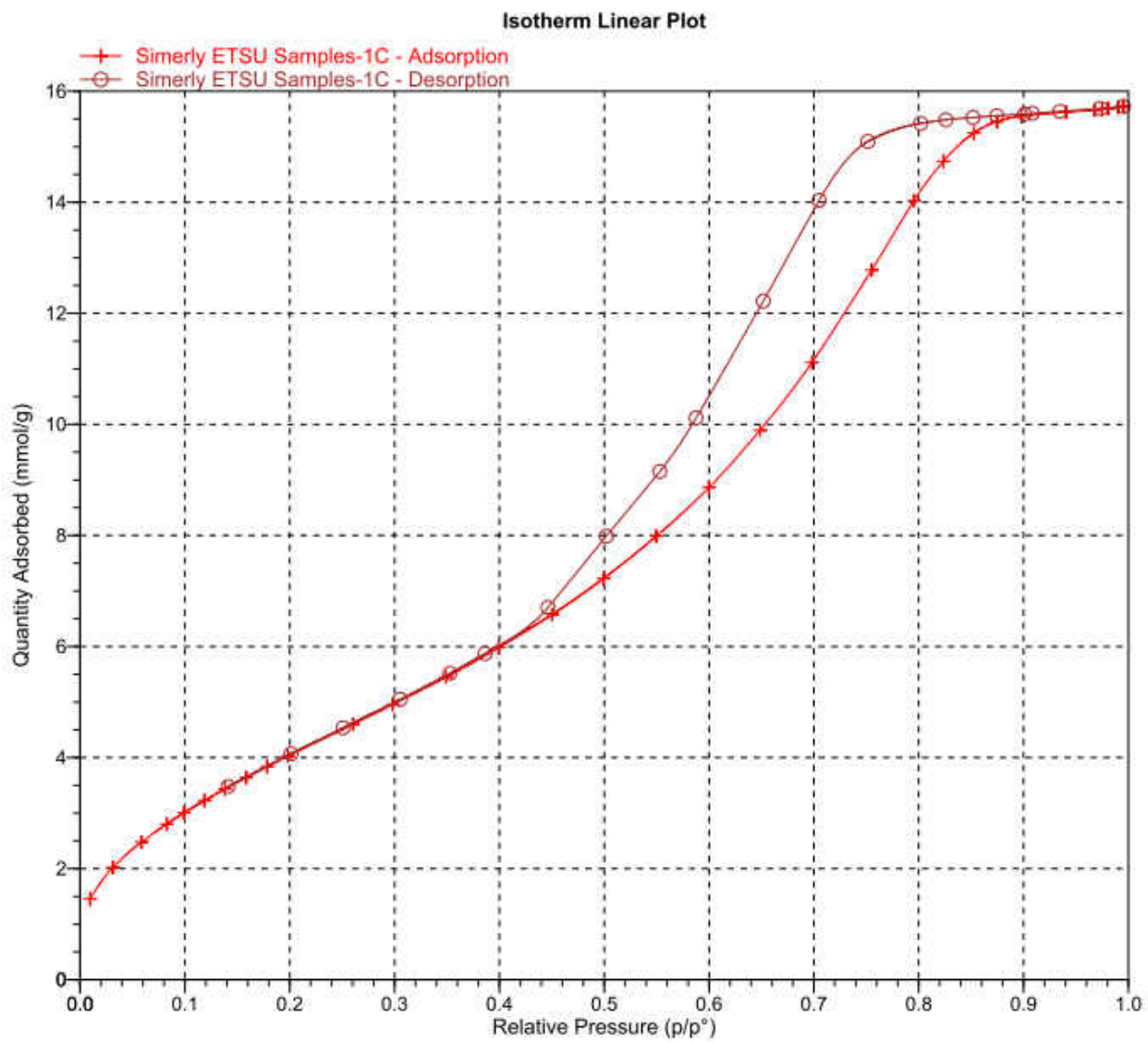


Figure 39. Adsorption/Desorption Isotherm of **21**.

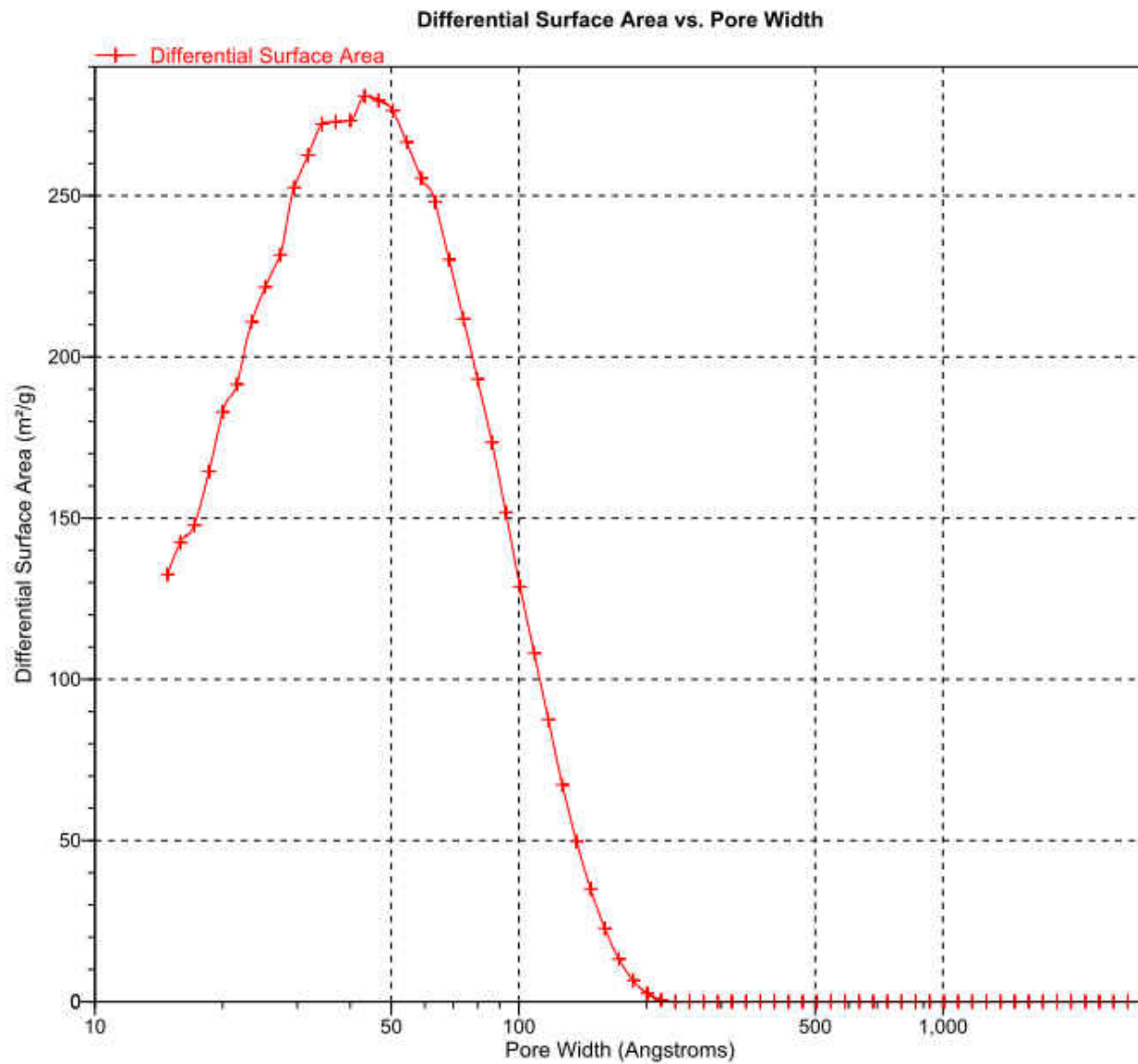


Figure 40. Pore Size Distribution of **21**.

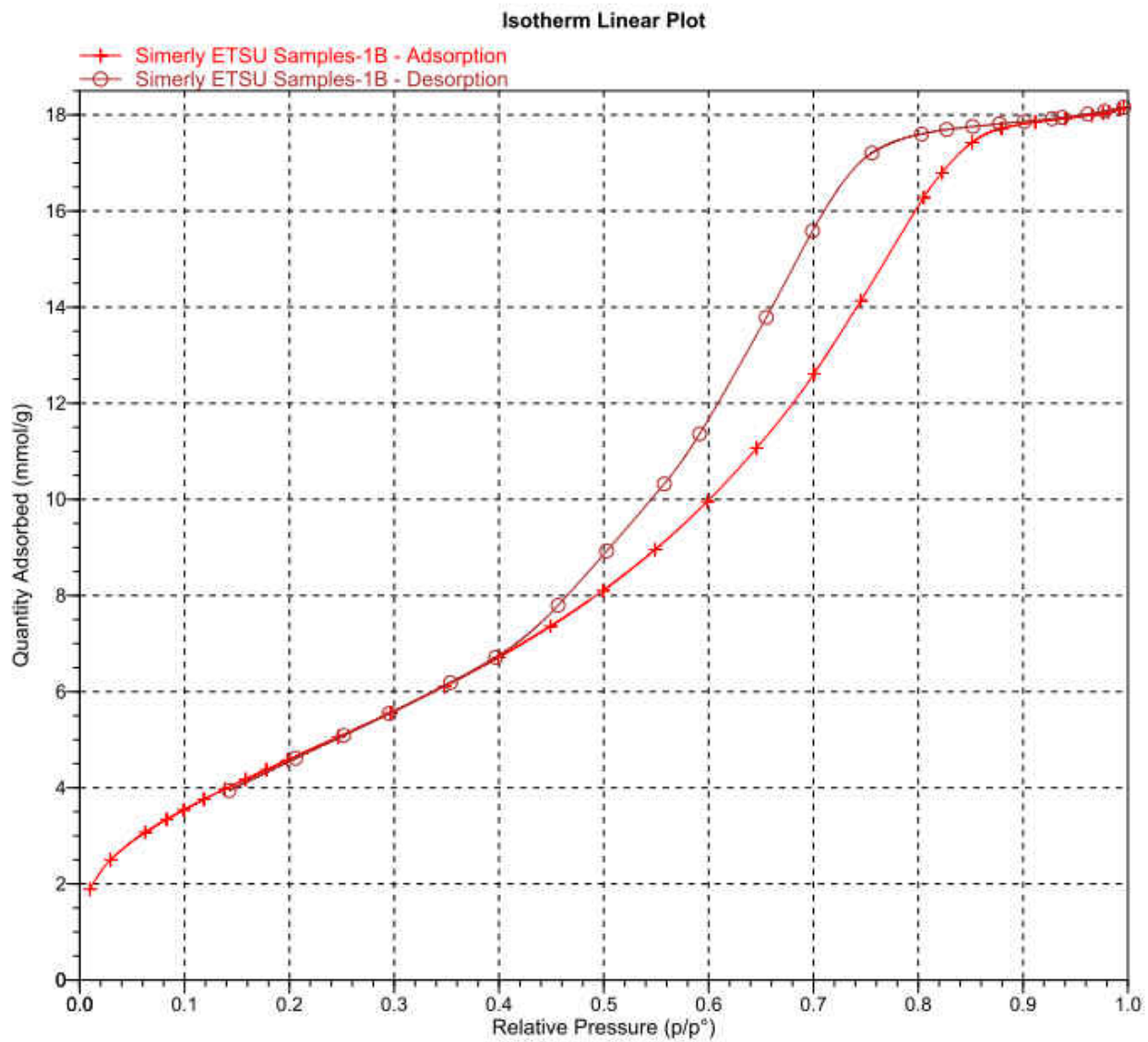


Figure 41. Adsorption/Desorption Isotherm of **22**.

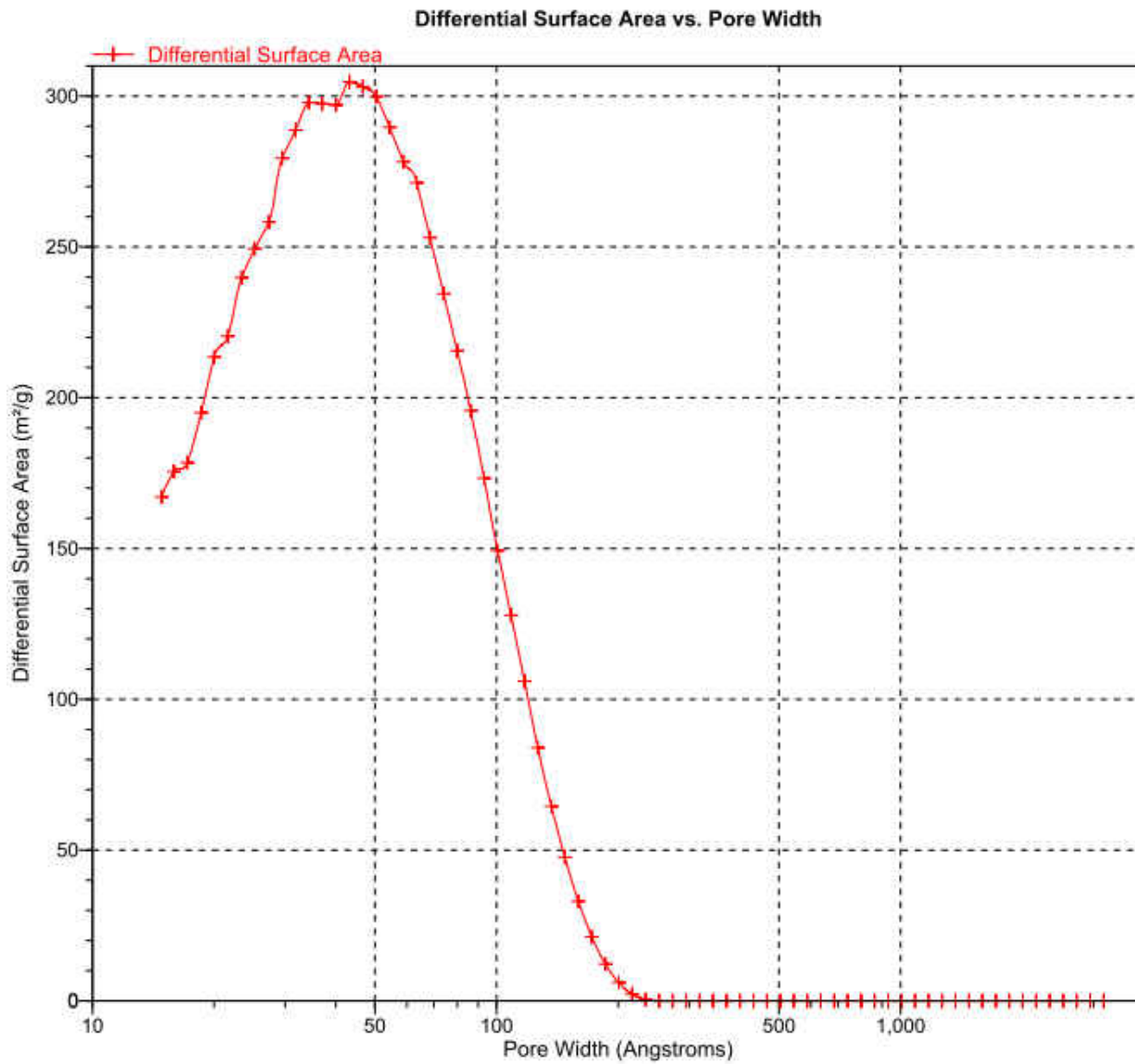


Figure 42. Pore Size Distribution of **22**.

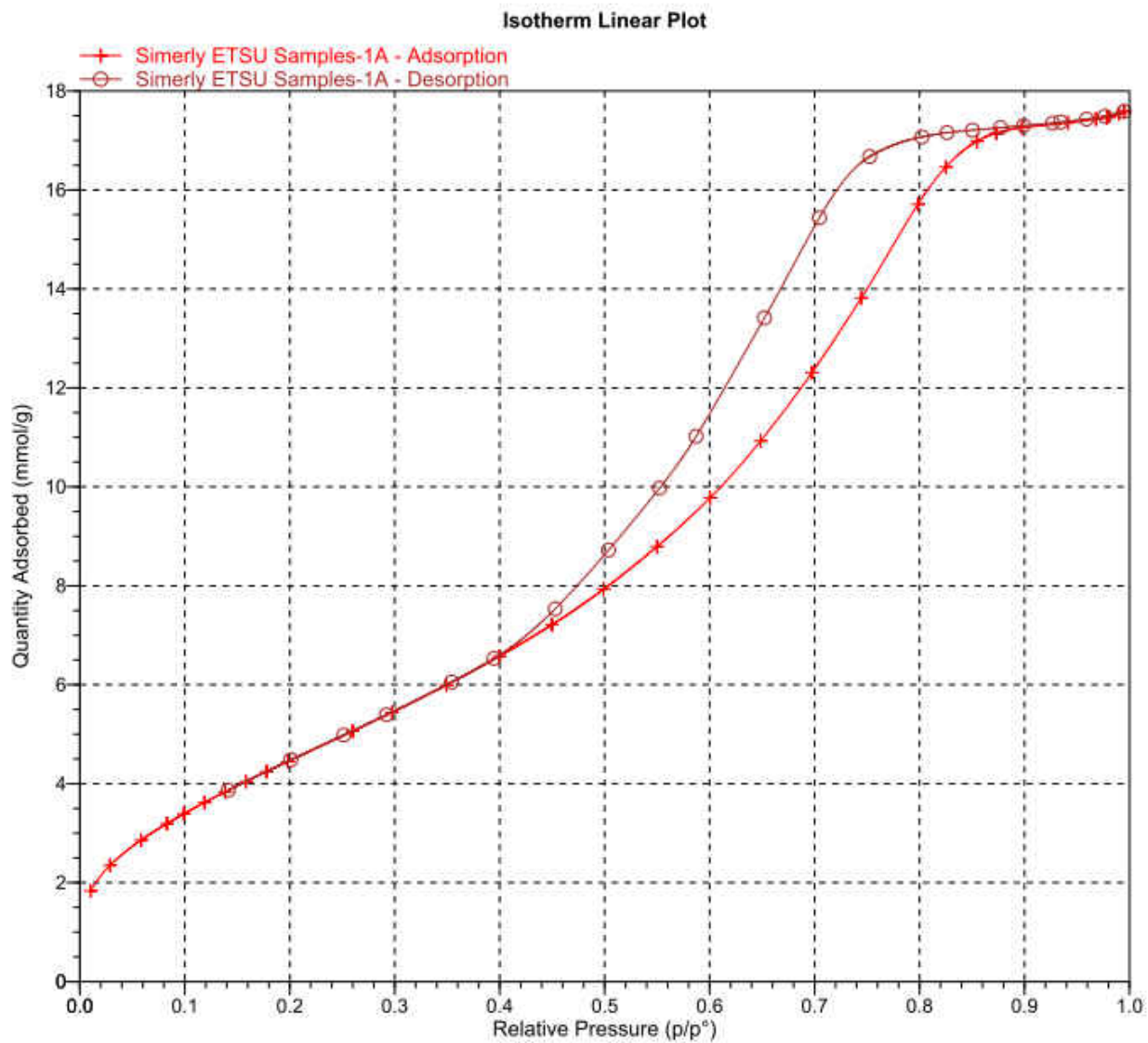


Figure 43. Adsorption/Desorption Isotherm of 23.

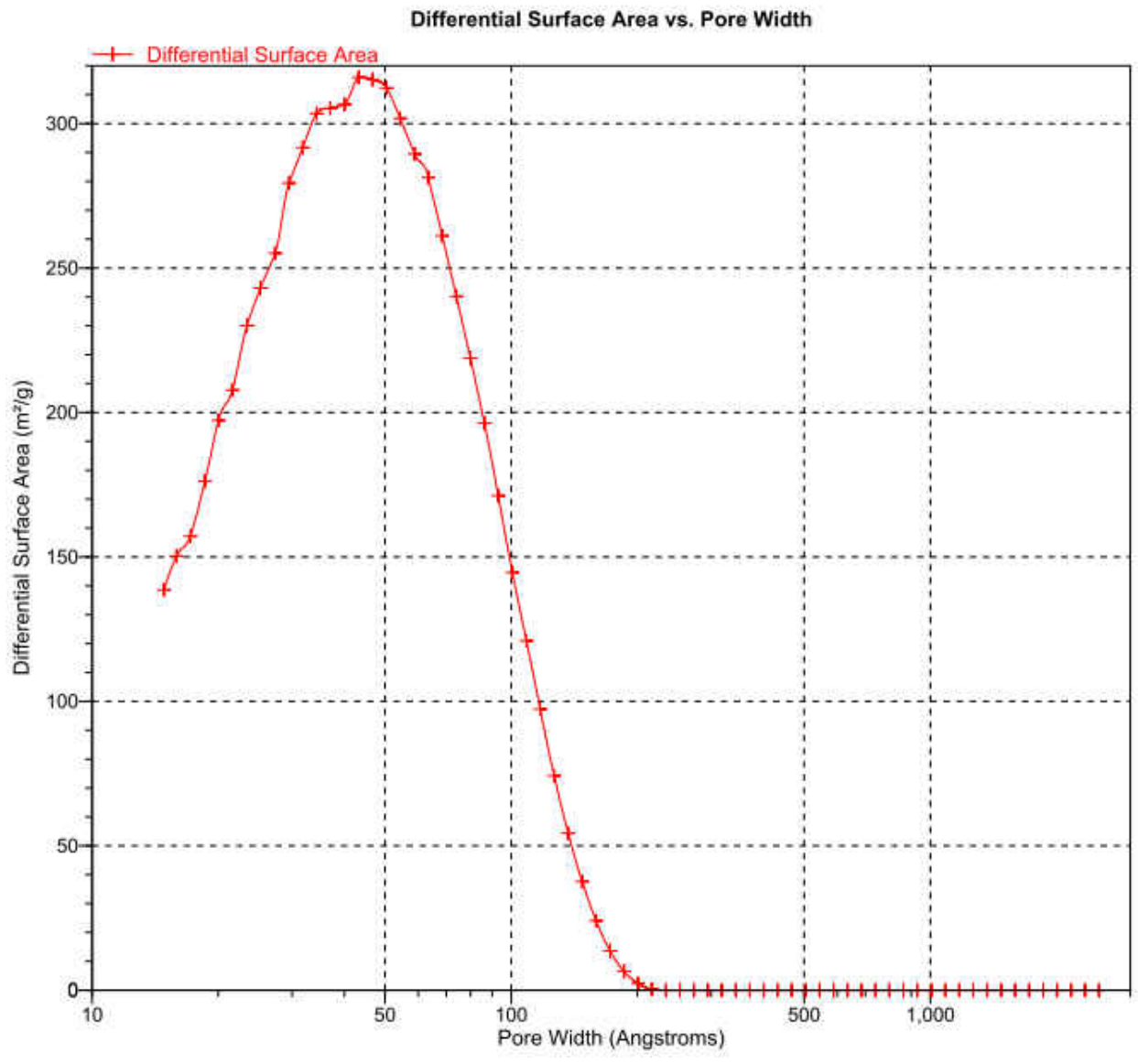


Figure 44. Pore Size Distribution of **23**.

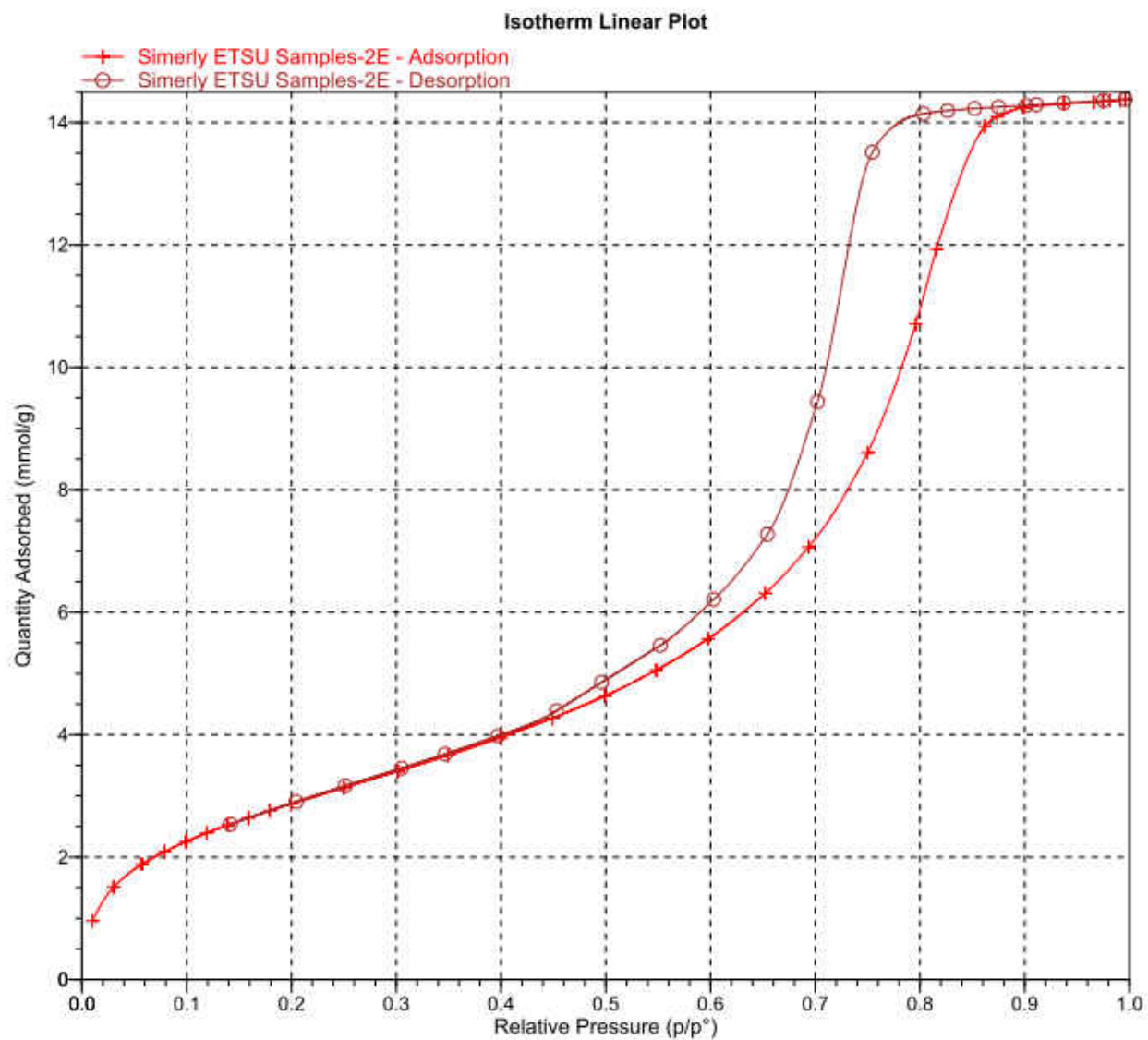


Figure 45. Adsorption/Desorption Isotherm of **24**.

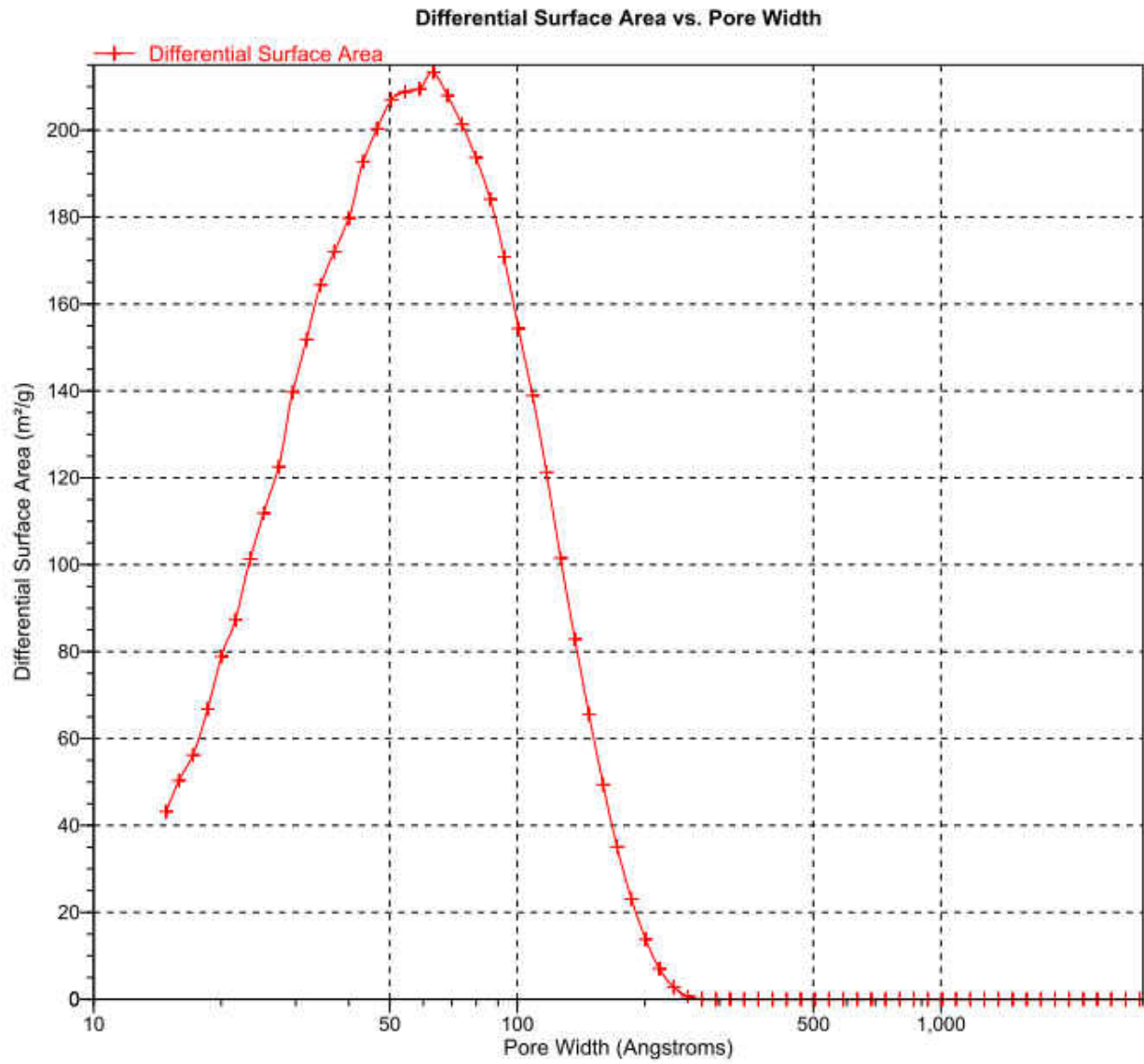


Figure 46. Pore Size Distribution of **24**.

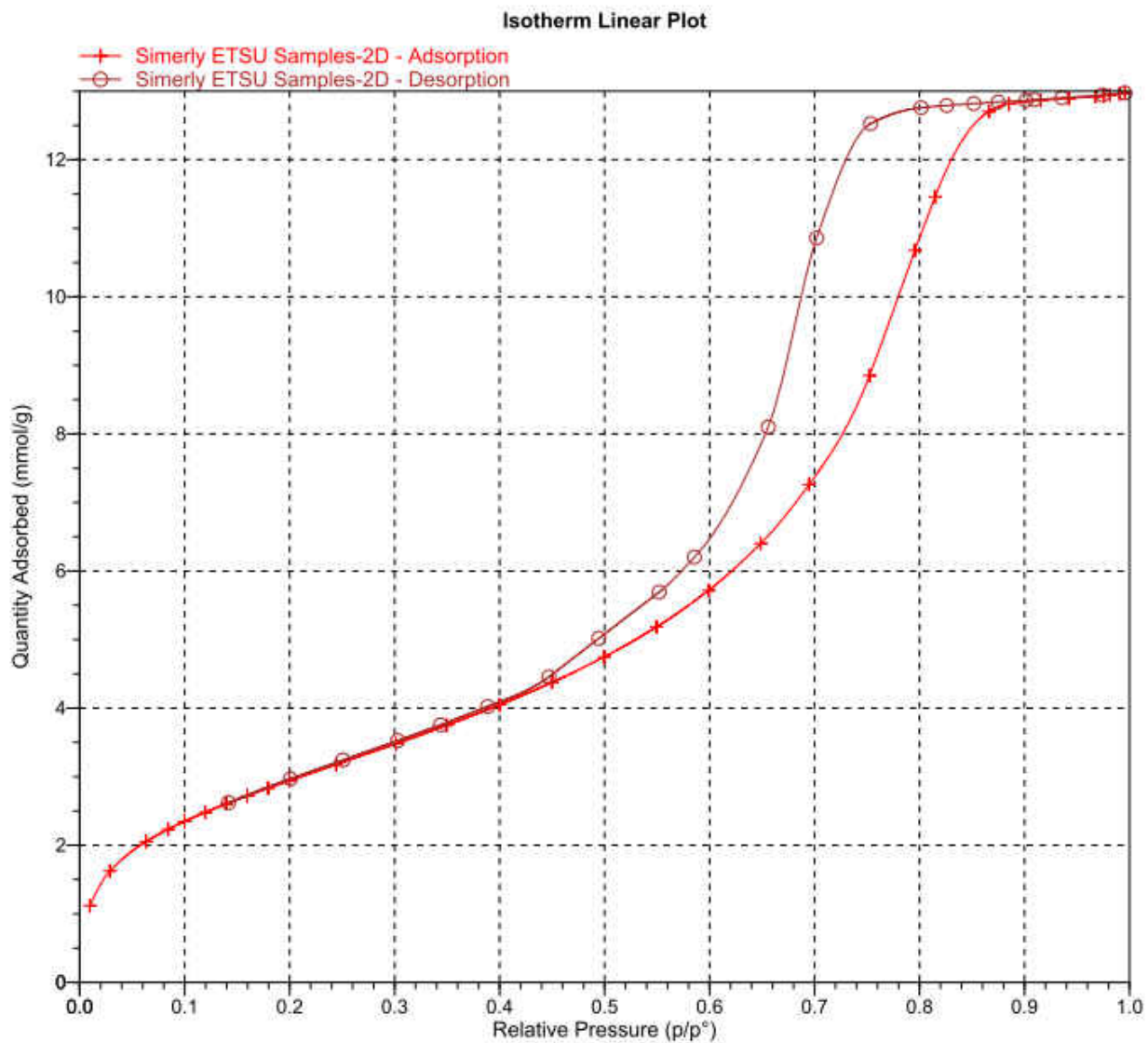


Figure 47. Adsorption/Desorption Isotherm of **25**.

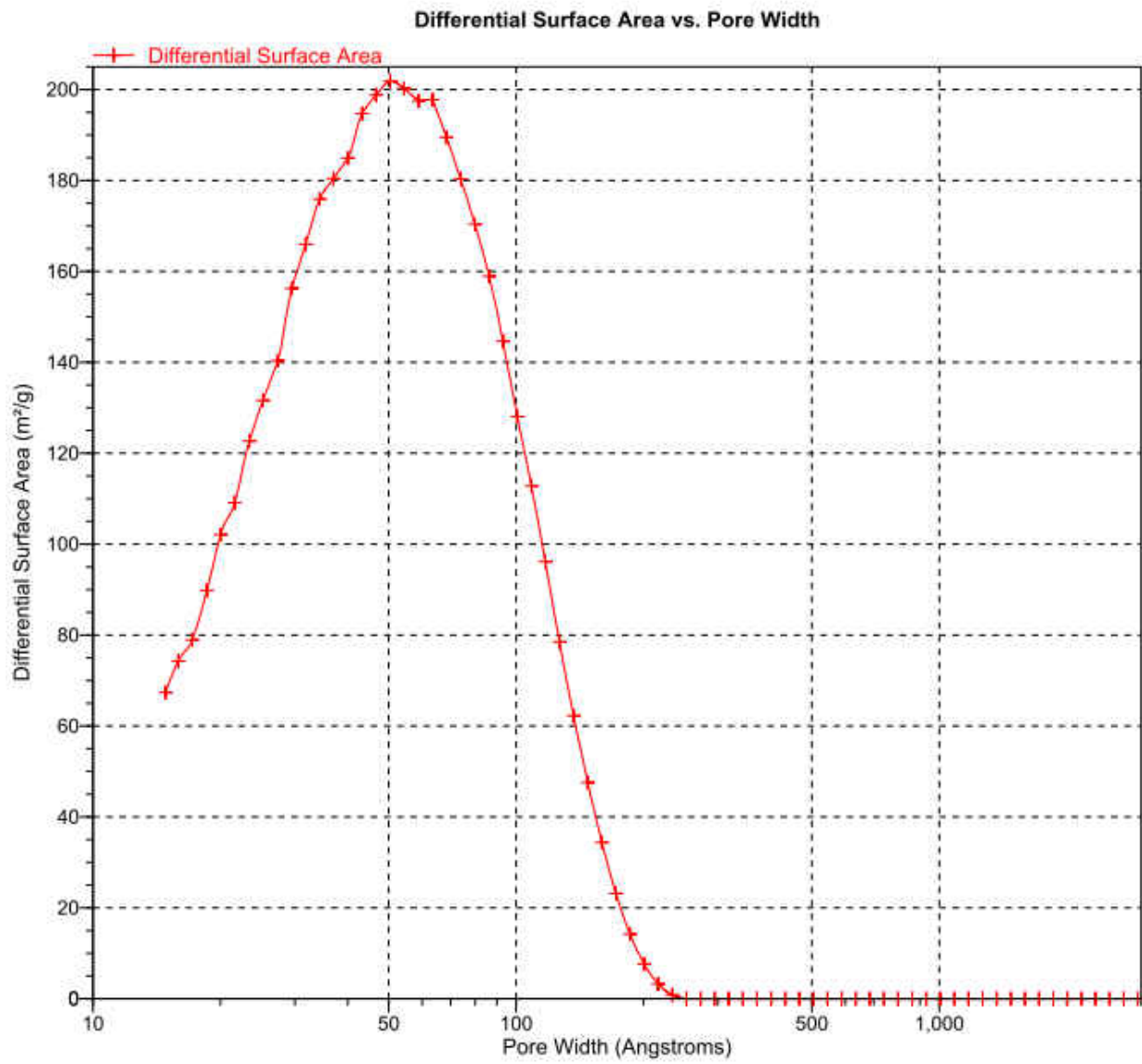


Figure 48. Pore Size Distribution of 25.

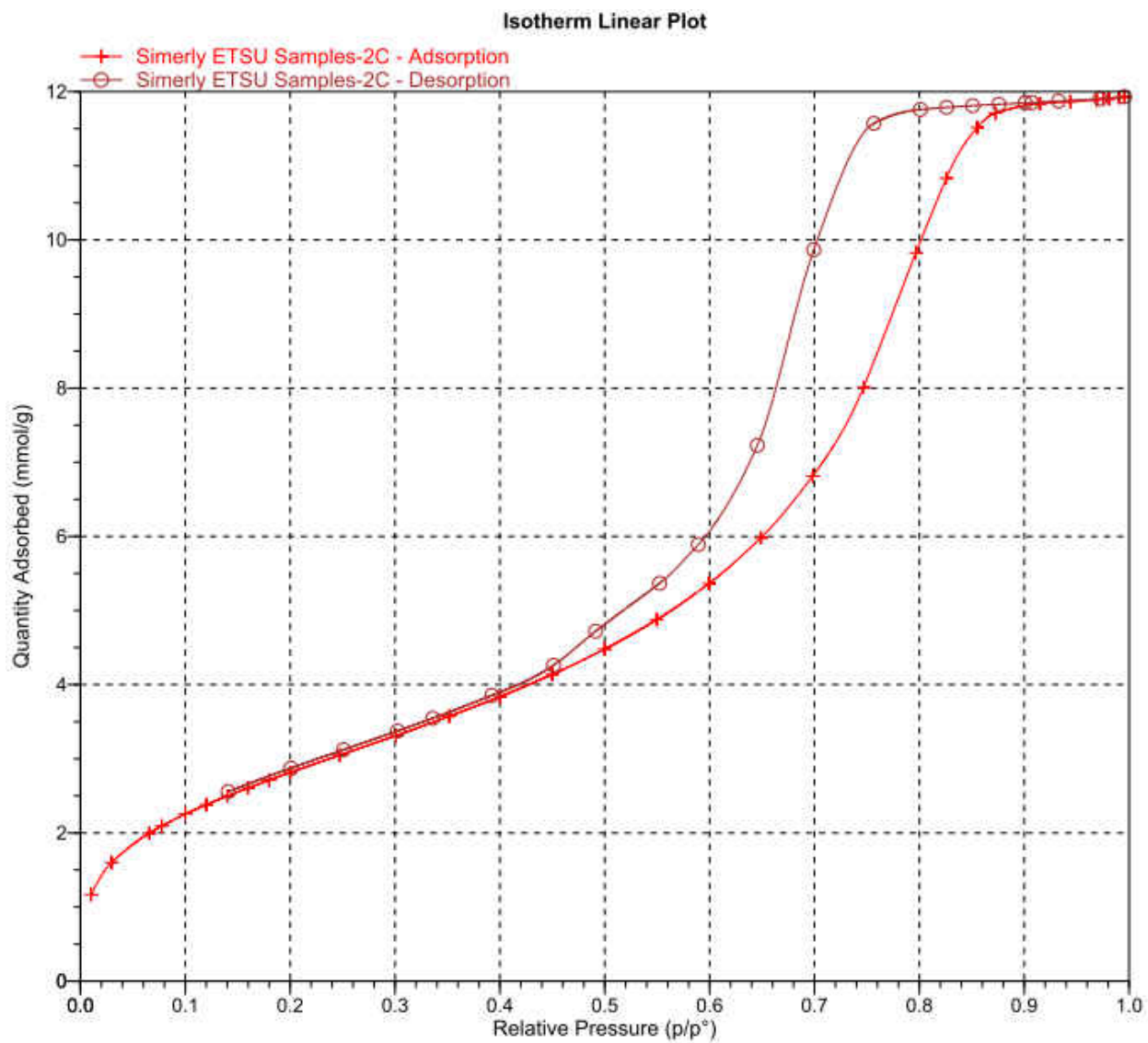


Figure 49. Adsorption/Desorption Isotherm **26**.

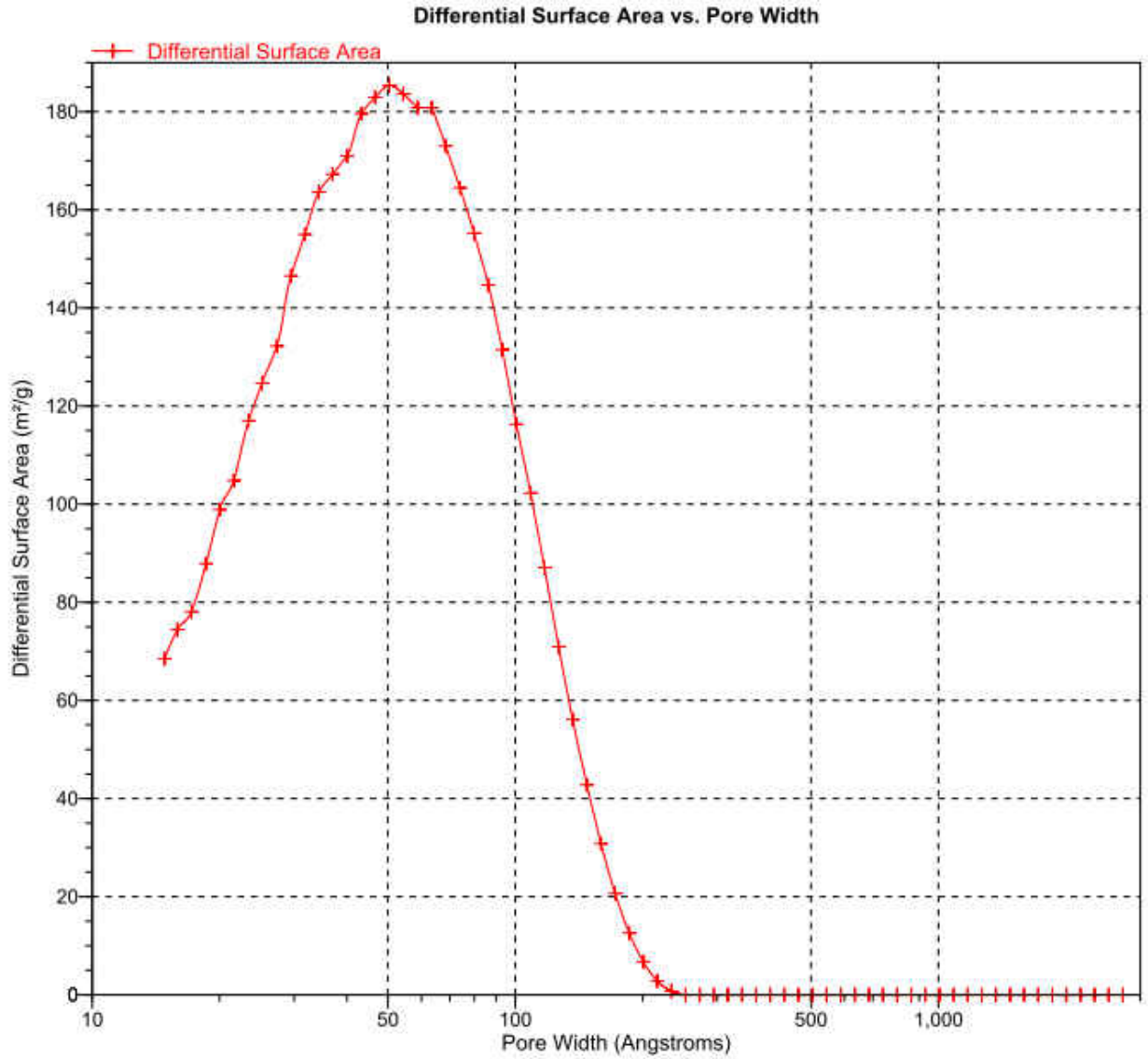


Figure 50. Pore Size Distribution of **26**.

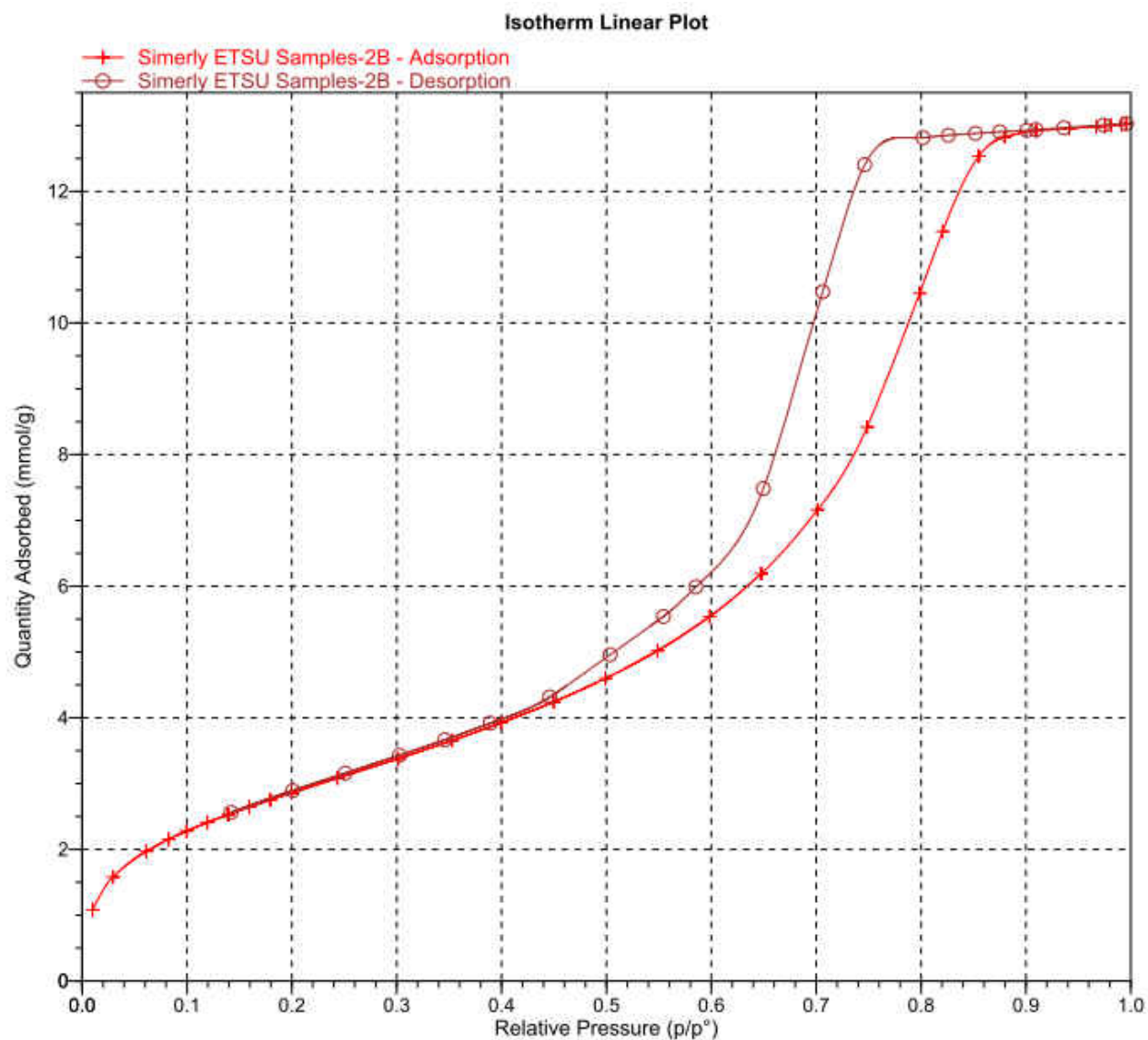


Figure 51. Adsorption/Desorption Isotherm of **27**.

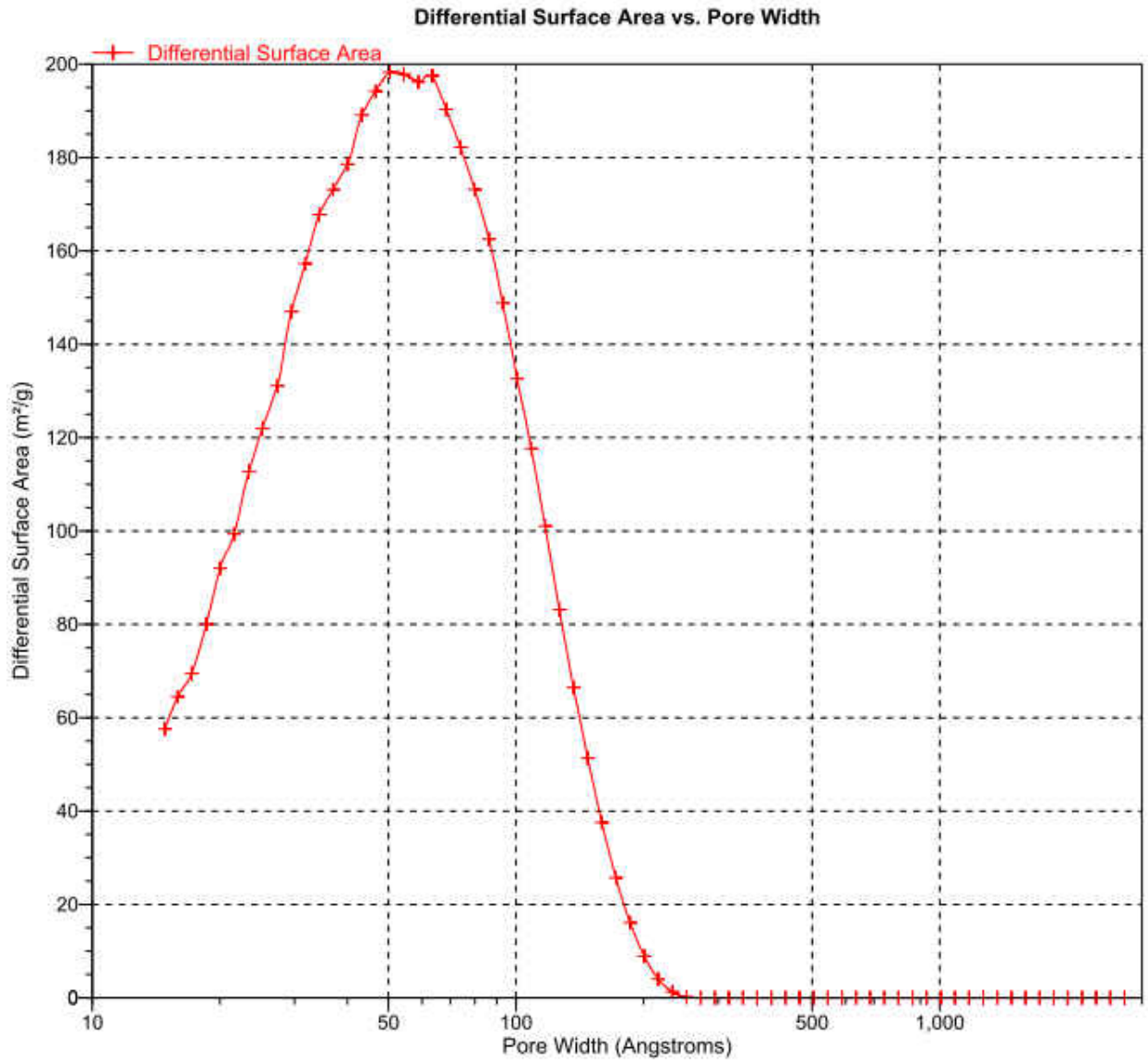


Figure 52. Pore Size Distribution of **27**.

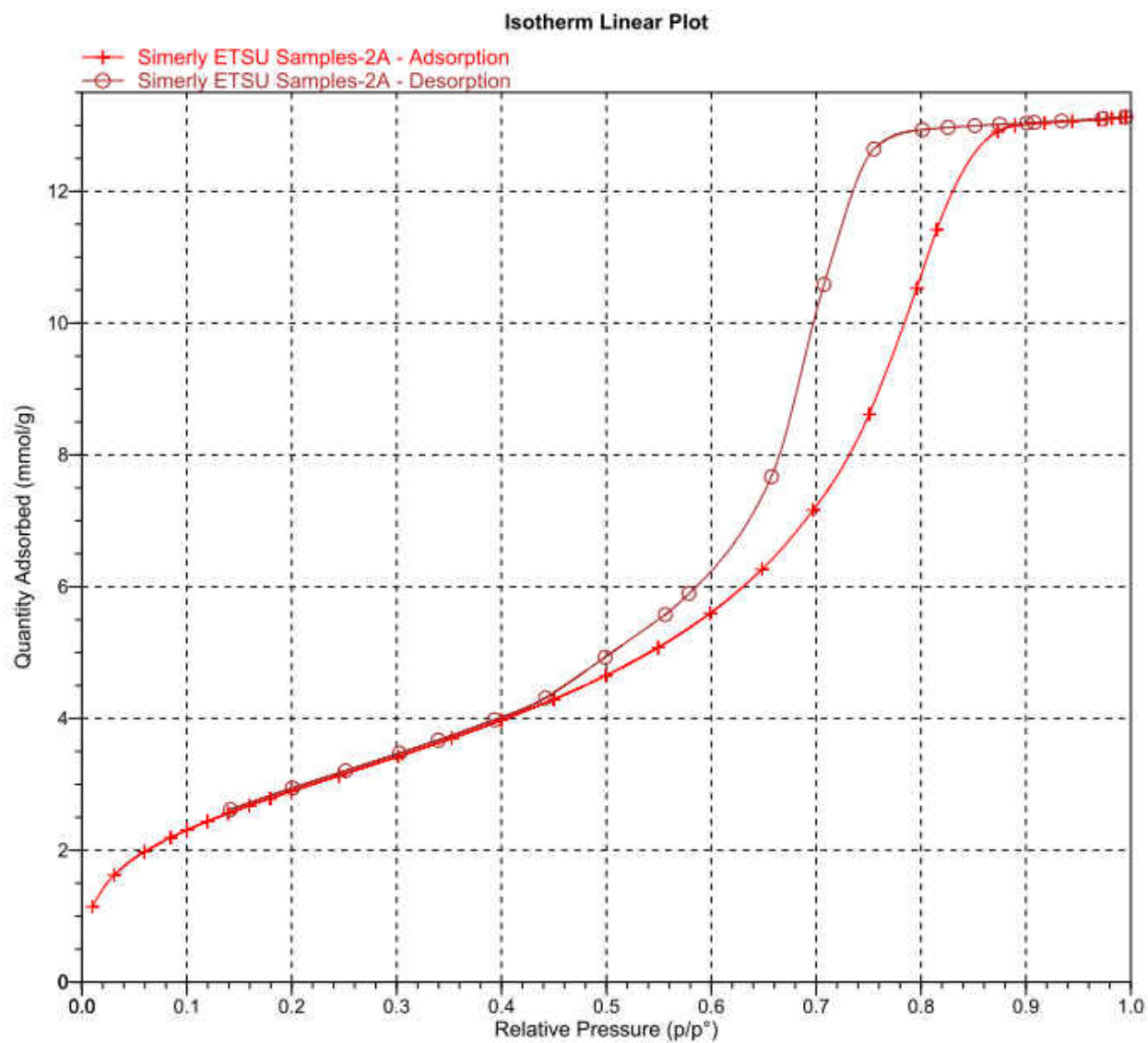


Figure 53. Adsorption/Desorption Isotherm of **28**.

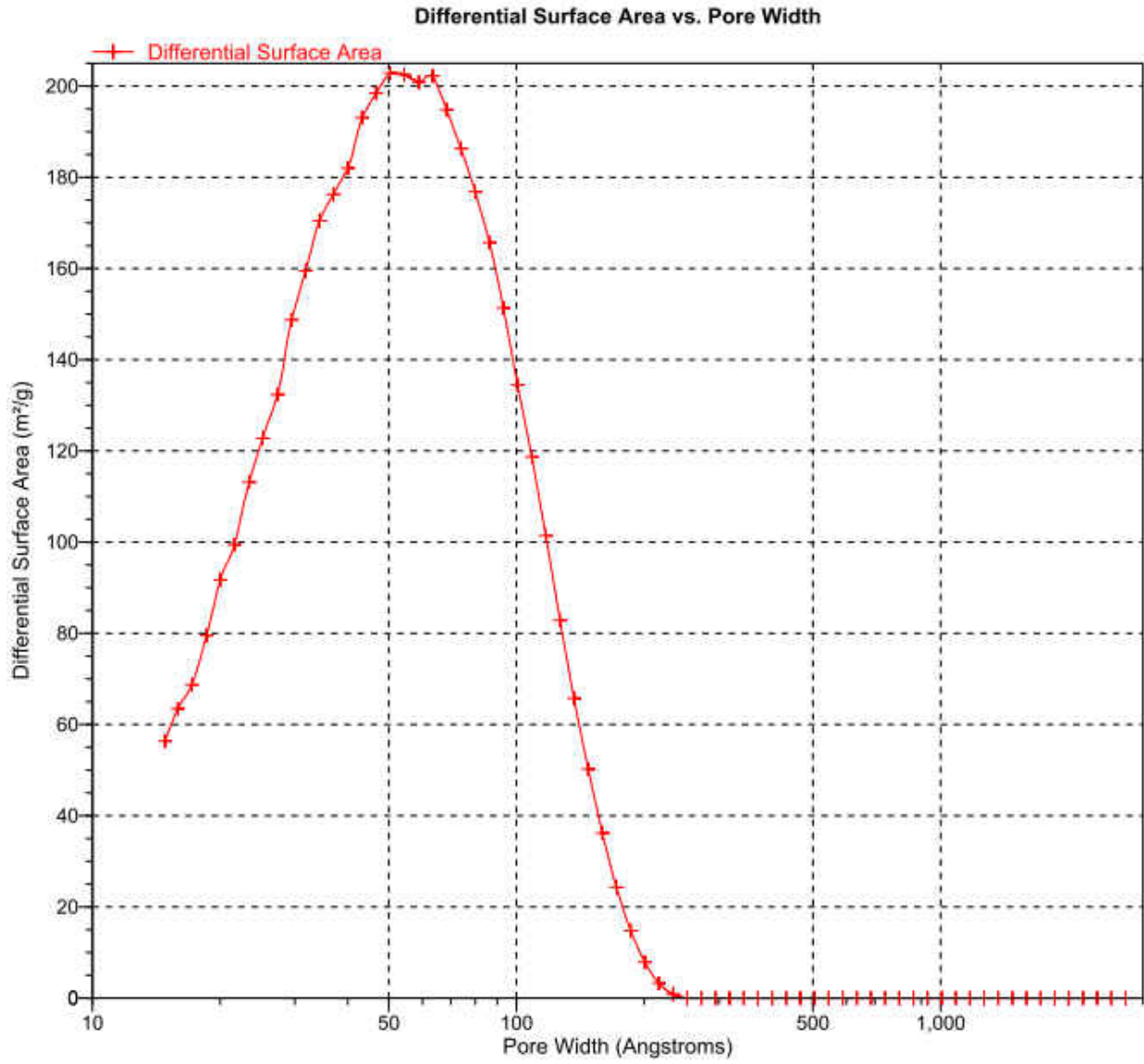


Figure 54. Pore Size Distribution of **28**.

APPENDIX D

Atomic Absorption Calibration Curve

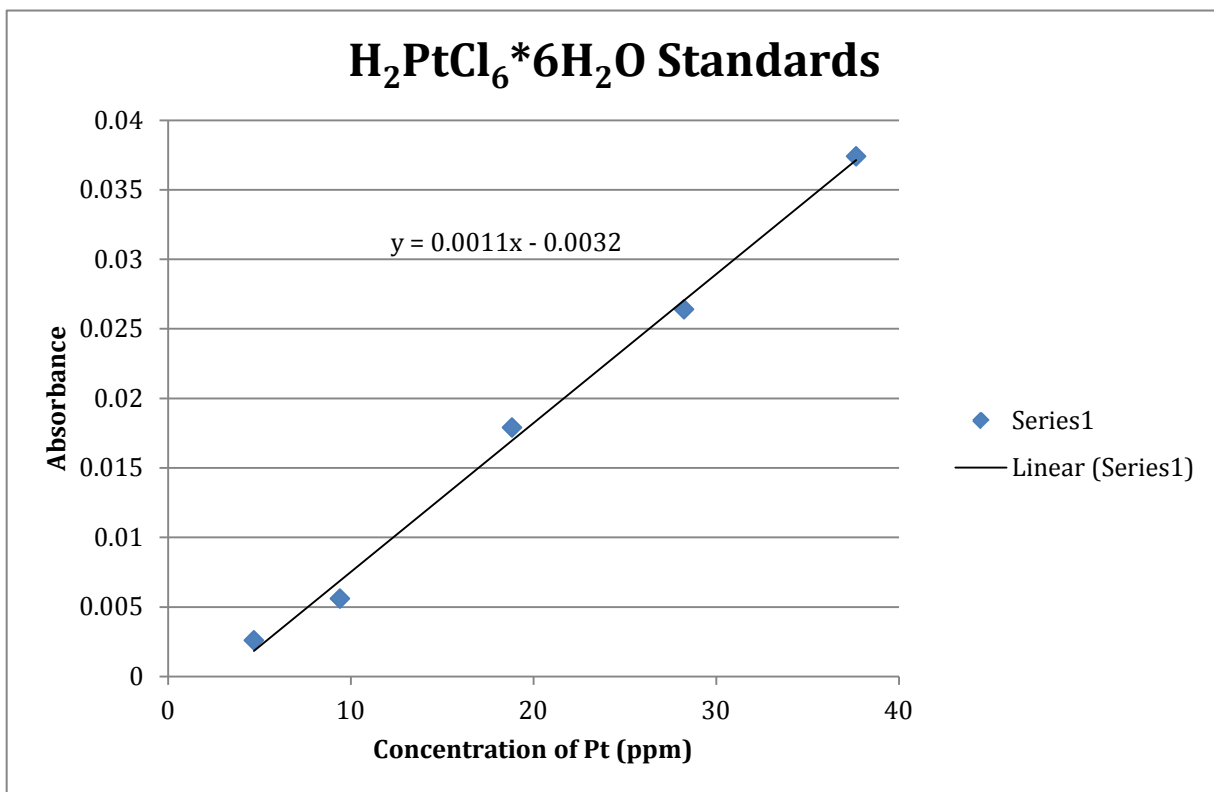


Figure 55. Calibration Curve of Pt Standards for AAS.

VITA

THOMAS MAX SIMERLY

Personal Data: Date of Birth: April 27, 1988
Place of Birth: Elizabethton, Tennessee
Marital Status: Single

Education: Public Schools, Unicoi County, Tennessee
B.S. Biochemistry, King College, Bristol, Tennessee 2010
M.S. Chemistry, East Tennessee State University, Johnson City,
Tennessee 2012

Professional Experience: Research Assistant, Pharmacology, East Tennessee State
University, Johnson City, Tennessee 2008
Research Assistant, Physiology, East Tennessee State
University, Johnson City, Tennessee 2010-2011
Lab Analyst, Eastman Chemical Company, Kingsport, Tennessee
2010-2012
Graduate Assistant, East Tennessee State University, Johnson City,
Tennessee 2011-2012

Awards: Outstanding Chemistry Senior of 2010, Northeast Tennessee
Section of the American Chemical Society, 2010
Outstanding Teaching Assistant Award, East Tennessee State
University, 2011
2nd Place Poster Presentation in Graduate Students – Master’s
Candidates Natural Sciences, 2012

Research Experience: Histamine Receptors in Mouse Atrium, Pharmacology, East
Tennessee State University, 2008
Phosphoinositide-3-kinase/Akt-Dependent Signaling is Required
for Maintenance of [Ca²⁺]_i, I_{Ca}, and Ca²⁺ Transients in
HL-1 Cardiomyocytes, Physiology, East Tennessee State
University, 2010-2011
Immobilized Bis-Indenyl Ligands for Stable and Cost-Effective

Metallocene Catalysts of Hydrogenation and
Polymerization Reactions, Chemistry, East Tennessee
State University, 2010-2012

Publications:

Simerly, T.; Zhou, G.; Golovko, L.; Tychinin, I.; Trachevsky, V.;
Gomza, Y.; Vasiliev, A. Highly Functionalized Bridged
Silsesquioxanes. *J. Sol-Gel. Sci. Technol.* **2012**.

Simerly, T.; Graves, B.; Li, C.; Williams, D.; Wondergem, R.
Phosphoinositide-3-kinase/Akt-Dependent Signaling is
Required for Maintenance of $[Ca^{2+}]_i$, ICa, and Ca^{2+}
Transients in HL-1 Cardiomyocytes. *J. Biomed. Sci.* **2012**.

Simerly, T.; Milligan, T.; Mohseni, R.; Vasiliev, A.
Immobilization of Ethylene Bis-Indenyl Ligands on
Functionalized Silica Gel. *Tetrahedron Lett.* **2012**.